Rab26 mediates selective targeting of synaptic vesicles to the autophagy pathway

Dissertation

For the award of the degree
"Doctor of Philosophy" (Dr. rer. nat.)
Division of Mathematics and Natural Sciences
of the Georg-August-Universität Göttingen

Submitted by
Beyenech Binotti

Born in Ethiopia

Citizenship Italian

Göttingen, 2014

Thesis supervisor:

Prof Dr. Reinhard Jahn
Department of Neurobiology, Max Planck Institute for Biophysical Chemistry

Members of the thesis committee:

Prof. Dr.Peter Rehling
Department of Biochemistry II, University of Göttingen
Prof. Dr. Mikael Simons
Department of Neurology, Max Planck Institute for Experimental Medicine, University of Göttingen

Extended thesis comittee:

Prof. Dr. Michael Thumm
Department of Biochemistry II, University of Göttingen
Prof. Dr. Oliver Schlüter
Molecular Neurobiology, European Neuroscience Institute (ENI), Göttingen
Prof. Dr. Blanche Schwappach
Department of Molecular Biology, University of Göttingen

Date of submission of the PhD Thesis: 31.01.2014

Date of oral examination: 17.03.2014

Affidavit

I declare that my Ph.D. thesis entitled “Rab26 mediates selective targeting of synaptic vesicles to the autophagy pathway” has been written independently and with no other sources and aids than quoted.

Beyenech Binotti

Göttingen, 2014

“To Cornelius with whom I began and share my wonderful project of life.”

“To Simone for his happiness and serenity that taught me how to face life´s challenges.”

Table of contents

List of Figures

List of Tables

Abstract

In recent years it has been shown that macroautophagy regulates the turnover of postsynaptic receptors and modulates presynaptic neurotransmission. However it is still unclear whether the presynaptic protein turnover is regulated by the same pathway. It was previously shown in our laboratory that the small GTPase Rab26 is highly enriched in the synaptic vesicle fraction (Nathan Pavlos, unpublished data). The real implication of its presence on the synaptic vesicle membranes though has not been investigated so far. The aim of this project was to characterize the functional role of Rab26 in neurons. We wanted to find out in which pathway Rab26 is implicated and if it contributes in regulating the synaptic vesicle (SV) cycle. I employed well established biochemical and cell biology approaches such as immunoprecipitation, GST pulldown, immunoisolation as well as immunocytochemistry and electron microscopy to address these questions. The systems in which I applied these techniques were cultured hippocampal neurons, HeLa ss6 and HEK 293T cell lines. During this study it was possible to obtain several findings. I could demonstrate that Rab26 is a neuronal small GTPase Rab protein which is associated with a subset of synaptic vesicles. It has the ability to oligomerize, to cluster vesicles and it interacts with one of the essential core components of the autophagosome machinery, Atg16L1. Furthermore it is selectively targeting recycled synaptic vesicles. This led us to conclude that Rab26 might be an important key regulator of synaptic vesicle quality control. Furthermore the identification of the interaction between Rab26 and Atg16L1 made it possible to connect recycled synaptic vesicles with the autophagy pathway. In addition we could offer an alternative mode of synaptic vesicle endocytosis that bypasses the Rab5-dependent pathway and converges with the late endosome/autolysosome pathway. All these aspects listed here will be discussed further in detail in the following paragraphs.

1 Introduction

1.1 Synapse

Neurons have a distinct and peculiar morphology that reflects their functional intracellular compartmentalization. They consist of a central part called either cell body or soma where the nucleus resides and where most of the synthesis occurs and of proximal and peripheral regions called axons and neurites. These arbors are fine and long extensions responsible for establishing contact with the neighboring neurons forming the so called neuronal network. The contact site is known as synapse.

The term synapse (from Greek *synapsis* that means conjunction) was first introduced in 1897 by the physiologist Charles Sherrington who first stated that the connection between neurons was neither direct nor physical. Synapses are one of the most specialized units of the neuronal network. They allow neurons to communicate with other neuronal cell types or with effector cells (such as muscle cells) through chemical or electrical signals. The synapse is formed principally by two parts that differ both morphologically and chemically. The presynaptic terminal contains a specialized type of vesicles named synaptic vesicles (SVs) in which the neurotransmitters (the chemical signals) are stored. The postsynaptic terminal is where the post synaptic receptors are located with their ligand binding sites exposed to the synaptic cleft in which the neurotransmitters (NTs) are released from the presynaptic terminal. The two parts are connected together by a specific set of cell-adhesion molecules (Chua *et al.* 2010). The signal first arrives at the presynaptic plasma membrane (PM) in the form of an electric impulse and induces then the opening of the calcium channels. The influx of calcium (Ca^{2+}) in the nerve terminal drives exocytosis of the synaptic vesicles that fuse with the PM and release the neurotransmitters by exocytosis into the synaptic cleft. There they bind to the receptors located on the postsynaptic membrane where the chemical signal is converted into a change of the electrical property of the membrane (Südhof 2008) (Figure 1). The release of the neurotransmitters is temporally and spatially regulated and occurs in a specific site of the presynaptic PM named active zone (AZ). This site of release is called the cytomatrix at the active zone (CAZ) and it is composed of the presynaptic PM and a huge number of proteins. Under the electron microscope this area appears electron dense and is therefore

easily recognizable. The directionality of the exocytosis of the synaptic vesicles is finely regulated and is driven by three major molecular events: docking, priming and fusion of SVs that take place at the active zone (Figure 1).

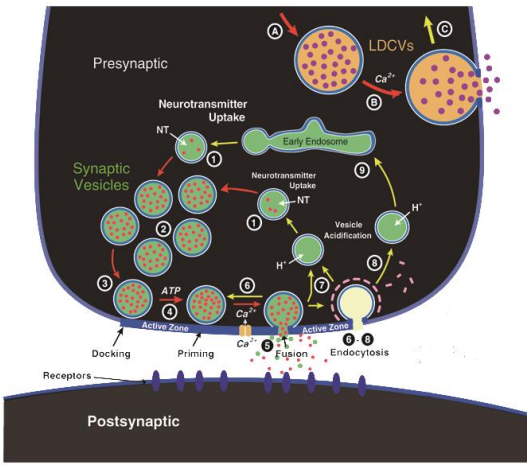

Figure 1 Key events of SV exocytosis.

Schematic representation of the exocytosis events that drive synaptic transmission. Synaptic vesicles release the neurotransmitters (NTs) in a coordinated fashion that requires three fundamental steps: docking, priming and fusion of SV with the PM. Image modified from Südhof (2008).

1.1.1 Steps of synaptic vesicle exocytosis

The release of NTs occurs mainly by exocytosis of synaptic vesicles that fuse with the presynaptic membrane. Synaptic vesicles filled with neurotransmitters are first delivered to the release site, the active zone, and then docked with the presynaptic plasma membrane. Subsequently the molecular machinery required for the exocytosis is recruited on the synaptic vesicles. This step is called "priming". In the final step the vesicle membrane fuses with the PM and the neurotransmitters are released into the synaptic cleft where they bind to the postsynaptic receptors that transduce the signal downstream. Below a more detailed description of the three mechanisms of synaptic vesicle exocytosis will be given: docking, priming and fusion.

Docking is the first step of SV exocytosis. Its definition is based mainly on a morphological observation. The docked SVs can be easily identified by electron microscopy. In fact their distance from the plasma membrane is not measurable or less than 30 nm (Xu-Friedman *et al.* 2001, Hammarlund *et al.* 2007, Verhage and Sorensen 2008). The process of docking controls the correct arrangement of synaptic vesicles in close proximity to the active zone. However the docking machinery is not yet fully understood.

The small GTPase Rab proteins (such as Rab3 and Rab27) and Rab effector proteins such as Rabphilin and Rab3 interacting molecule (RIM) are known to be involved in positioning synaptic vesicles at the level of the presynaptic PM. A fundamental role in SV docking is played by the so called RIM-containing protein complex which is composed of the active zone proteins such as piccolo, RIM, bassoon, ERKs and α-liprin (Südhof 2012).

Priming is the reaction that converts the docked (unprimed pool) to the ready releasable pool (RRP). It is an ATP-dependent process that gives fusion competency to the docked synaptic vesicles that become ready to fuse with the PM upon Ca^{2+} influx (Becherer and Rettig 2006, Verhage and Sorensen 2008).

The molecular mechanism that drives the priming event is well investigated and understood. The priming reaction requires the formation of a trimetric SNARE complex (the minimal core machinery for membrane fusion) in which the R-SNARE Synaptobrevin on the side of synaptic vesicle membrane forms a stable complex with the Q-SNAREs SNAP-25 and Syntaxin on the side of the PM. In a mechanism called SNARE complex zippering, the complex pulls the two membranes close to each other (Fasshauer *et al.* 1998, Lonart and Sudhof 2000, Sorensen *et al.* 2006).

An essential factor of the priming step is Munc-13 (Brose *et al.* 2000). Mice deficient of this protein lack the RRP, have their synapse transmission impaired and have an increased number of docked vesicles (Aravamudan *et al.* 1999, Augustin *et al.* 1999, Richmond *et al.* 1999). Munc-13 together with RIM and Rab3 assists synaptic vesicles towards the recruitment of the priming machinery (Betz *et al.* 2001).

Fusion is the last step of synaptic vesicle exocytosis (Südhof 2013). It is the most investigated and best understood mechanism (Jahn and Fasshauer 2012). It is promoted upon calcium influx driven by the arrival of an action potential that induces the opening of the voltage-gated Ca^{2+} channels. Once the calcium enters the synaptic terminal, it binds to

both C_2 domains (C2A and C2B) of Synaptotagmin, the calcium sensor SV protein that triggers membrane fusion (Geppert *et al.* 1994, Chapman *et al.* 1996). The C2A and C2B domains are able to interact with different phospholipids on the membrane of synaptic vesicles only upon calcium biding (van den Bogaart *et al.* 2012). The SNAREs are the driving force of the fusion. The formation of a quaternary *trans* SNARE complex (Chapman *et al.* 1995, Dai *et al.* 2007) is driven by a zippering mechanism that runs from their cytosolic tails towards their transmembrane domains. This process releases the energy necessary for membrane fusion (Jahn and Scheller 2006, Sorensen *et al.* 2006).

1.1.2 Synaptic vesicle retrieval

To sustain efficient neurotransmitter release a tight coupling of exo- and endocytosis is required. In this way synaptic vesicles undergo several rounds of exocytosis and endocytosis without compromising synaptic transmission.

The first evidence of synaptic vesicles retrieval goes back to 1973 (Heuser and Reese 1973), and since then a lot of progress was made in understanding vesicle recycling from the plasma membrane (PM) to the cytosol. The vesicle retrieval at the synapse can occur in at least three ways: Clathrin-mediated endocytosis (CME), "kiss-and-run" mode as shown in Figure 2, and bulk endocytosis. Recent experimental data showed the existence of a fourth possible way of synaptic vesicle recycling called "ultrafast" endocytosis that occurs in terms of milliseconds after stimulation (50 ms to 100 ms) and takes place outside of the active zone (Watanabe *et al.* 2013).

The "kiss-and run" endocytosis is very fast whereas the bulk endocytosis is considerably slower. The first mode was observed upon vesicle stimulation at a very low frequency. The formation of an uncoated vesicle pinch could be seen within 1 to 2 sec after stimulation (Fesce *et al.* 1994). These observations led to the hypothesis that exocytosis and endocytosis were linked by the formation of a transient fusion pore. In this way the "kiss-and run" theory was introduced. The synaptic vesicles are first attached to the active zone, and then they fuse without a complete membrane collapse with the plasma membrane, just forming a fusion pore through which they release their content. Then in less than 2 seconds they are endocytosed back while keeping their protein and lipid composition and thereby their vesicle identity. This mechanism is still very controversial within the field (Rizzoli and Jahn 2007). Bulk endocytosis occurs upon prolonged and strong stimulation (Rizzoli

and Betz 2005). Large regions of the presynaptic terminal PM are invaginated as a tubular or cistern-like structure from which vesicles can bud off and recycle back for multiple cycles of exo- and endocytosis (Miller and Heuser 1984, Clayton and Cousin 2008).

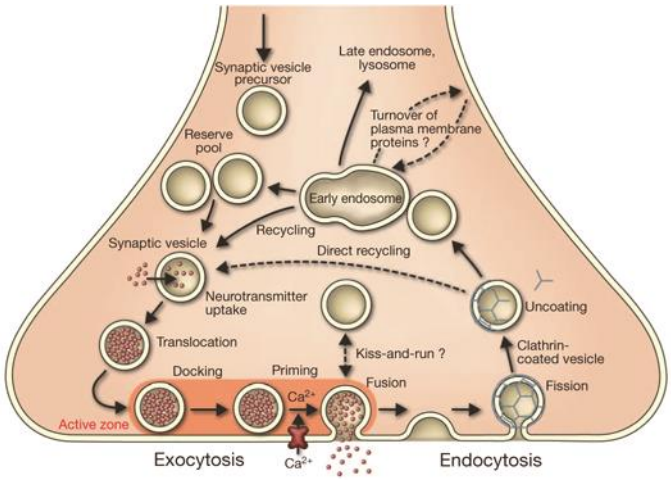

Figure 2 The synaptic vesicle cycle.
Schematic representation of the SV recycling pathway in the pre-synaptic terminal. Image taken from Jahn and Fasshauer (2012).

The clathrin-mediated endocytosis (CME) is well characterized. It is the best understood and investigated molecular mechanism of endocytosis. It is accepted that the main pathway for synaptic vesicle recycling is based on the CME pathway (Granseth *et al.* 2006). Although CME is a "housekeeping" process, in synapses it acquired several adaptations that make this pathway neuron specific (Jahn and Sudhof 1994, Ferguson *et al.* 2007). Proteomic studies showed that synaptic vesicle proteins are the main cargo of the clathrin coated vesicles (CCV) (Blondeau *et al.* 2004). Isolation of synaptic vesicles from rat brain revealed high concentration of endosomal components (Takamori *et al.* 2006). The protein machinery of the CME pathway consists of a large number of proteins that include mainly clathrin, adaptor proteins such as AP-2, epsin, eps15, AP180, Intersectin, Dynamin, Synaptojanin, and Amphiphysin, (Slepnev and De Camilli 2000, McMahon and Boucrot 2011). Clathrin mediated endocytosis occurs in a sequential manner and the CCVs are morphologically recognizable by their typical lattice-like coat (Pearse 1976, Ferguson *et al.* 2008). Clathrin alone does not bind to the membrane. Adaptors and accessory proteins

are essential for correct nucleation and cargo recognition. First adaptor proteins such as AP-2 are recruited on the presynaptic membrane in the sites where phosphatidylinositol-4**,** 5-bisphosphate (PIP2) is clustered. Here AP-2 recognizes the specific cargo (such as Synaptotagmin, Zhang *et al.* (1994)), recruits clathrin, and initiates the membrane invagination in concert with AP180 promoting the formation of the clathrin triskelion that induces membrane curvature. Subsequently the invaginated portion of the PM buds with the formation of a bud neck. Amphiphysin mediates Dynamin recruitment which promotes membrane fission (Hinshaw and Schmid 1995, Roux *et al.* 2006). At this point CCVs are formed and are transported in the cytosol. Finally Synaptojanin promotes uncoating hydrolyzing PIP2 (Chang-Ileto *et al.* 2011). The energy required for the coat disassembly comes from the ATPase Hsc70 that is recruited on the CCVs by its cofactor Auxilin that binds both AP-2 and Clathrin. Subsequently Clathrin and adaptor proteins are dissociated from the vesicles and recycled back to a new nucleation module for a subsequent round of endocytosis. CME in the nerve terminal is a relatively fast mechanism compare to other non-neuronal cell types and occurs within 15-20 seconds (Heuser and Reese 1973, Miller and Heuser 1984, Jockusch *et al.* 2005, Granseth *et al.* 2006, Balaji and Ryan 2007).

After uncoating the recycled synaptic vesicles can be either directly recycled to populate the RRP (after being re-loaded with neurotransmitters), or fuse with the sorting endosome. From the sorting endosome vesicles can be recycled and regenerated by an additional mechanism that requires budding and uncoating (Sudhof 2004) (Figure 2). Alternatively from the sorting compartment other vesicle types can bud and donate membrane to the later stage endosomes such as late endosomes/multivesicular bodies (LE/MVBs) and lysosomes/autophagosomes (Figure 2) that are most likely involved in the turnover of pre-synaptic components (Tsukita and Ishikawa 1980).

1.2 Synapse turnover

Synaptic vesicles undergo several rounds of exocytosis and endocytosis. Therefore a fine regulation of the turnover of synaptic components is required for the synaptic machinery to function properly.

Synthesis of synaptic proteins was originally thought to occur in the cell body and the proteins would then be transported via the axons to the synapses. But it became visible that protein synthesis in neurons can also occur locally (Steward and Levy 1982, Holt and Schuman 2013). In fact there are different evidences that show that proteins synthesis takes place in neurons at the level of the different subcellular compartments (Aakalu *et al.* 2001, Dahm *et al.* 2008, Martin 2010).

The understanding of synaptic vesicle turnover is far from being completely elucidated.

What is the mechanism that regulates the degradation of the presynaptic proteins? How can recycled synaptic vesicles be selectively targeted to the degradation pathway? This is a fascinating and poorly understood process.

There are two major degradative pathways: the ubiquitin-mediated degradation and the autophagosome/lysosome pathways.

1.2.1 Ubiquitin mediated degradation

Many studies reported that protein synthesis and degradation are involved in synaptic plasticity (Campbell and Holt 2001) and that most of the proteins are degraded by the ubiquitin proteasome pathway (Hershko and Ciechanover 1998, Voges *et al.* 1999). Thomas and Wyman (1984) showed for the first time an involvement of ubiquitinylation in axonal outgrowth in drosophila giant fibers. Since then it became clear that this mechanism is indeed an essential and highly regulated pathway, which modulates the neuronal development, plasticity and connectivity as well as synapse formation (Muralidhar and Thomas 1993, DiAntonio *et al.* 2001, Murphey *et al.* 2003, Yao *et al.* 2007, Yi and Ehlers 2007, Lee *et al.* 2008). There are at least two types of degradation pathways in which the ubiquitin conjugation system is involved in: the proteasome and the MVB/lysosome pathway.

Ubiquitin is a very small protein (76 amino acids). It is one of the post-translational modifications that the cell uses for the regulation of protein abundance and quality control. Specific enzymes catalyze the ubiquitinylation reaction: the ubiquitin-activating enzymes (E1s) that transfer ubiquitin to the second enzyme, the ubiquitin-conjugating enzymes (E2s) that bind simultaneously the substrate and the ubiquitin ligases (E3s). E3s transfer the ubiquitin from E2 to the substrate (Komander and Rape 2012). The covalent attachment of one or more ubiquitins (polyubiquitin chain) targets the substrates to one of the ubiquitin-degradation pathways.

1.2.1.1 The ubiquitin proteasome system (UPS)

The proteasome (26S) is a big multi-subunit protease formed by a catalytic core (20S proteasome) and by two regulatory factors (19S particles) (Finley 2009).
The ubiquitin-proteasome system (UPS) is a local and reversible process which usually plays a role in the turnover of short-lived proteins (Hegde *et al.* 1993, Hegde *et al.* 1997, Hershko and Ciechanover 1998). The substrates need to have a chain of at least 4 ubiquitins attached in order to be degraded efficiently by the catalytic core of the proteasome (Thrower *et al.* 2000).
The UPS is critical for presynaptic function. It is involved in the regulation of the abundance of the presynaptic proteins. Defects in this system strongly affect synapse physiology. Inhibition of the proteasome causes accumulation of the presynaptic protein Munc-13 compromising the neurotransmitter release (Speese *et al.* 2003). The synaptic E3 ligase (SCRAPPER) regulates the degradation of RIM1 (Yao *et al.* 2007). Moreover proteasome blockage increases FM-dye uptake thereby affecting the SV cycle (Willeumier *et al.* 2006).
UPS is involved also in the regulation of neuronal physiology. By regulating the level of small GTPase such as Rap and Rho family members the ubiquitin degradation system regulates neuronal differentiation, synapse formation and elimination (Schwamborn *et al.* 2007).

1.2.1.2 The ubiquitin dependent endosomal sorting

The second ubiquitin-based degradation system is dependent on the interaction with the endocytic pathway. In contrast to the UPS where polyubiquitinylation of the substrates is required, in this type of degradation instead the targets are labeled usually by a single ubiquitin molecule or by a multi-monoubiquitinylation (Haglund *et al.* 2003).

The molecular basis of the ubiquitin-dependent endosomal sorting is based on a conserved mechanism: the ESCRTs machinery (endosomal sorting complex for transport) that is formed by four complexes: ESCRT0, ESCRT-I, ESCRT-II, and ESCRT-III which in a sequentially manner are recruited on the endosome to modulate the formation of intraluminal vesicles (ILVs) that internalize proteins that are intended to be delivered to the lysosome for degradation. The best investigated cargoes of this pathway are ubiquitinylated membrane receptor proteins (Katzmann *et al.* 2002), such as the epidermal growth factor receptor (EGFR) (Roxrud *et al.* 2008). Once the cargo is ubiquitinylated by a specific E3 ligase (d'Azzo *et al.* 2005) it is internalized by CME into endosomal membranes. The ESCRT machinery acts at this level. ESCRT-0, I and II contain subunits that have ubiquitin interacting motif (UIM) and retain the cargoes on the endosomal membrane to prevent their recycling back to the PM. Then ESCRT-III is recruited to promote membrane curvature, budding and abscission of the new formed ILV. The multi vesicle endosome (MVE), called also multi vesicular body (MVB) fuses with the lysosome where the cargoes are degraded (for details see review Raiborg and Stenmark (2009)).

Contrary to the UPS, the degradation of presynaptic components by the ubiquitin-dependent sorting endosome pathway is less investigated. Haberman *et al.* (2012) proposed the existence of an endo-lysosome degradation pathway that is linked with the SV cycle. But at the post-synaptic level the ubiquitin-based endocytosis pathway was shown to regulate the surface abundance of postsynaptic receptors such as the AMPAR (Patrick *et al.* 2003, Lee *et al.* 2004) and the $GABA_AR$ (Bedford *et al.* 2001).

Both type of ubiquitin-degradation systems converge with the second main proteolytic machinery, the autophagosome-lysosome pathway, either at the regulatory or at the substrate level. In the following chapter a more detailed description of the autophagy pathway it will be given.

1.2.2 Autophagosome/lysosome pathway

The autophagosome/lysosome pathway is the second proteolysis pathway where usually long-lived proteins are digested (Dunn 1994, Shehata *et al.* 2012). Neurons are highly differentiated and polarized. This specialization serves to fulfill their intrinsic role of communicating with other cells which often times are very far away from each other. It was described by electron microscopy in the 1960´s that upon injury, neuronal cell bodies and axons were showing an accumulation of autophagic compartments with very distinct characteristics: double membrane structures engulfing cytoplasmic contents (Wettstein and Sotelo 1963, Schlote 1966, Holtzman *et al.* 1967, Blumcke *et al.* 1968, Lampert and Schochet 1968). There are three major conserved autophagy pathways: macroautophagy, microautophagy, and chaperone-mediated autophagy (CMA). Each subtype applies different mechanisms to engulf cytoplasmic content and delivers materials for degradation into the lysosome.

Microautophagy is the "self-eating" process that requires inward invagination of the lysosomal membrane thereby engulfing small portions of cytoplasmic content for degradation. It is the least understood mechanism and little is known about the molecular machinery that governs this uptake (Li *et al.* 2012).

CMA is a selective self-eating process that results in degradation of specific soluble proteins (Cuervo and Dice 2000) that have an internal recognition motif (KFEQ) (Chiang and Dice 1988, Dice and Chiang 1989). Proteins that carry these sequences are recognized by chaperons mainly by Hsc70 and Hsp90 through the interaction with the lysosomal receptor LAMP2A which delivers the unfolded proteins to the lysosome for their digestion (Dice 2007, Mizushima 2011). Chaperone mediated autophagy is conserved in most of the cell types and is activated during long-term nutrient starvation and oxidative stress (Kiffin *et al.* 2004, Finn and Dice 2005). It is involved in the clearance of aggresomes such as mutants of α-Synuclein (Cuervo *et al.* 2004). The pathological α-Synuclein is not properly translocated into the lysosome though it is still able to bind to LAMP2A receptor. This blocks the degradation of the other CMA substrates. Inefficient activity of the CMA pathway leads to the activation of the non-selective autophagy process that is the macroautophagy.

Macroautophagy is the canonical autophagy pathway. The term autophagy originates from the Greek word "phagy" that means to eat and "auto" stays for self. The word was first introduced by Christian De Duve in 1966. It is a conserved cellular process, an intracellular membrane trafficking pathway that is active at a basal level. The cells use this pathway to get rid of misfolded proteins and damaged organelles. Macroautophagy is an important process strictly required for cellular survival. In fact the activity of this pathway is greatly enhanced during particular situations such as nutrient deprivation, physical and chemical stress, or during microbial invasions. In all these circumstances autophagy is used to degrade proteins and macromolecules to supply the cell with the necessary building blocks releasing amino acids, nucleotides, and other monomeric components. In detail, as shown in Figure 3, pieces of double membrane structures called either phagophore, isolation membrane, or PAS (pre-autophagosomal structure) progressively expand around the target cytoplasm. The PAS encloses to form the autophagosome that can undergo fusion with endocytic compartments such as early endosomes and MVBs (Orsi *et al.* 2010, Hyttinen *et al.* 2013) and becomes an intermediate autophagic compartment called amphisome. The autophagy pathway ends with the fusion of the autophagosome with the lysosome transforming into an autolysosome (Tanida *et al.* 2005, Nakatogawa *et al.* 2009). The lysosomal proteases break down both the inner membrane of the autophagosome and the cytoplasmic contents. The catabolic products are subsequently recycled back to the cytosol and used as substrates for the biosynthetic pathways (Xie and Klionsky 2007).

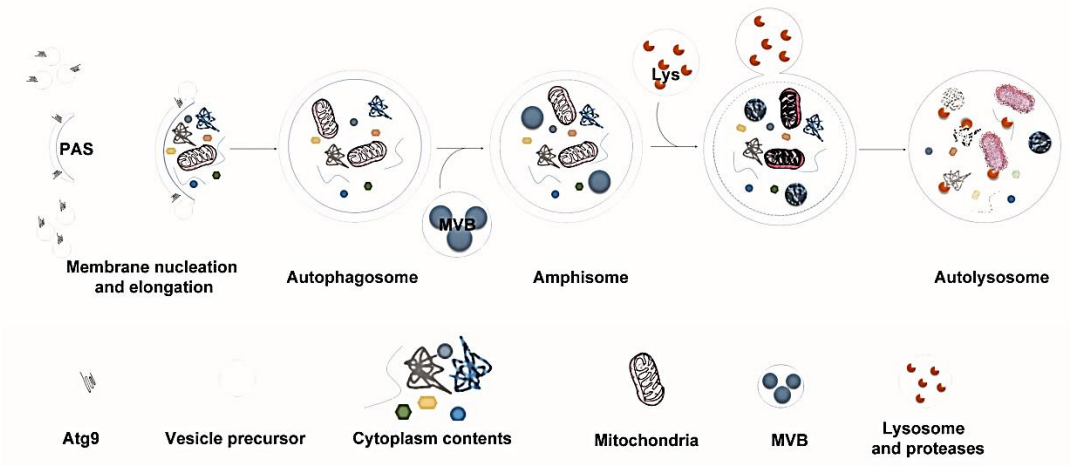

Figure 3 Schematic representation of the canonical autophagy pathway

1.2.3 Molecular machinery that drives macroautophagy

Macroautophagy is formed by a complex degradative machinery that includes at least 30 autophagy related (Atg) genes, which encode Atg proteins (Xie and Klionsky 2007, Suzuki and Ohsumi 2010). There are three fundamental steps: the phagophore/isolation membrane biogenesis, the elongation/enclosure, and finally the autophagosome maturation. Each step of the autophagosome biogenesis and maturation is finely controlled by a subset of Atg proteins (Nakatogawa *et al.* 2009, Stanley *et al.* 2013) (see Figure 4).

Autophagosome formation initiates at the PAS. The nucleation factors that trigger the recruitment of the other Atg proteins depend on the Atg1 complex that includes Atg1/ULK1-4 kinase, Atg17, Atg29 and Atg31. Their assembly on the PAS is independent on the nutrient condition (Suzuki *et al.* 2007, Kabeya *et al.* 2009).

During starvation or treatment with rapamycin, the mammalian target of rapamycin (mTOR) is inhibited. This causes Atg13 dephosphorylation which under these conditions is able to bind to the Atg1 complex.

Subsequently the Atg9 complex is recruited on the PAS. This complex is formed by Atg9 itself (in yeast and mammals) and Atg23 and Atg27, in yeast with no counterpart in mammalian cells. The two proteins are respectively a peripheral membrane protein and a type I integral membrane protein (Tucker *et al.* 2003, Yen *et al.* 2007). Atg9 is the only multispanning membrane protein (Noda et al. 2000) and it is believed that Atg9 supplies the PAS with vesicles for the elongation of the isolation membrane. It was shown in yeast and proposed in mammals that Atg9 shuttles between the PAS and a peripheral pool that appears to be formed by vesicle clusters (Mari *et al.* 2010, Mari and Reggiori 2010, Webber and Tooze 2010). The next step is the recruitment of the Vps34/class III PI3-kinase complex to which other Atg components such as Vps34, Vps15, Vps30/Atg6, and Atg14 belong. This complex is necessary for PIP3 production that acts as a molecular anchor allowing other Atg proteins to be recruited onto the membrane. These PIP3 binding proteins are the so called PROPPINS (β-propeller proteins that bind Phosphoinositides). Two Atg proteins are part of the PROPPINs family, Atg18 and Atg21. Atg18 is an adaptor protein which in complex with Atg2 mediates Atg9 cycles (Krick *et al.* 2012, Busse *et al.* 2013, Thumm *et al.* 2013). Atg21 instead is a member of the cytoplasm to vacuole targeting (Cvt) pathway a selective type of autophagy in yeast used to deliver the hydrolase aminopeptidase I to the vacuole (Lynch-Day and Klionsky 2010).

The core components of the membrane elongation step are the two ubiquitin like proteins Atg12 and Atg8/LC3 (Mizushima *et al.* 2011).

Shortly Atg12 is first attached to Atg7, an E1-like enzyme, then is transferred to the E2-like protein Atg10 which then promotes the conjugation of Atg12 to Atg5, (Mizushima *et al.* 1998). The Atg5-Atg12 complex is subsequently bound to Atg16L1 by direct interaction with Atg5. Atg16L1 promotes oligomerisation of the trimeric complexes allowing the formation of the huge Atg16 complex that is essential for autophagosome progression and maturation (Mizushima *et al.* 2003).

Atg8/LC3 is the second ubiquitin-like protein of the autophagy pathway. LC3 is associated to the autophagosome membrane during each step of autophagosome formation. It has been widely characterized and is used as a canonical autophagosome marker due to its ability to bind to the autophagosome membrane upon starvation (Klionsky *et al*. 2008, Rubinsztein *et al.* 2009). In order to be lipidated, an endopeptidase, namely Atg4, cleaves the C-terminal residues of LC3 in a way that the c-terminal Glycine is exposed (Hemelaar *et al.* 2003). This LC3 is a cytosolic form and it is called LC3-I. Atg7 activates LC3-I and transfers the protein to Atg3 that catalyzes the formation of a covalent bound between LC3-I and phosphatidylethanolamine (PE) and its conversion in LC3-II (Tanida *et al.* 2002). Under these conditions LC3-II acts as an integral component of the autophagosome membrane (Tanida *et al.* 2006).

After the autophagosome maturation the inner membrane-associated LC3-II is degraded by lysosomal proteases. The LC3-II in the outer membrane is released into the cytosolic pool by the action of Atg4 that cleaves the PE from LC3-II converting it into LC3-I that is ready for subsequent lipidation rounds (Tanida *et al.* 2004).

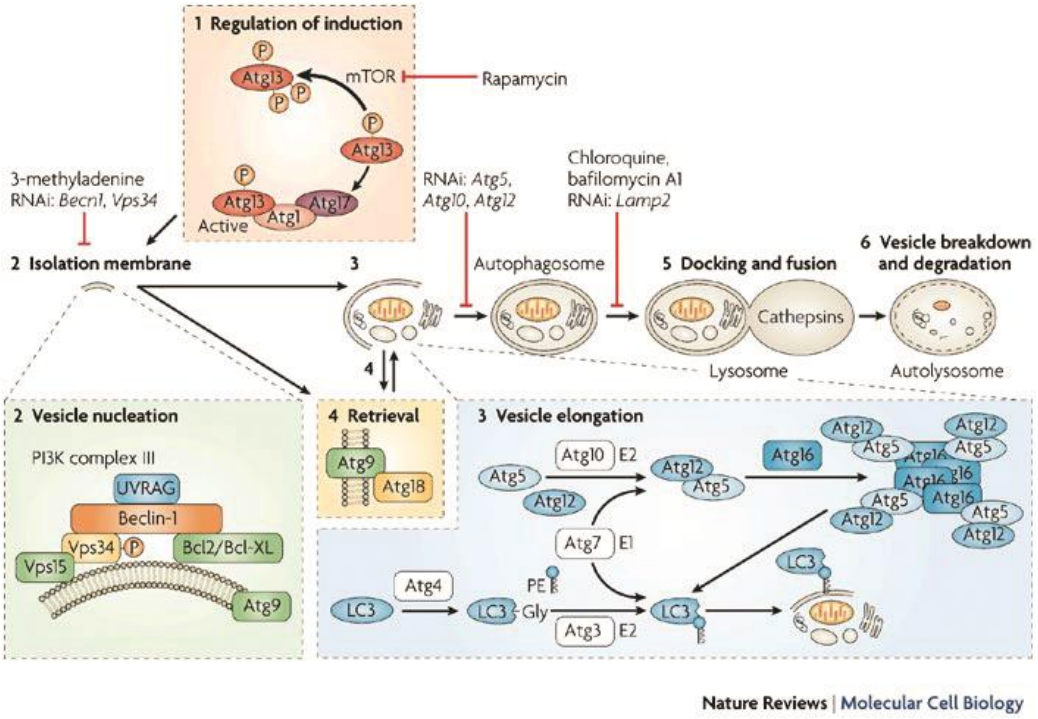

Figure 4 The molecular machinery of the autophagy pathway

Each step of autophagosome formation is driven by a specific set of Atg proteins. Inhibition of mTOR causes phosphorylation of the Atg1 complex that activates the recruitment of the nucleation factors (PI3K complex III) on the isolation membrane (PAS). The Atg9 complex shuttle between the PAS and the vesicle precursors supplying the immature autophagosome with membranes promoting membrane elongation that requires the recruitment of the Atg5-Atg12-Atg16 complex (the ubiquitin-like conjugating system). This complex by activating and recruiting LC3 promotes not only the elongation, but also the enclosure of the autophagosome compartment. After fusion with the lysosome, LC3 is cleaved from the outer membrane by the action of the endopeptidase Atg4 and recycled to the cytosolic pool. Image taken by Maiuri *et al.* (2007).

1.2.4 Cross-talk between autophagy and endosome pathways

Autophagy and endosomes are very close related pathways. They not only share molecular players, but since both are catabolic machinery, they both fuse with lysosome. They converge at a certain point in their pathway forming a hybrid compartment called amphisome derived from the fusion between autophagosome and LE/MVB (Berg *et al.* 1998, Fader *et al.* 2008) (Figure 3).

A number of molecular players are involved in the proper progression during autophagosome maturation which includes the small GTPase Rab proteins and the SNAREs.

SNARE proteins, the minimal machinery for membrane fusion (Jahn and Scheller 2006, Jahn and Fasshauer 2012), assist the fusion steps between endosomes and autophagosomes. An increased numbers of studies demonstrate the importance of SNAREs in the autophagy pathway. They mediate fusion with LE/MVB (Fader and Colombo 2009, Fader *et al.* 2009) and with the lysosome (Renna *et al.* 2011). Syntaxin-17 was recently shown to be a resident autophagosomal membrane SNARE protein that assists autophagosome biogenesis and maturation (Itakura *et al.* 2012, Hamasaki *et al.* 2013, Takats *et al.* 2013)

The small GTPases Rab proteins are also essential factors in driving the autophagosome towards the endosome-lysosome pathway (Chua *et al.* 2011) with the help of their regulators and effector proteins. They are present at the level of each step of autophagosome biogenesis, formation and maturation. For example Rab1 and Rab33 are thought to be involved in the early stage supplying the growing isolation membrane with precursors membranes coming either from ER (Lamb *et al.* 2013) or Golgi (Itoh *et al.* 2008). Rab7 was shown to be crucial for autophagosome maturation (Hyttinen *et al.* 2013). It is required for fusion of late endosomes with the autophagosome (Gutierrez *et al.* 2004, Jager *et al.* 2004). A direct connection between Rab7 and the autophagosome is the newly discovered FYCO protein that contains a FYVE domain as well as coiled coil domain. This protein acts as a Rab7 effector and a LC3-interacting protein (Pankiv *et al.* 2010).

1.3 An overview on the small GTPase Rab proteins

In my study I investigated the role of the small GTPase Rab26 and its involvement in synaptic function. As mentioned above Rab proteins play an important function in the regulation of intracellular membrane trafficking.
Of particular interest for my studies was the implication of Rab26 in presynaptic protein turnover by looking at less investigated degradative pathways: ubiquitin-based endosomal degradation and the autophagosome/lysosome pathway for pre-synaptic proteins.
Below I will give an overview on how the small GTPases work at the molecular level and how they are spatially and temporally regulated with a special emphasis on neuronal Rab proteins and Rab26.

1.3.1 Rab proteins

Rab26 is a member of the Rab proteins the biggest subgroup of the Ras superfamily (Stenmark and Olkkonen 2001, Hutagalung and Novick 2011). The Ras protein family is composed of more than 170 members (Colicelli 2004). According to functional and structural similarities they are subdivided in at least five different Ras-like GTPase subfamilies: Ras, Rho, Rab, Arf/Sar1 and Ran. They are highly conserved among all eukaryotes and are involved in different aspects of cellular physiology: gene expression is often regulated by Ras proteins. Cytoskeleton organization requires the Rho family. Necleo-cytoplasmic import-export is driven by the Ran proteins. Vesicle transport is mediated by both Arf and Rab proteins (Stenmark and Olkkonen 2001, Wennerberg *et al.* 2005).
The first Rab protein identified was the yeast Ypt1p. It was categorized as a yeast homologue of Ras like-proteins with uncharacterized function (Gallwitz *et al.* 1983). Subsequent analysis carried out by Schmidt et al. in (1986) and (1988) showed that Ypt1p is an essential yeast protein that is involved in microtubule organization and modulate intracellular calcium concentration. The involvement of Rab proteins in membrane trafficking was first observed by a yeast genetic screen that allow the identification of several temperature sensitive (*ts*) yeast (sec) mutants that cause accumulation of secretory vesicles in the cytoplasm (Novick and Schekman 1979, Novick *et al.* 1980, Waters and Pfeffer 1999).

These mutants block the secretory pathway. Sec4p was the first Rab protein to be identified as close relative to Ras-like proteins involved in vesicle secretion. The *ts sec4* was observed to block the secretory vesicle pathway at the exit site between Golgi and the membrane surface (Salminen and Novick 1987, Waters and Pfeffer 1999).

When the first Rab proteins where discovered, their function was mainly restricted to tethering of secretory vesicles (Salminen and Novick 1987). In the last 30 years from the discovery of the first Rab proteins, the role of these small GTPases have been extensively studied and it was found that they are not only implicated in vesicle tethering, but also involved in different aspects of intracellular membrane trafficking, from exocytosis and endocytosis, to more specialized types of membrane trafficking such as the autophagy pathway (1.2.2). They are involved in cargo selection, vesicle formation, tethering, docking and membrane identity definition (Hutagalung and Novick 2011). Their versatility is dependent on their ability to recruit different effector proteins (Grosshans *et al.* 2006) that aid them in most of their different cellular functions: in the endocytic pathway, in degradative processes and in several neuronal function (Ng and Tang 2008, Stenmark 2009, Hutagalung and Novick 2011).

The Rab subfamily is composed of more than 70 members (around 11 in yeast and more than 60 in humans), that are subdivided according their function and structural similarities (see Figure 5A). At least one member of each group has a crystal structure solved in their GTP or GDP states allowing a general overview in their "modus operandi". They have a common and conserved primary structures (Pfeffer 2005, Brighouse *et al.* 2010) (Figure 5B). The Rab family domain (RabF) is the GTPase domain which in the ternary structure corresponds to the "swich region" that is formed by 6 β-strands and 5 α- helices. This motif includes the switch I and II regions the nucleotide binding site. The GTPase domain is present in all Rab members (Figure 5 grey box). Within each subgroup of Rabs a conserved sequences is observed: the Rab subfamily domain (RabSF showed in Figure 5 with black boxes). These motifs are located upstream and downstream of the GTPase domain and represent the regions where the effector proteins bind. The C-terminal portion is the hypervariable region that is specific to each Rab proteins. The last 2 cysteine residues (cc) are postraslationally modified by the attachment of two geranylgeranyl anchors essential for the membrane insertion of Rabs after their activation.

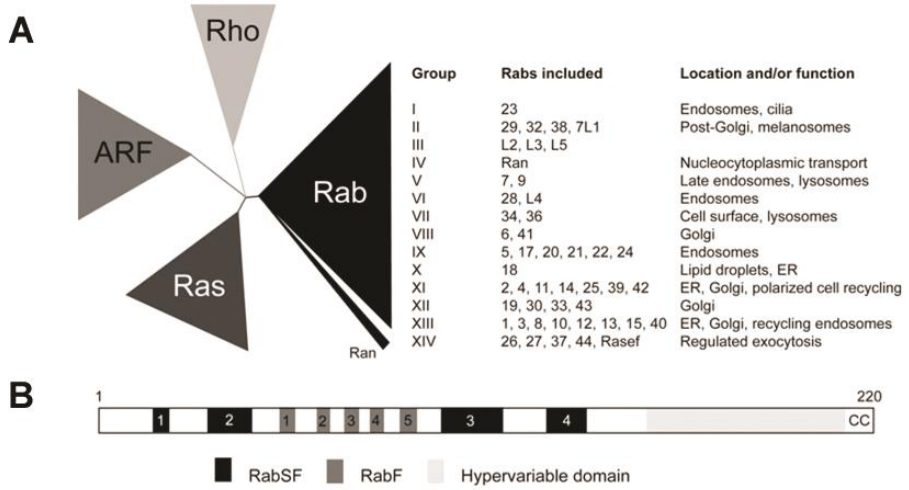

Figure 5 Schematic representation of Ras superfamily

(A) Rab proteins are the largest group of the small GTPases. They are clustered in several subfamilies according to their sequence and functional similarities. In (**B**) the primary structures that define the Rab domains are shown: RabF corresponds to the domain common to all the Rab family members; RabSF is the domain conserved within the Rab subfamilies. The C-terminal portion is the hypervariable region and is specific for each Rab proteins. At the very end of the sequence two cysteine residues (CC) are highlighted: they are the amino acids that are geranylgeranylated. Figure modified from Brighouse *et al.* (2010).

1.3.1.1 The Rab cycle and membrane association and dissociation

Rab proteins as all the small GTPase have an intrinsic ability to hydrolyze GTP in GDP + Pi. The switch on/off states corresponds to the activation/inactivation state of Rabs and it is an essential mechanism that controls not only spatially but also temporally the function of these small GTPases. The kinetics of the nucleotide-dependent cycle are finely regulated and accelerated by specific proteins (Cherfils and Zeghouf 2013): GTPase exchange factors (GEFs), GTPase activating proteins (GAPs) (Goody *et al.* 2005) and GDP dissociator inhibitors (GDIs) that control Rab membrane association dissociation (Pfeffer and Aivazian 2004, Goody *et al.* 2005). Therefore in order to understand membrane traffic it is essential to apprehend the mechanism of action of the small GTPase cycle.

The intrinsically low ability to hydrolyze GTP in GDP + Pi, is accelerated by the regulator proteins GTPase-activating proteins (GAPs) (Barr and Lambright 2010). RabGAP proteins have a common domain called TBC1 (Tre-2/Cdc16/Bub2) that it was first identified in yeast in a genetic screen (Strom *et al.* 1993, Du *et al.* 1998, Albert and Gallwitz 1999).

With a mechanism similar to RasGAPs the TBC1 domain has the so called Arginine/glutamine “fingers” that protrude into the GTPase pocket and stimulate the GTP hydrolysis (Albert *et al.* 1999, Pan *et al.* 2006), converting RabGTP (active form) in

RabGDP (inactive form). GAP proteins are the "inhibitors" of Rab activity. In fact the inability to hydrolysis GTP either by Rab point mutation in the GTPase domain or by loss of function of the specific GAP protein is sufficient to alter the endocytic pathway. An example is given by the constitutive activation of the early endosome marker Rab5. RabGAP-5 depletion induces uncontrolled membrane fusion and formation of large endosome whereas RabGAP-5 overexpression blocks the endocytic pathway (Haas *et al.* 2005).

The activation of Rabs is catalyzed by the GEF proteins that allow the exchange of GDP with GTP. A big numbers of GAP proteins (around 38) were characterized (Fuchs *et al.* 2007, Haas *et al.* 2007) and observed to be specific for the different Rab proteins. On the other hand due to the difficulty of finding conserved and common domains, only a few GEFs were identified leaving a huge numbers of Rab proteins with unknown activating factors (Yoshimura *et al.* 2010, Hutagalung and Novick 2011). The few identified GEFs have unrelated protein structures (Barr and Lambright 2010). Structural analysis revealed that the VPS9 domain of Rabex-5 (Rab5-GEF) shows conserved residues that bind the switch I and II regions and promotes the replacement of GDP with GTP (Delprato *et al.* 2004). Elegant experiments performed by Gerondopoulos *et al.* (2012) and by Blumer *et al.* (2013) showed how GEFs alone are able to target specific Rab proteins on the specific membranes.

It is the cooperative role of GEF and GAP proteins that defines the spatial and temporal regulation of Rab function within the cells and on the specific membrane domains (Wennerberg *et al.* 2005). Once Rabs are activated, they are able to recruit specific effector proteins on their target sites initiating therefore the specific signal.

The active form of Rab proteins (RabGTP form) is membrane bound whereas the RabGDP form is generally cytosolic. The association to the membrane is GTP dependent and is possible due to the presence of a lipid anchor, the geranylgeranyl motif.

Newly synthesized Rab proteins similarly to many Ras family members bind to GDP and undergo post translational modifications. Rab escort proteins (REPs), factors restricted only to Rab families, form a complex with RabGDP that is recognized by the prenylating enzyme geranylgeranyltransferase (GGTase) that attaches covalently two geranylgeranyl motifs to the last two cysteine residues of the small GTPase. REPs act on Rab proteins till the small GTPase is associated to the specific membrane but they are not involved in the membrane association-dissociation cycle of Rabs. The retrieval of Rabs from the membrane is accomplished by RabGDI which keeps Rab inactive in the soluble pool

(Goody *et al.* 2005, Wu *et al.* 2010). It is well studied how RabGDI removes Rab proteins from the membrane (Ignatev *et al.* 2008). RabGDI binds preferentially to the prenylated GDP form of Rab proteins. (Sanford *et al.* 1995, Wu *et al.* 2010). Sasaki *et al.* (1990) identified and purified from bovine brain cytosol a protein that inhibited the dissociation of GDP (called GDI) from a Ras-like protein. Garrett *et al.* (1994) showed that yeast GDI proteins regulate the membrane association of Sec4 and depletion of this regulator inhibits dissociation of Sec4 from the membrane and loss of the Sec4 cytosolic pool. RabGDIs therefore not only extract Rab proteins from the membrane, but are crucial for the correct balance of the Rab cycles and therefore for vesicle trafficking. For a subsequent round of membrane cycle, Rab proteins are displaced from RabGDI by the GDI-displacement factor (GDF) (Sivars *et al.* 2003) with a still not completely understood mechanism. Rab proteins are transported to the membrane where the specific GEF proteins are located. GEFs catalyze the displacement of GDP with GTP thereby activating Rab that is now able to initiate the signal by recruiting specific effectors for the specific function for which the small GTPases are responsible. The GAPs inactivate Rab proteins by stimulating the GTP hydrolysis. Now RabGDI is able to extract RabGDP from the membrane to the cytosol pools and the cycle can reinitiate. In Figure 6 is depicted the mechanism of Rab cycle.

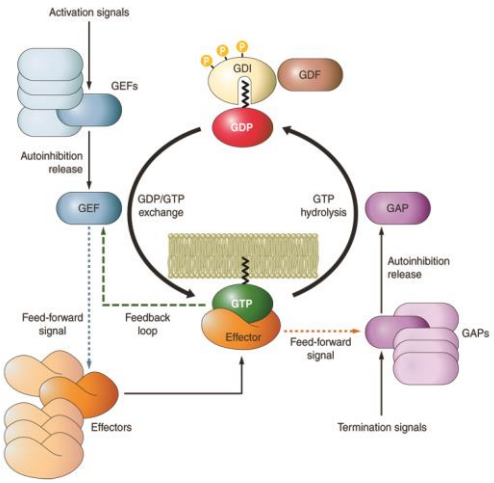

Figure 6 Rab GTPase cycle

Schematic representation of Rab nucleotide and membrane association-dissociation cycle (Cherfils and Zeghouf 2013)

1.3.2 Rab26 and the neuronal secretory Rab proteins

Our group identified several Rab proteins that are differentially enriched in highly purified synaptic vesicles isolated from rat brain homogenates (Pavlos *et al.* 2010) suggesting that many Rabs are involved in controlling not only the synaptic vesicle cycle but more in general are involved in different aspects of neuronal activity (Ng and Tang 2008). Proteomic study showed that the small GTPase Rab26 was found in the purified synaptic vesicle fraction (Takamori *et al.* 2006). Biochemical analysis supported that indeed Rab26 was highly enriched in the isolated synaptic vesicle fraction (Nathan Pavlos, unpublished data). The observation of Rab26 being highly enriched in the SV fraction motivated us to investigate more deeply the role of Rab26 in synapse.

Rab26 is a poorly characterized Rab protein and is a close relative to the secretory small GTPase Rab37 (Masuda *et al.* 2000). It was first grouped as a member of the Rab3 family together with Rab27 and classified as a secretory Rab protein with RIM being its potential effector protein (Fukuda 2003, Fukuda 2008). Rab26 was first observed in tissues where the secretion is tightly regulated such as brain, kidney and pancreas by in-situ hybridization using Rab3a as a probe (Wagner *et al.* 1995). Subsequent findings proved that the human Rab26 was preferentially and highly expressed in brain areas, such as amygdala, cerebellum and hippocampus (Seki *et al.* 2000). Indirect evidence suggests an involvement of Rab26 in the regulation of exocrine granule maturation and cell surface localization of membrane receptors. (Tian *et al.* 2010, Li *et al.* 2012). Jin and Mills (2014) showed for the first time Rab26 as a novel lysosomal associated protein.
Rab26 was proposed to be a Rab3a homologue and predicted to regulate synaptic vesicles exocytosis (Wagner *et al.* 1995). The neuronal exocytosis machinery is modulated by the two well investigated neuronal Rab proteins: Rab3s and Rab27s.

Rab3 has four isoforms Rab3A, B C and D. Rab3D is the non-neuronal Rab3 isoform, is known to be highly expressed in osteoclasts and is involved in bone growth (Pavlos *et al.* 2005). Rab3abc are the most abundant small GTPases in neurons and are highly enriched in SV fraction (Pavlos *et al.* 2010). Around ten Rab3 proteins were calculated to be associated to the membrane of one synaptic vesicle (Takamori *et al.* 2006). Rab3s are amongst the most investigated small GTPases. They are known to modulate neurotransmitter release, but unexpectedly it was the Rab3GEF KO that was showing a strong reduction in synaptic vesicle release when compared to the quadruple KO of all four

Rab3s (only 30% reduction) (Schluter *et al.* 2004). The same effect was observed in the *C. elegance* Rab3 homologue where the GEF (Aex-3) causes the major transmission defect (Iwasaki *et al.* 1997, Nonet *et al.* 1997).

Rab27 is present in two different isoforms, Rab27A and Rab27B that differ at the functional level and in their intracellular distribution (Ostrowski *et al.* 2010). Rab27A is highly expressed outside of the central nervous system (CNS). Rab27B is the second most abundant small GTPase in the brain. It is shown to be involved in the modulation of synaptic vesicle endo/exocytosis and neurotransmitter release. It shares several common features with Rab3 such as sequence similarity and localization on the secretary vesicles. Furthermore it is regulated by the same Rab3GEF in mammals and Aex-3 in *C-elegans* (Mahoney *et al.* 2006). Rab3s and Rab27 also share common effector proteins such as Rabphillin (Fukuda 2003, Fukuda 2008). In addition it was recently shown that Rab27B is also required for synaptic vesicle recycling in a Ca^{2+} dependent manner (Pavlos *et al.* 2010). In fact upon Rab27 depletion or expression of Rab27 GTP/GDP locked mutants the recycling mechanism of synaptic vesicles is impaired (Mahoney *et al.* 2006, Pavlos *et al.* 2010). Contrary to Rab3 which cycles between the cytosolic pool and the membrane bound state during the synaptic vesicle cycle, Rab27B remains tightly associated to the membrane during all stages of the SV cycle. Rab27B seems to be resistant to GDI extraction in its GDP form. Strikingly structural studies showed that the GDP form of Rab27 undergoes homodimerization suggesting the existence of Rab27GDP as an inactive homodimer (Chavas *et al.* 2007, Pavlos *et al.* 2010).

As a mentioned above in section 1.3.1 Rab proteins act at the level of vesicle formation, budding, transport, tethering and docking. They function in concert with their effector proteins. The most studied neuronal Rab effectors are Rabphilins and RIMs. Rabphilin acts as a Rab3 and Rab27 effector; whereas RIMs are only Rab3 effectors. Therefore their roles reflect the function of their specific Rab GTPase in their GTP configuration. Rabphilins are cytosolic proteins and are recruited to the plasma membrane by Rab3. Their function appears to be strictly linked to the Rab3 cycle. Their function is still unclear since Rabphilin KO mice do not show any obvious synaptic dysfunctions (Schluter *et al.* 1999). RIMs are members of the presynaptic protein complex that builds the active zone (AZ). All the AZ proteins are essential for correct synaptic vesicle exocytosis. The AZ is composed by the RIM complex that includes: Munc13, Piccolo, Bassoon, ELKS and α-Liprin (Chua

et al. 2010). Contrary to Rabphilins, RIMs appear to be essential for long term potentiation (Kaeser and Sudhof 2005), but the absence of the RIM gene does not cause any alteration in the number and quality of the docked synaptic vesicles (Koushika *et al.* 2001).

Though it was reported that RIM was interacting directly also with Rab26 (Fukuda 2003), a surprising preliminary experiments performed by Nathan Pavlos revealed that overexpression of Rab26 in neurons gave an exciting and interesting phenotype that distanced Rab26 from the expected exocytosis towards an unknown synaptic autophagy pathway.

2 Results

2.1 Rab26 is a neuronal small GTPase

Several studies reported how Rab proteins and their regulators and effectors are implicated in the modulation of the different steps of the synaptic vesicle pathway (Ng and Tang 2008). For example in our lab Pavlos *et al.* (2010) revealed that many Rab proteins are found to be enriched or differentially represented in neurons together with the most well-known synaptic Rab proteins Rab3 and Rab27. Amongst them we found enrichment of the small GTPase Rab26 in synaptic vesicles isolated from rat brain homogenate (for protocol see section 4.2.3.4). Therefore in a first experiment I wanted to clarify if Rab26 is associated on the synaptic vesicle membranes using as a sample the different subcellular fractions of rat brain and checking the enrichment profile by western blotting.

The enrichment of Rab26 and Synaptophysin in highly purified vesicles is represented in Figure 7A (lane SV). Very low signal could be detected in the nuclear fraction (P1), in the post nuclear supernatant (S1), in the cytosolic fraction (S2 and S3), in the synaptosome fraction (P2) and in the presynaptic membranes (LP1). The level of Rab26 was considerably higher in the crude synaptic vesicles (LP2) and highly enriched in the pure synaptic vesicle (SV) fractions. The well-known synaptic vesicle marker Synaptophysin showed a comparable pattern of enrichment though its signal in the SV fraction was significantly higher.

Next I analyzed if Rab26 was directly associated to the synaptic vesicle membrane and if so whether these vesicles would be a subpopulation with characteristic morphology. In order to investigate this hypothesis, I made use of the immunoisolation (II) assay, a very powerful technique that allows the isolation of specific organelles and therefore the analysis of their membrane-protein composition.

For this purpose the crude synaptic vesicle fractions (LP2) were re-suspended in immunoisolation buffer (for protocol see chapter 4.2.3.6) and incubated with immunobeads (Eupergit C1Z methacrylate microbeads) coupled either to monoclonal Synaptophysin (7.2) antibody or to monoclonal Rab26 (163E12) antibody. The beads were then washed extensively and eluted with loading dye. The vesicle composition was analyzed by Western blot (Figure 7B).

Excitingly the Rab26 antibody was pulling down a subset of Synaptophysin positive vesicles, whereas Synaptophysin was able to immunoisolate almost all the Rab26 positive vesicles. This can be seen comparing the II and SN lanes for Rab26 (left) and for Synaptophysin (right). In parallel immunoprecipitation (IP) was performed using the same conditions with the only difference of the addition of Triton X-100 (Tx). Triton as expected solubilized the membranes and in the presence of Tx both Rab26 and Synaptophysin were detected only in the supernatant fraction and not in the IP. This suggested that the two proteins are on the same vesicles and that they do not interact directly.

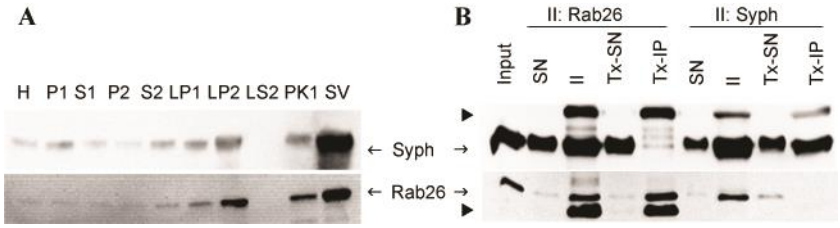

Figure 7 Rab26 is a synaptic vesicle protein

(A) Rab26 is enriched in the pure SV fraction. Synaptophysin was used as a synaptic vesicle marker. The blot represents the subcellular fractionation of rat brain homogenate. **(B)** Rab26 and Synaptophysin reside on the same vesicle membrane. SN, supernatant; II, Immunoisolation, Tx, Triton-x-100; IP, immunoprecipitation. LP2 was used as starting material. Arrows indicate the Rab26 and Synaptophysin bands. Arrowheads show the antibody light or the heavy chain bands. Immunoisolation was performed by Janina Boyken. The monoclonal anti-Rab26 and anti Syph antibodies used in this study are from Synaptic System.

Once clarified that Rab26 was associated with the synaptic vesicle membrane, in a next step I investigated if there was any difference in morphology between Rab26 and Synaptophysin vesicles. For this purpose I decided to use electron microscopy.

Immunoisolated Rab26- and Synaptophysin-positive vesicles were subjected to electron microscopy analysis. After data processing, the two sets of images were compared (Figure 8A). Very few vesicles per beads were immunoisolated in the Rab26 immunobeads compared to the Synaptophysin sample that showed a large number of coupled particles. Further analysis pointed out that the two populations were not different in terms of size and morphology. In fact vesicles size distribution was analyzed by measuring the diameters of particles coupled to the beads (Figure 8B and C).

Around 300-400 vesicles were counted and the size average was calculated (Figure 8C). The values were plotted in a graph (Figure 8B). No obvious differences could be observed in the vesicle size between Synaptophysin (in brown line) and Rab26 (in green line). Both showed a similar size profile with a peak at a synaptic vesicle diameter of 40-45 nm. To control the quality of the immunoisolation, the isolated vesicles against Rab26 and Synaptophysin were compared with the IgG negative control and analyzed by WB (Figure 8D). Immunoisolation of synaptic vesicles was only efficient in presence of either anti Rab26 or anti Synaptophysin antibodies but not with IgG coupled beads.

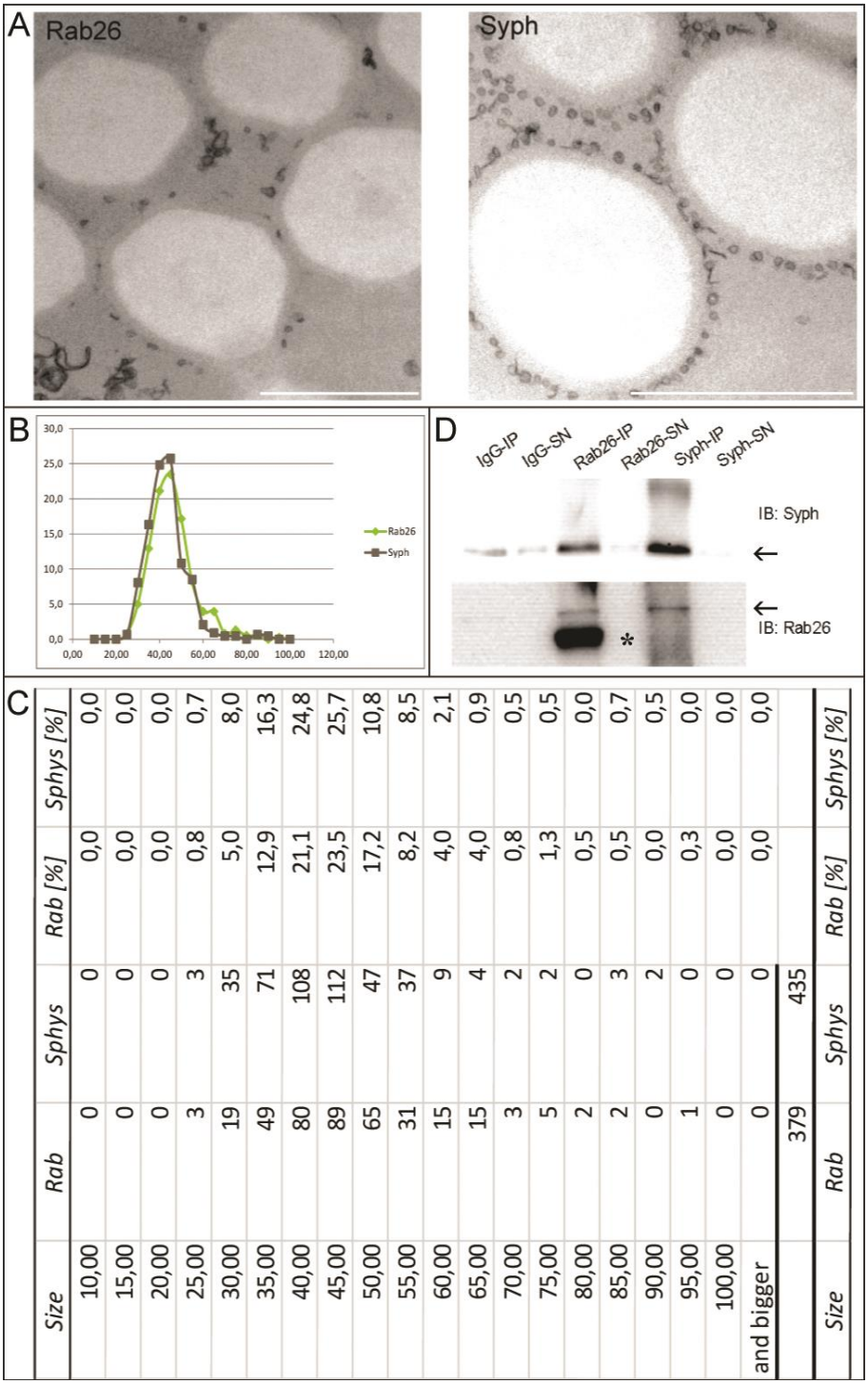

Size	Rab	Sphys	Rab [%]	Sphys [%]	Rab	Sphys	Rab [%]	Sphys [%]
10,00	0	0	0,0	0,0				
15,00	0	0	0,0	0,0				
20,00	0	0	0,0	0,0				
25,00	3	3	0,8	0,7				
30,00	19	35	5,0	8,0				
35,00	49	71	12,9	16,3				
40,00	80	108	21,1	24,8				
45,00	89	112	23,5	25,7				
50,00	65	47	17,2	10,8				
55,00	31	37	8,2	8,5				
60,00	15	9	4,0	2,1				
65,00	15	4	4,0	0,9				
70,00	3	2	0,8	0,5				
75,00	5	2	1,3	0,5				
80,00	2	0	0,5	0,0				
85,00	2	3	0,5	0,7				
90,00	0	2	0,0	0,5				
95,00	1	0	0,3	0,0				
100,00	0	0	0,0	0,0				
and bigger	0	0	0,0	0,0				
	379	435						

Figure 8 Size distribution of Rab26 positive vesicles

(A) Rab26 positive vesicles appear to be a subpopulation of SVs, scale bar, 1 µm. **(B)** The graph represents the size distribution of Rab26 positive vesicles in green and Synaptophysin positive vesicles in grey. In both case the size average is 40 nm as expected for SVs. **(C)** The table below is the summary of the counted vesicle diameters used for plotting the size distribution profile both for Rab26 and for Synaptophysin, Syph. Figure **(D)** Represents a WB of Rab26 and Synaptophysin coupled beads after the immunoisolation compared with the IgG beads. Arrows indicate respectively the Syph band and the Rab26 band. The asterisk represents the light chain of the antibody used for the immunoisolation. Electron microscopy and quantification analysis was performed by Dietmar Riedel.

2.1.1 Rab26 is a SV protein

I decided to use immunocytochemistry to confirm the hypothesis that Rab26 is not only a neuronal small GTPase, but also colocalizes with synaptic vesicle markers.

Brain tissue sections of 2 years old mice were stained with the monoclonal anti Rab26 antibody in combination with a neuronal nuclei marker (NeuN, a neuronal transcription factor) and with DAPI a general nuclear dye. Rab26 (in green), and NeuN (in red), are coexpressed in the same cell types as shown in the magnified area at the right side. The arrow and the arrowhead highlight the neuronal and the non-neuronal cells respectively (Figure 9A).

Dissociated hippocampal neurons were co-labeled with monoclonal Rab26 antibody (green) and with the monoclonal Synaptotagmin I antibody (red) (Figure 9B). This experiment confirmed the results obtained by immunoisolation as described in paragraph 2.1. In fact a subset of Synaptotagmin positive puncta was colocalizing with Rab26 puncta. The region within the white rectangular box is magnified next to the picture and highlights the cell body and the proximal regions of the neuronal cell. The arrows indicate the co-localization. The *in vivo* data support the hypothesis that Rab26 is expressed in neurons and has a punctate-like pattern that marks a subset of synaptic vesicles.

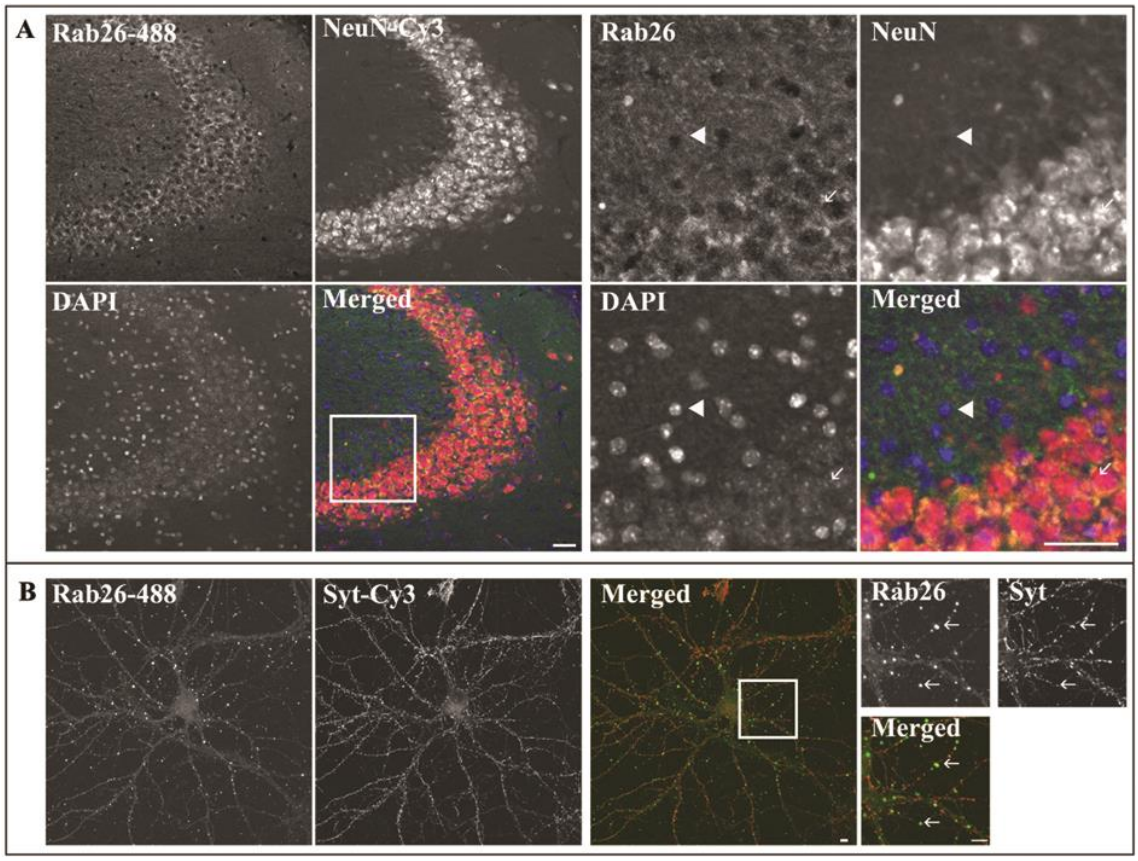

Figure 9 Rab26 is a neuronal Rab protein

(**A**) Rab26 is expressed in the same cells as the neuronal marker NeuN (arrow) but not in other cell types indicated by the single stain of DAPI (arrowhead). Brain sections of 2 years old mice. The stain was performed by Sigrid Schmidt. **(B)** Endogenous Rab26 shows a punctate pattern that colocalizes with a subset of Synaptotagmin1 (arrows). Dissociated rat hippocampal neurons were used on day 16 in vitro (DIV 16). Anti-mouse Rab26 was observed with Alexafoluor-488, green; anti-rabbit Syt, Synaptotagmin-1was visualized with Cy3, red; nucleus with DAPI, blue.

2.2 Overexpression of Rab26 results in cluster formation

2.2.1 The GFP tag influences the Rab26 phenotype

Single point mutations in the nucleotide binding region of Rab proteins that cause defects in their membrane-cytosol cycle are well established (as an example see Li and Stahl (1993)). The constitutively active form (GTP bound) is called GTP-locked conformation. This substitution does not allow the small GTPases to hydrolyze GTP therefore they are in an active configuration and always associated to the membrane. The dominant negative form, (GDP-form) is referred also as the GDP-locked form. Under this condition Rab proteins are found mainly in the cytosolic pool.

By the alignment with mouse Rab37 (the closest homologue of Rab26) for which these mutations are reported (Masuda *et al.* 2000), it was possible to identify the amino acid residues whose substitutions create the constitutively active (CA, Q123L) and dominant negative (DN, T77N and N177I) forms of Rab26.

The most common and well established method to study the intracellular distribution and functions of Rab proteins is the use of the green fluorescent protein (GFP) (Sonnichsen *et al.* 2000) or other smaller tags such as Flag. To use the most suitable tag the phenotypes of the differentially labeled Rab26 proteins and the mutants were compared in neurons and in a heterologous system such as HeLa cells with the endogenous distribution or overexpression of the untagged protein visualized with the help of specific antibody.

The differently tagged Rab26 versions (EGFP, mGFP, Flag-, and untagged variants) were transiently transfected in HeLa cells to observe their expression profile. As it can be seen in Figure 10A EGFP-Rab26 WT, QL, and TN (lane 1), Flag-Rab26 WT, QL, and TN (lane 2), and the untagged variants (lane 3), expressed the proteins in a comparable way. The DN form shows very low expression level in a tag independent manner.

Next I analyzed the behavior of the different tags by immunocytochemistry. HeLa cells were transiently transfected making use of the commercially available reagent, Lipofectamine 2000 (Invitrogen). The intracellular distribution of Rab26 was comparable between the different tags but the morphology of the Rab26 puncta and the time required for their formation was notably different. The GFP variants provoked the formation of huge puncta after only 24 hours of overexpression. The Flag- and the untagged version instead caused significant puncta formation starting from 48 hours of overexpression.

These observations suggested that the puncta generation caused by Rab26 overexpression was enhanced by the presence of GFP (Figure 10B). This effect could be observed both for EGFP and mGFP. EGFP differs from mGFP by only a single point mutation (A206K) that renders EGFP monomeric (mGFP). Therefore the weak self-dimerization property of EGFP might explain the observed big puncta formation.

Next the two different GFP tagged Rab26 were compared. Generally once the small GTPases are bound to GTP, they are recruited on the specific membrane targets, and inserted in the membrane bilayer by their geranylgeranyl motif, a posttranslational modification that requires a specific enzyme called geranylgeranyltransferase (GGTase) (for details see section 1.3.1.1). To investigate if the two variants of GFP-Rab26WT were membrane associated a differential centrifugation experiments was performed. Figure 10C highlights how EGFP- and mGFP-Rab26 were found both in the cytosolic and in the membrane fractions. P1 and P2 are the heavy membrane fractions which correspond to nuclei and mitochondria. Mitofilin, a mitochondrial inner membrane protein, was used to visualize the mitochondria membrane fraction. Vesicles such as early endosomes, lysosomes, and autophagosomes can be found in the P3 fraction. Here LC3B was used as the autophagosome marker. EGFP alone was mainly found in the soluble fraction, and in the post nuclear supernatant (PNS), S2, and in S3. mGFP-Rab26WT and EGFP-Rab26WT behaved in similar way in HeLa and we decided to proceed using the EGFP-Rab26 variants to investigate the subcellular localization of the recombinant Rab26 in neurons.

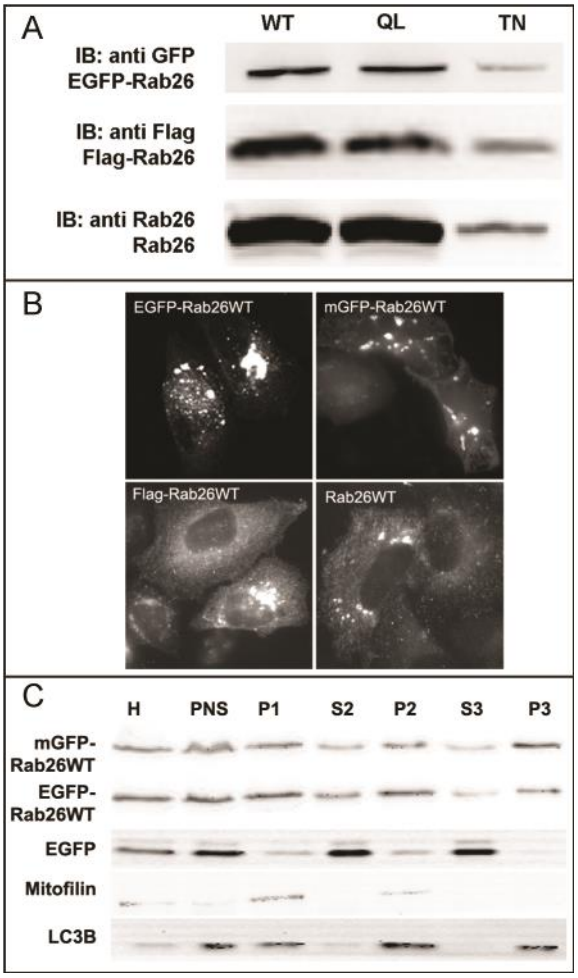

Figure 10 GFP-tag enhances Rab26 phenotype

(A) Expression level of the different Rab26 variants. Rab26WT and QL are showing comparable expression level. Rab26TN instead appears to have lower expression in a tag independent manner. **(B)** Transient expression of the different Rab26WT variants. EGFP- and mGFP-Rab26WT form huge puncta around the perinuclear regions after 24 hrs overexpression. Flag-Rab26WT and untagged Rab26WT show a more reduced phenotype with puncta appearing after 48 hours transfection. **(C)** Differential centrifugation of HeLa extracts transiently expressing EGFP-/mGFP-Rab26WT or EGFP alone. The two Rab26WT variants are preferentially found in the membrane fraction indicated by the upper label (P1, P2, and P3). EGFP was used as a negative control, and is preferentially in the soluble fractions (PNS, post nuclear supernatant; S2 and S3). Mitofilin, a mitochondrial inner membrane protein, was observed in P1 and P2 the autophagosomal protein LC3 in P1, P2, and P3. Both proteins were used as a membrane bound marker respectively for mitochondria and autophagosome membranes.

Subsequently we used the different EGFP-Rab26 mutants to characterize their phenotype in dissociated hippocampal neurons. We were expecting to see puncta like structures similar to the phenotype observed at the endogenous level in neurons (Figure 9B).

The overexpression of the EGFP-Rab26WT, QL, and TN/NI in cultured neurons showed a surprising phenotype. Interestingly EGFP-Rab26WT formed large and bright clusters around the perinuclear regions and on the entire length of the neurites. Unexpectedly the QL was showing moderate punctate structures localized preferentially at the neuronal branches. The proximal and the perinuclear regions instead showed intense and diffuse distribution. The DN forms (EGFP-Rab26TN and NI) of Rab26 appear diffuse having occasional puncta in close proximity of the cell body (Figure 11A). When compared with the endogenous distribution (Figure 9B) the EGFP-Rab26WTpuncta are again more numerous and their size is considerably increased.

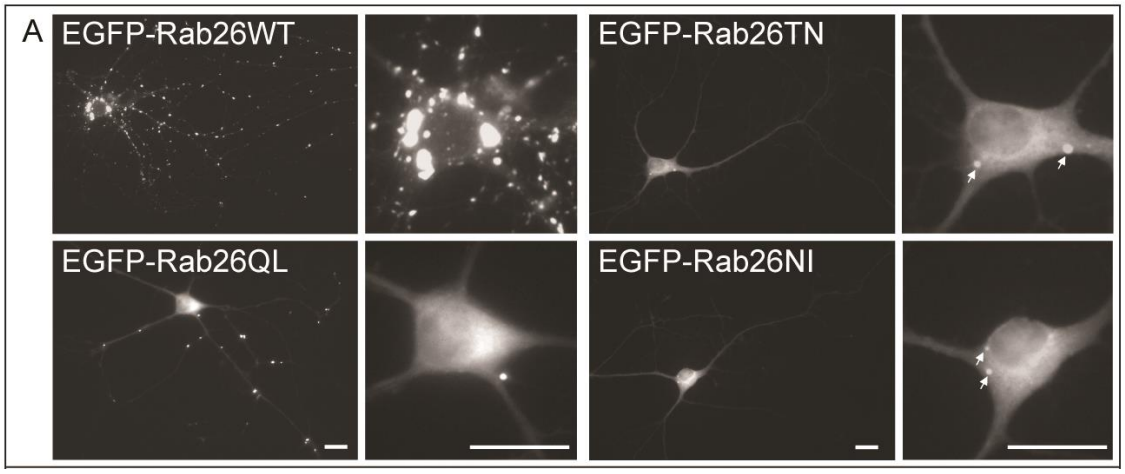

Figure 11 EGFP-Rab26 causes huge puncta structures in neurons

(A) Overexpression of EGFP-Rab26WT is responsible for huge puncta formation. The constitutively active form (EGFP-Rab26QL) shows a reduced phenotype and the dominant negative forms (EGFP-Rab26TN/NI) appear diffuse with small puncta distributed in the cytosol (arrows). The rat hippocampal neurons were fixed at DIV7 , scale bar 10 µm. Figures are given by Nathan Pavlos (data not published).

2.2.2 Rab26 clusters SV proteins in neurons

Given its strong phenotype, EGFP-Rab26WT was used to investigate the intracellular distribution of Rab26 relative to a variety of different endomembrane markers in neurons. We expected to see -similar to endogenous Rab26 - that EGFP-Rab26WT labels synaptic vesicles. Indeed it was exciting to observed that those huge and bright puncta described in the previous paragraph were preferentially colocalizing with synaptic vesicle markers such as Synaptobrevin, Synaptophysin, Synaptotagmin I and Rab3a both in the soma (Figure 12A) and in the axons (Figure 12B) but not with EEA1, an early endosomal marker. The linescans next to each figure represent the colocalization profile. In addition coexpression of EGFP-Rab26WT with the neuropeptide RFP-NPY caused huge clusters of NPY in the cell body and in the axon that colocalize with EGFP-Rab26WT (Figure 12A and B).

No other intracellular organelles were affected in their morphology or distribution upon EGFP-Rab26WT overexpression, but some of the organelle markers showed significant colocalization (Figure 13). More in detail it can be seen that Rab26 did not colocalize with EEA1 and Transferrin (Tnf) suggesting no involvement with early endosomes or the recycling pool (Figure 13A and B). Rab26 did not disrupt the Golgi apparatus as visualized by the GM130 protein (Figure 13E) and the distribution of the late endosomal SNARE Vti1b was not affected (Figure 13F**)**. On the other hand EGFP-Rab26WT seemed to reside in part on the lysosome membrane labeled with LAMP2 a lysosomal receptor protein (Figure 13**C**), suggesting that Rab26 is associated at some point with the lysosome compartment. In addition SNARE proteins that are involved in vesicle maturation (VAMP4 and Sytaxin-6) were partially affected by the EGFP-Rab26WT overexpression. Linescans show a partial colocalization (Figure 13G, H**)**. In addition Rab26-positive structures contained the neuropeptide Secretogranin II (SgII) (Figure 13 I), suggesting the view that the Rab26-induced clusters include not only SVs but also large dense core vesicles.

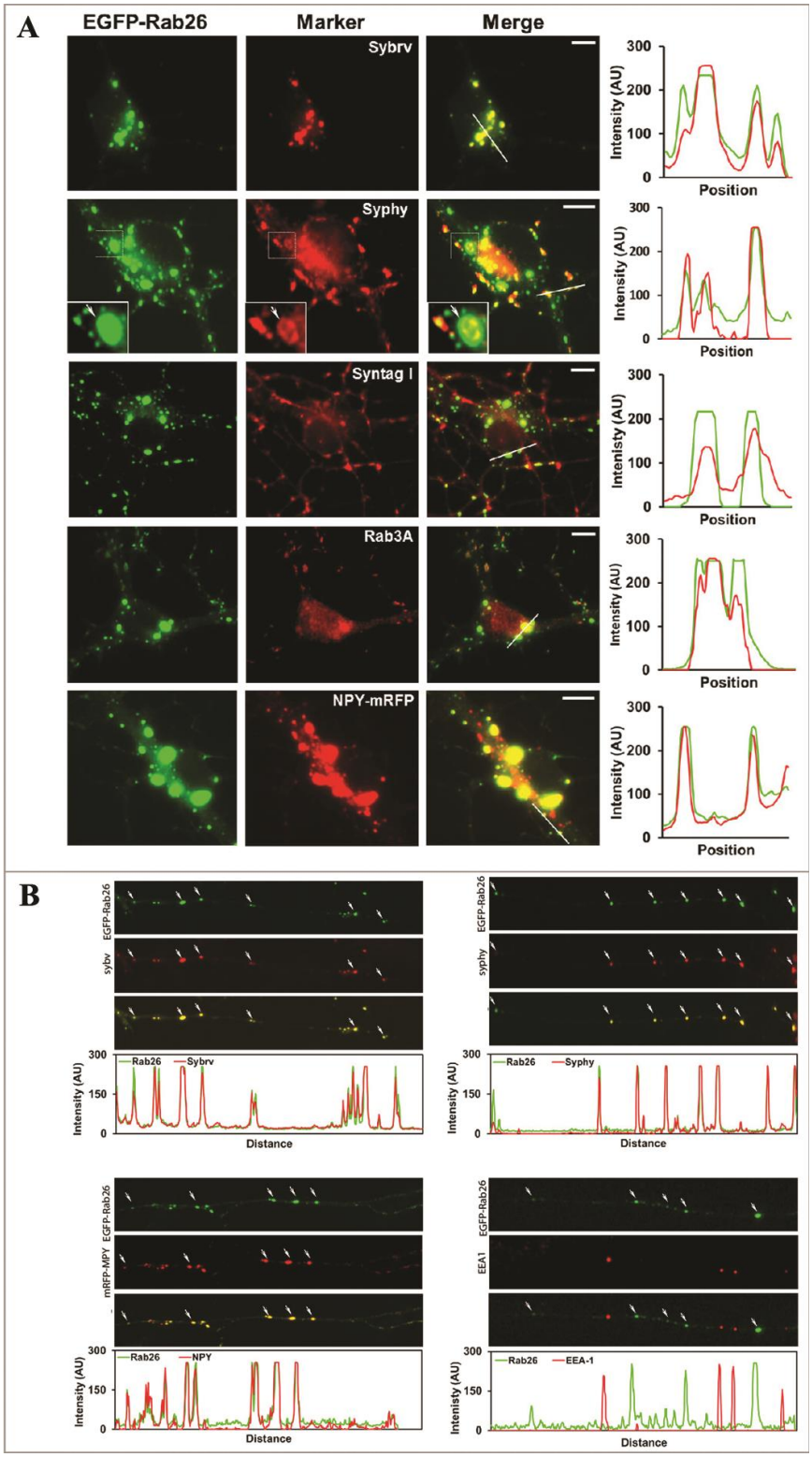

Figure 12 EGFP-Rab26 colocalizes with presynaptic markers

(A) EGFP-Rab26WT colocalizes with the synaptic vesicle protein markers at the level of the neuronal soma. Rab26 causes huge clusters of Synaptobrevin, (Sybv); Synaptophysin, (Syphy); Synaptotagmin I, (Syntag I) and Rab3A. Coexpression with RFP-NPY show drastic accumulation of the neuropeptide itself in the soma, scale bar 5 µm. **(B)** The synaptic vesicle proteins colocalize with EGFP-Rab26WT also at the level of the axon (arrows). No overlap was observed with the early endosomal marker EEA1 (arrows). Data kindly given by Nathan Pavlos (unpublished results)**.**

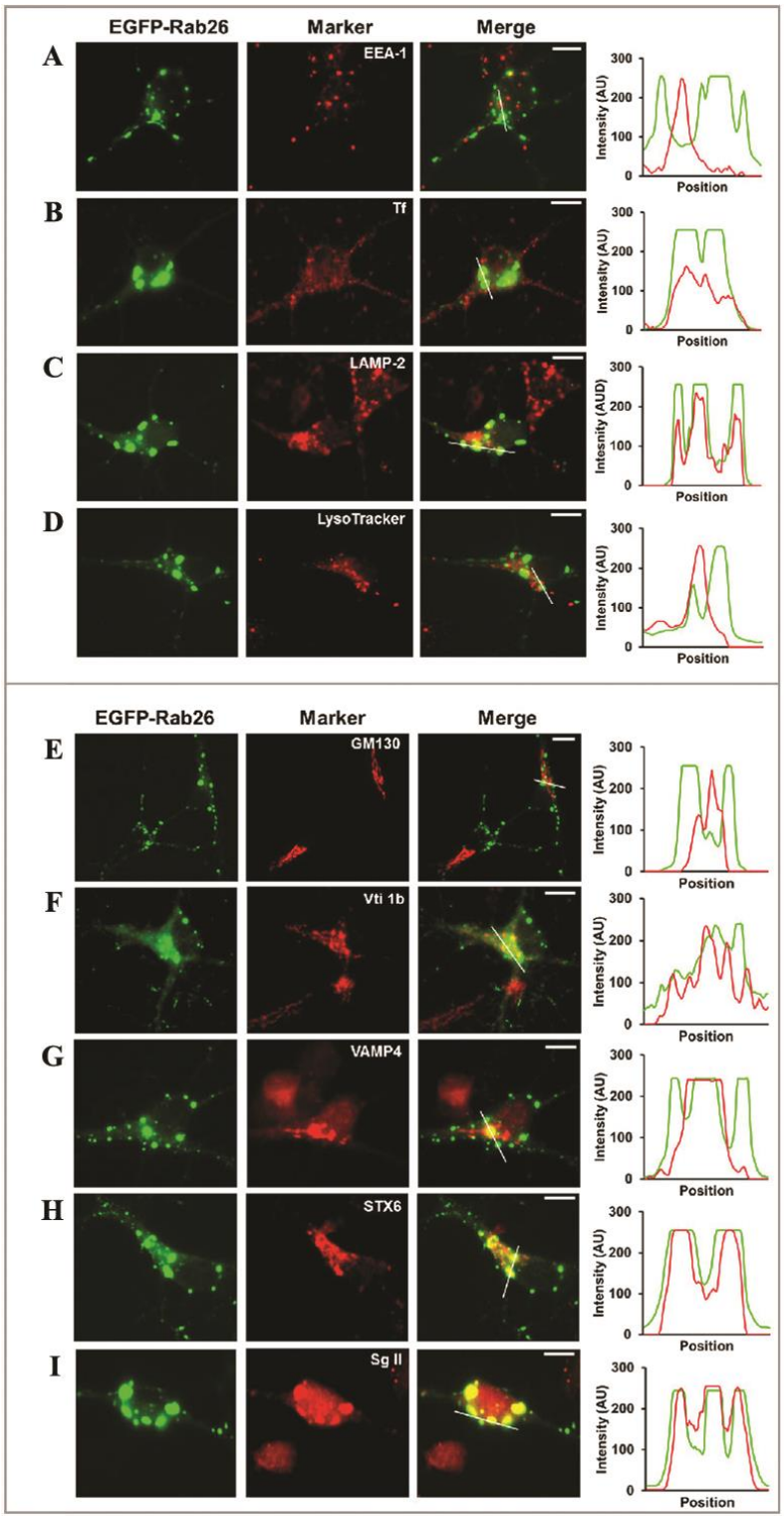

Figure 13 EGFP-Rab26 intracellular distribution in neurons

EGFP-Rab26WT does not colocalize with EEA-1 and Tnf **(A and B)**. Significant colocalization could be observed with LAMP2, a lysosomal marker but not with Lysotracker **(C and D)**. The overexpression of Rab26WT does not affect Golgi distribution visualized by GM130 **(E)**. The SNARE proteins Vti1b and VAMP4 show little overlap. Sytaxin6 (SYX6) instead is extensively colocalizing **(F, G, and H)**. EGFP-Rab26WT clusters also Secretogranin II (SgII) **(I).** Linescans are represented next to the corresponding figure. Scale bar,5 µm Both panel are kindly given by Nathan Pavlos (Unpublished results)

To clarify if the EGFP tag might enhance the Rab26 phenotype I compared its localization with the intracellular distribution of Flag-tagged Rab26 in neurons. The localization was not affected since we could still observe Flag-Rab26 on the synaptic vesicle compartment due to its overlap with Syt1 (Figure 14). Both Flag and EGFP-Rab26WT and QL had the ability to cause puncta formation (Figure 12 and Figure 14A and B). The TN form failed to colocalize with Synaptotagmin-1(Figure 14C).

The analysis of the intracellular distribution of Rab26 at the level of the soma and the axon highlights that Rab26 preferentially resides in the synaptic vesicle pool. The absence of colocalization with EEA1, but the partial overlap with early endosomal SNARE proteins suggests a potential role of Rab26 in targeting synaptic vesicles to the late endosome/lysosomal pathway due the overlap with LAMP2.

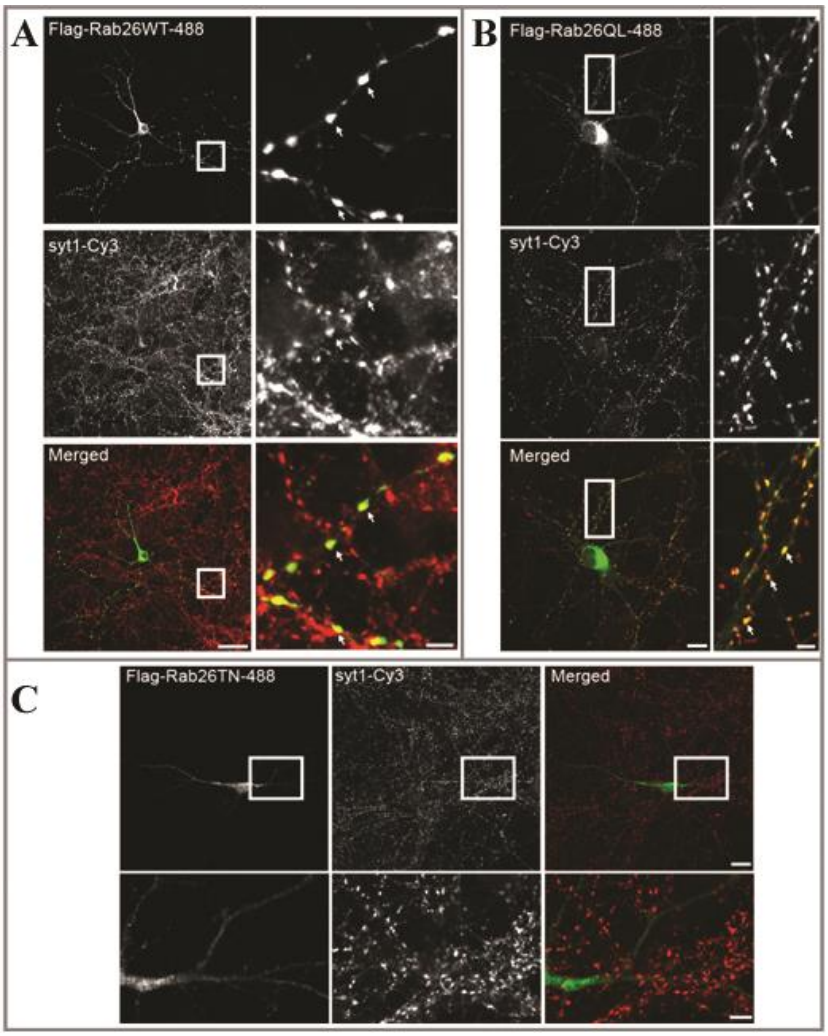

Figure 14 Rab26 is enriched at the synapse

(A) Flag-Rab26WT forms huge puncta at the neurite level that are colocalizing with endogenous Syt1 visualized in red. White boxes are represented as a magnified area next to each panel. **(B)** Flag-Rab26QL forms a punctate pattern that is colocalizing with Syt1 in red. The white box is represented as a magnified region close to the respective image. Arrows indicate colocalization. **(C)** Flag-Rab26TN is retained in the proximal region and appears to have small puncta that fail to colocalize with Syt1. Syt1, Synaptotagmin-1; 488, Alexa Fluor 488. High dense rat hippocampal culture; 46 hrs overexpression, DIV 9.

2.2.3 EGFP-Rab26 clusters recycled synaptic vesicles.

Previously we observed that Rab26 resides on a subset of synaptic vesicles. It was of fundamental importance to find out which kind of structures EGFP-Rab26WT is causing.
We decided to use electron microscopy to answer these questions.
In neuron cultures overexpressing EGFP-Rab26WT, Rab26 was immunolabeled with 5 nm gold particles and either endogenous Synaptobrevin (upper panel) or endogenous Synaptophysin (lower panel) were immunolabeled with 10 nm diameter of gold particles. Electron microscopy analysis showed that both Rab26 and both the presynaptic markers are localized in the same vesicle pool (Figure 15A). Intriguingly the ultrastructure studies showed that the bright and big puncta that are observed by immunofluorescence microscopy, were a massive vesicle clusters. But which kind of synaptic vesicle are we looking at?
To address this question I performed an *in vivo* recycling assay where I incubated the neurons with a pre-labeled antibody that recognizes the luminal domain of Synaptotagmin-1(synaptic system) during the 24 hours of overexpression of EGFP-Rab26. The luminal tail of Synaptotagmin is accessible to the antibody only after the exocytosis of the neurotransmitters in to the synaptic cleft prior to the recycling event. Upon endocytosis the antibody is localized specifically in the lumen of recycled vesicles. Subsequently the neurons were fixed with 4% PFA and analyzed by confocal microscope. It was exciting to see that EGFP-Rab26WT and QL colocalized extensively with recycled synaptic vesicles (indicated in red). Regarding the dominant negative form of Rab26 no Synaptotagmin clusters were observed neither in the soma nor in the periphery of the neurons (Figure 15B).

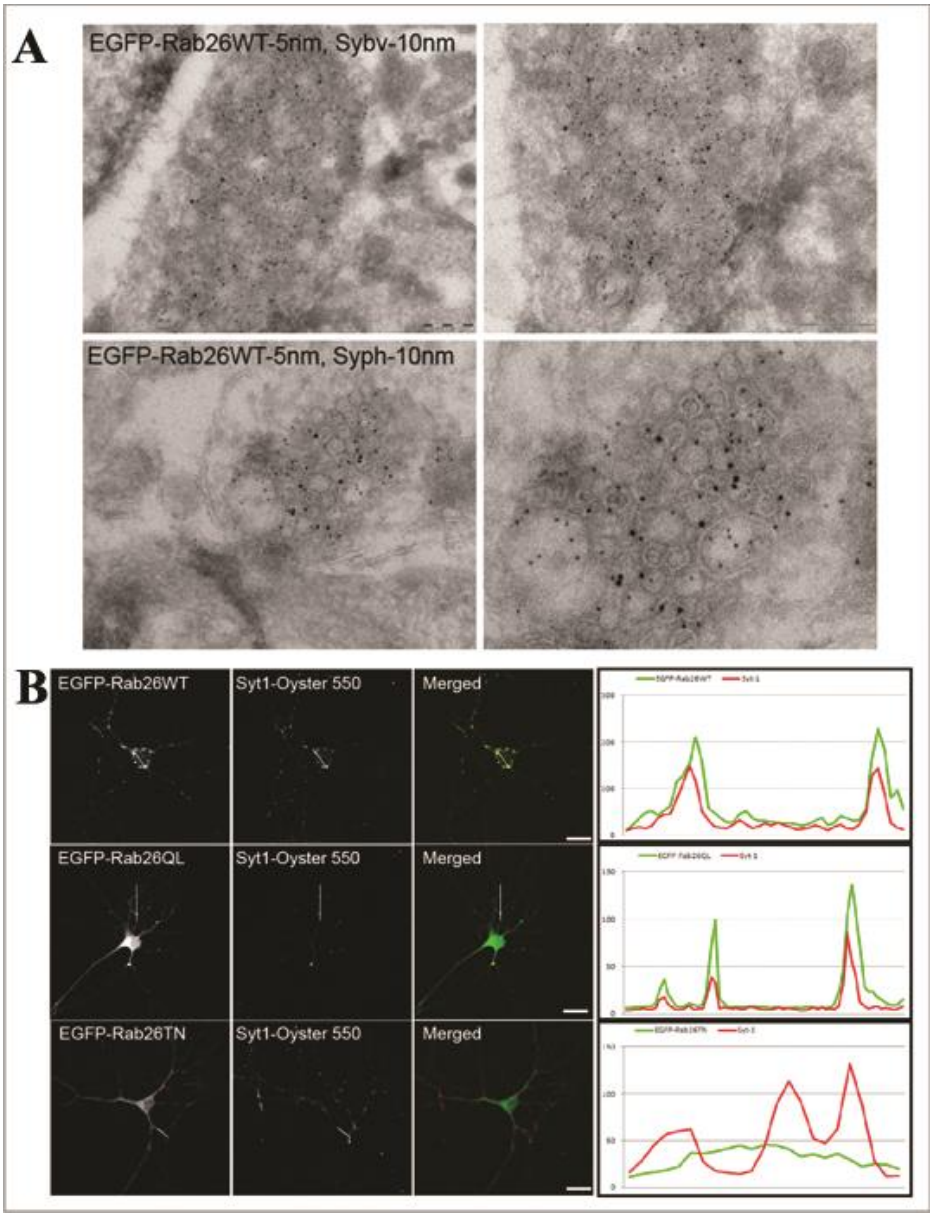

Figure 15 Rab26 targets a subset of recycled synaptic vesicles

(A) Immuno gold electron microscopy shows that EGFP-Rab26WT (5 nm particle) resides on a subset of synaptic vesicles labeled either with Synaptobrevin (upper) or with Synaptophysin (below) (Sybv-10 nm, and Syph-10 nm respectively). Electron microscopy images were performed by Dirk Wenzel. **(B)** The *in vivo* recycling assay shows the colocalization of Rab26 clusters with recycled synaptic vesicles upon 24 hours incubation of neurons expressing EGFP-Rab26WT, QL and TN with the antibody that recognizes the luminal domain of Synaptotagmin-1 (Syt1_41.1 Oyster-550, Synaptic System). The colocalization was extensive in the case of Rab26WT. The constitutively active form showed also colocalization where the clusters are formed whereas the dominant negative form does not show any Synaptotagmin clusters DIV 8, Scale bar 10 µm.

Further analysis of the ultrastructure images revealed that these vesicle clusters were sometimes compartmentalized within membranous structures (Figure 16, arrow), or oftentimes without these engulfing membrane compartment behaving more like vesicle aggregates (Figure 15A). Moreover the vesicle clusters were also found in close proximity of an electron dense material or mitochondria (m) that recall degradative compartments (Figure 16).

Putting all this data together we could draw an exciting and fascinating picture: Rab26 is a SV protein and has the ability to cluster selectively recycled synaptic vesicles.

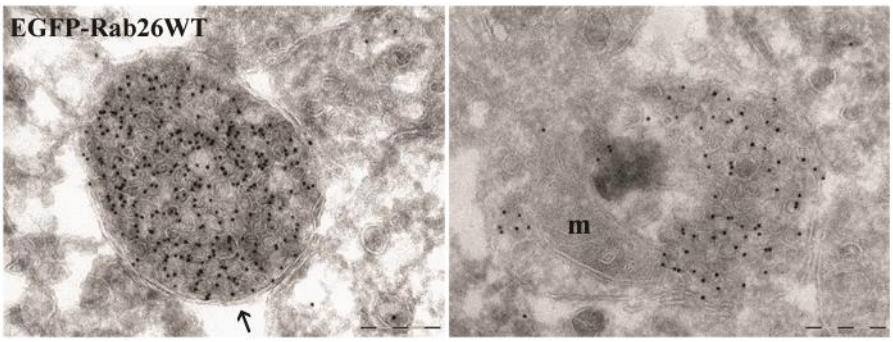

Figure 16 EGFP-Rab26WT causes vesicle clusters

Immunogold electron microscopy reveals that EGFP-Rab26WT clusters are massive vesicle aggregates that might be engulfed in membrane structures (arrows). The presence of mitochondria (m) and/or electron dense contents remind of degradative compartment. EGFP-Rab26WT was visualized by anti GFP antibody labeled with 10 nm gold particles. Scale bars are 200 nm. Electron microscopy was done by Dirk Wenzel.

2.3 Rab26-induced clusters in neurons represent intermediates of an autophagosomal pathway

Next we try to understand in which compartment the clustered vesicles are trapped.
The observation that EGFP-Rab26WT overlaps with the lysosomal marker (LAMP2) and the electron microscopy images brought us to speculate that we might be looking at a selective type of degradation pathway. But what does Rab26 have to do with synaptic vesicles and autophagosomes? Is it possible that Rab26 targets synaptic vesicles for degradation by the autophagosome/lysosome pathway? Are synaptic vesicles being degraded? Why? In order to answer some of these questions, I made use of canonical autophagy markers such as LC3 for mature autophagosomes and Atg16L1 for early autophagic compartments using cultured hippocampal neurons.
The Flag-Rab26 variants were coexpressed with GFP-LC3B. After 48 hours the neurons were fixed, subjected to immunostaining and analyzed by confocal microscopy (Figure 17). To our surprise the Flag-Rab26WT and the QL caused accumulation of the GFP-LC3B puncta along the distal region of the neurites (arrows). Flag-Rab26TN instead showed small puncta distributed throughout the neuronal arborization and GFP-LC3B appeared to have diffuse stain along the neuronal extensions (arrowheads).
Atg16L1 is one of the best investigated early autophagosome markers. It is essential for membrane elongation, LC3 lipidation and recruitment on the autophagosome membrane (Lamb *et al.* 2013). Furthermore it is also known to act as an effector for the Golgi resident small GTPase Rab33 (Fukuda and Itoh 2008, Itoh *et al.* 2008). For this reason I chose between many others early autophagosome markers (such as Atg1, Atg14, Atg5) Atg16L1.
Both endogenous Atg16L1 and Rab26 colocalized in neurons (Figure 18A, arrows). To validate this observation I overexpressed Flag-Rab26 constructs in cultured hippocampal neurons. Excitingly overexpression of Flag-Rab26WT and QL caused clustering of the endogenous Atg16L1 (Figure 18B, C; see arrows) suggesting that Rab26 might recruit Atg16L1 on the synaptic vesicle membranes at the very early stage of autophagosome formation. Instead the overexpression of the Flag-Rab26TN did not cluster Atg16L1. Furthermore Rab26TN small puncta did not show any colocalization with Atg16L1 (Figure 18D, arrows). Finally EGFP-Rab26WT was able to recruit Atg16L1 on the same compartment, but not the endogenous LC3B (Figure 18E, F. See arrows).

These results suggested that EGFP-Rab26WT most likely acts as dominant negative form and they support the hypothesis that Rab26 might reside both on SVs and on the autophagosome membrane.

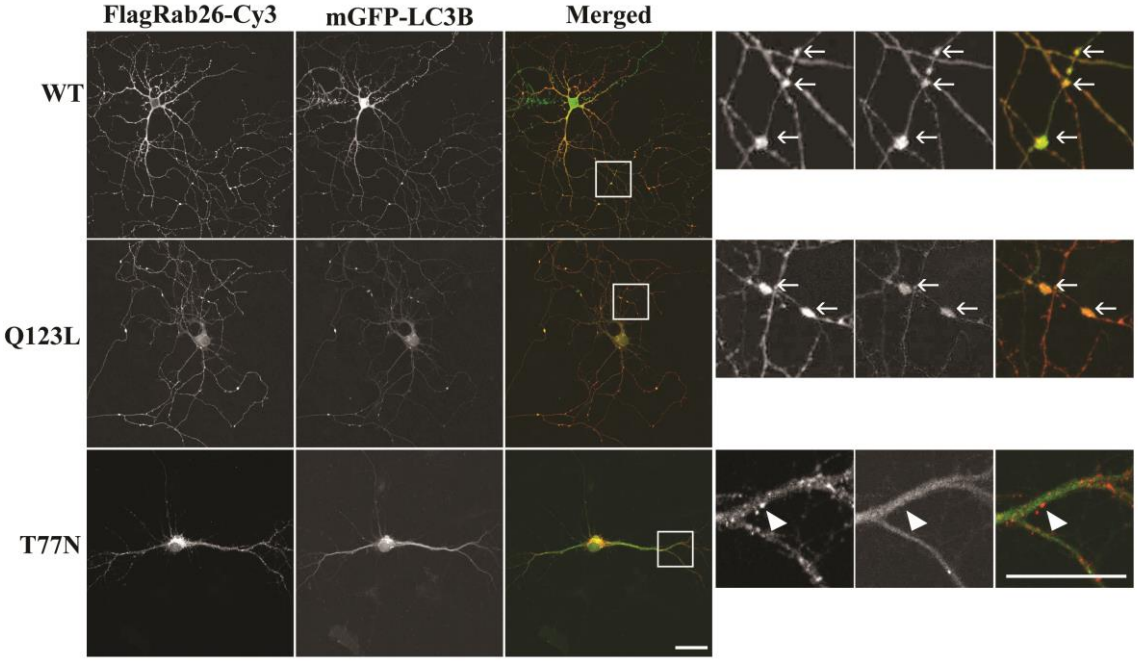

Figure 17 Rab26 clusters autophagosomes in neurons

Flag-Rab26WT and QL (arrows) and not the TN (arrowhead) cause LC3B clusters in the neurites. The white boxes are enlarged as a magnified area beside each panel.Scale bar, 10µm. Rat hippocampal neurons DIV 8.

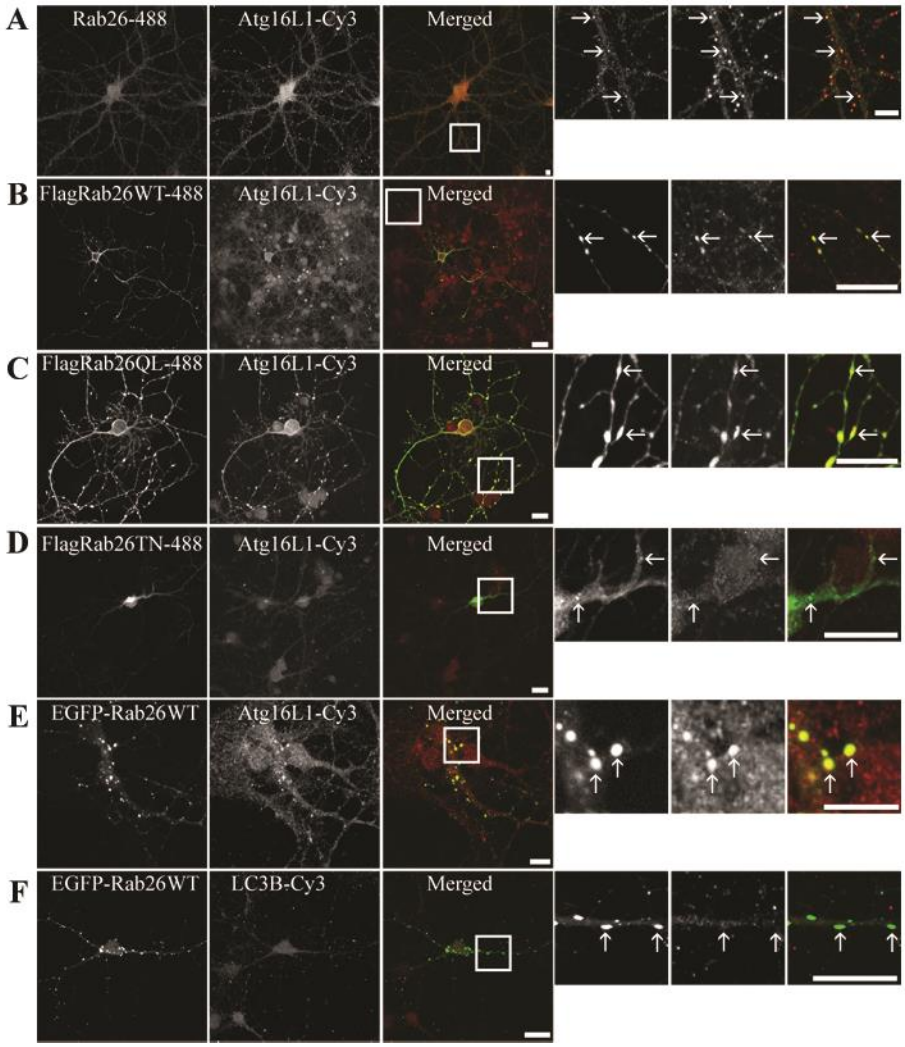

Figure 18 Rab26 recruits Atg16L1 to the same compartments

(A) Endogenous Rab26 (green) colocalizes with endogenous Atg16L1 (red) in dissociated hippocampal neurons DIV 16. The white boxes are enlarged as a magnified area next to each figure. Arrows indicate colocalization. (**B** and **C)** Overexpression of Flag-Rab26WT and QL cause endogenous Atg16L1 clusters in the neurite regions. (**D**) FlagRab26TN instead fails to recruit Atg16L1 that appears diffused also if Rab26 clusters are formed, arrow. (**E**) EGFP-RAb26WT traps endogenous Atg16L1 on the same clusters (arrows) but fails to recruit LC3B, (**F**, arrows). White boxes are represented beside each panel as a magnified area. The cells are hippocampal neurons, DIV 8. Scale bare, 10 µm

2.4 Rab26 labels late endosomes and autophagosomes in HeLa cells

In the first section of this work I performed my experiments mainly in neurons. I showed that Rab26 is a neuronal specific small GTPase. Furthermore in the light of all the experiments we could show by combination of light microscope and electron microscope that the overexpressed Rab26 provokes the formation of immense vesicle clusters that affect the distribution of the majority of pre-synaptic markers. Even more, colocalization of Rab26 with GFP-LC3B and Atg16L1 showed how Rab26 might be responsible for addressing selectively a subset of synaptic vesicles to the autophagy.
If Rab26 is involved in vesicle clustering or in triggering membranous compartments to the autophagosome it should accomplished its function also in other cell systems that do not have Rab26 native compartments (SVs) when ectopically expressed. HeLa cells were the heterologous system chosen to investigate this theory.

2.4.1 Rab26 phenotype in HeLa cells

First I analyzed the exogenous expression of EGFP-Rab26WT, QL and TN.
As described in neurons (Figure 11) also in HeLa the overexpression of EGFP-Rab26WT showed the strongest phenotype (Figure 19) whereas the QL appeared to be concentrated around the nucleus but with moderate features compare to the WT. EGFP-Rab26TN was mostly diffuse with some small puncta dispersed in the cytosol.

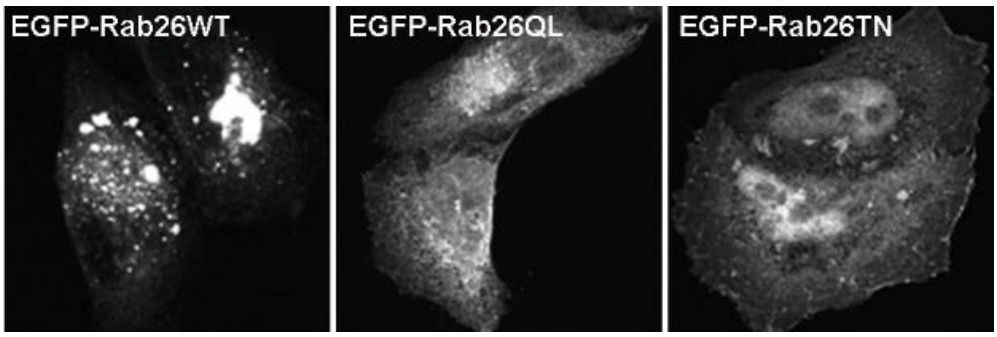

Figure 19 EGFP-Rab26WT forms huge puncta in HeLa cells

Overexpression of EGFP-Rab26WT and the mutants in HeLa shows comparable features to those observed in neurons. Cells where fixed after 24 hours of overexpression and analyzed by confocal microscope.

2.4.2 Rab26 compartmentalization in HeLa cells

To investigate in more detail Rab26 function, I chose HeLa cell lines since they are well-established model to study autophagy. In these experiments untagged Rab26 was chosen for the co-stain experiments. Like in neurons, also in HeLa different subcellular markers were used to investigate the intracellular localization of Rab26 (Figure 20).
For the recycling and the early endosomes respectively the Transferrin (Tnf) conjugated with fluorescent dye (Alexa Fluor 488) and RFP-Rab5QL were used as markers. To label the late endosomes was used EGFP-Rab7WT, EGFP-Rab33WT to visualize the Golgi apparatus and vesicle derived from Golgi (Itoh *et al.* 2008). RFP-LC3 instead was used to visualize the autophagosome organelles.
Transferrin receptors are down regulated upon binding to their ligand and internalized. Subsequently they are recycled back to the plasma membrane surface mediated by Rab4-Rab11 pathway (Mayle *et al.* 2012). For this assay fluorescently labeled transferrin was incubated for 30 min with HeLa cells transiently expressing Rab26. Both Rab26 and Tnf distribution were not disturbed (Figure 20A). Tnf (in green) was mainly distributed close to the plasma membrane. Rab26 instead appears to have a perinuclear distribution. This is in agreement with what was shown previously in neurons (Figure 13B). Coexpression of Rab26WT with RFP-Rab5QL does not affect the Rab26 distribution. RFP-Rab5QL appears to have the canonical phenotype (Stenmark *et al.* 1994, Roberts *et al.* 1999): enlarge endosomal compartments that are Rab26 negative (Figure 20B). This results show that as observed in neurons (Figure 13A) Rab5 and Rab26 follow a different pathway. A partial overlap and extensive colocalization could be observed respectively with EGFP-Rab33WT and with EGFP-Rab7WT (Figure 20C and D). Excitingly RFP-LC3 and Rab26WT were largely colocalizing (Figure 20E).

In the present studies HeLa cells were used as an “artificial” system, since they are neither polarized nor secretory cells. But the data observed using this heterologous system were of great importance since they strongly support the experiments obtained in neurons. Rab26 in the absence of its native compartment (SVs) is still able to perform its intrinsic activity: to cluster vesicles and to direct them to the autophagy pathway.
Further advantages in having used HeLa were showing for the first time that Rab26 was preferentially found in the late endosomal-autophagosome compartments. The partial overlap observed with Rab33 suggest that Rab26 might be involved also in the maturation

of autophagosome since it is known that Rab33 interacts directly with Atg16L1 a core component of the autophagosome machinery (Itoh 2008).

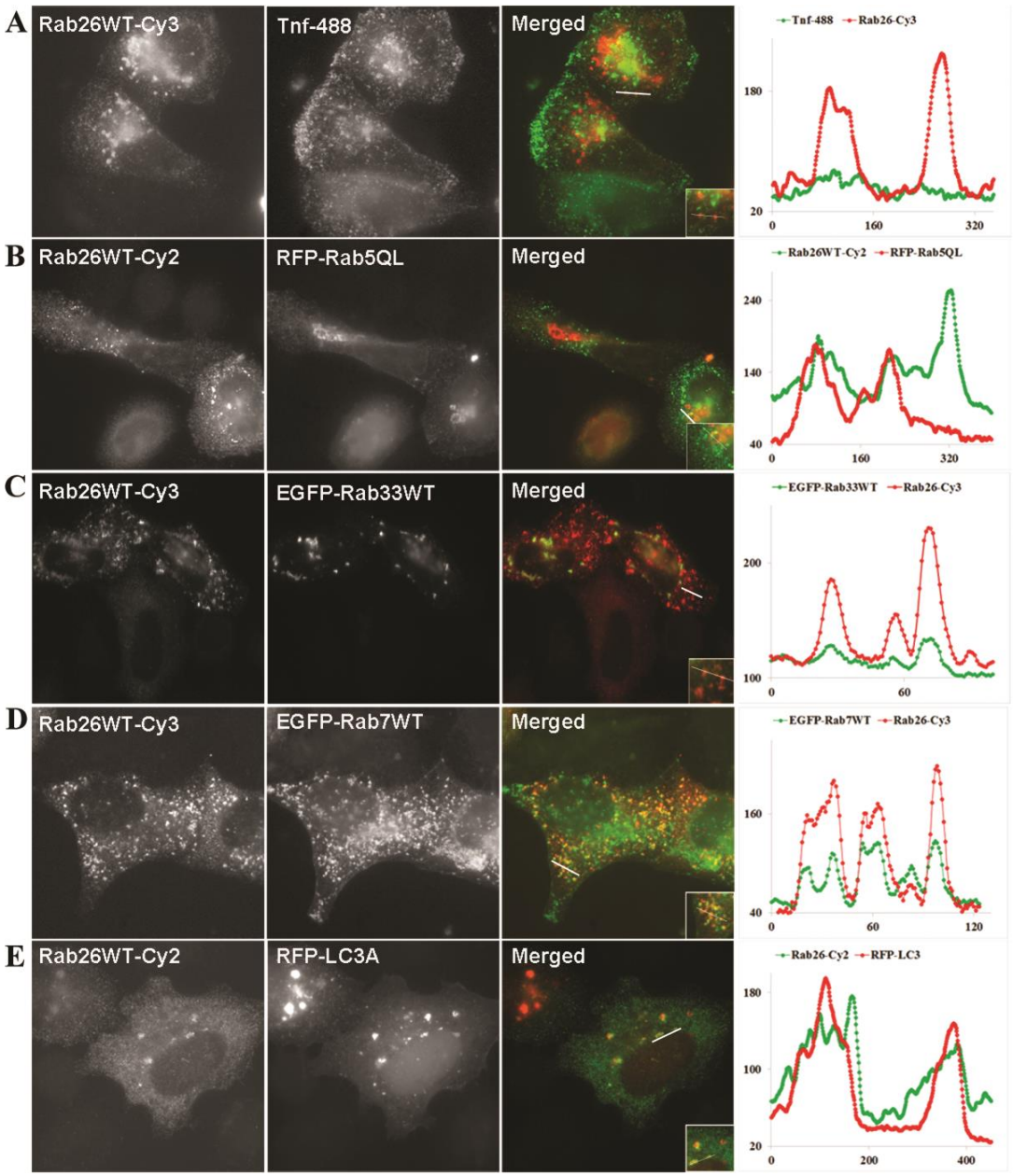

Figure 20 Rab26 compartmentalization in HeLa

Co-labeling of untagged Rab26 transiently expressed in HeLa with organelle markers revealed that Rab26 was preferentially associated with Rab7, LC3 compartments and partially overlapping with EGFP-Rab33 (**C**, **D**, and **E**) and not with the recycling and early endosomes visualized by Rab5 and Tnf (**A** and **B**). Beside each figure a linescan graph is indicated to show the colocalization profile.

2.4.3 Rab26 clusters degradative compartments

The colocalization experiments performed in HeLa converge with what was observed and described in neurons where it was shown clearly that Rab26 colocalizes with autophagosome markers, such as GFP-LC3 and endogenous Ag16L1 but not with early endosome markers. Furthermore the ultrastructural analysis in neurons showed that the EGFP-Rab26WT causes massive vesicle clusters (Figure 16). The observed colocalization of Rab26 with Rab7, LC3 and partially with Rab33 (Figure 20) was of crucial importance since it allowed me to address this study towards a specific intracellular membrane trafficking pathway. In fact these experiments revealed to be the additional and strong prove that Rab26 was implicated in the trafficking between late endosome and autophagosome/lysosome compartments.

In the next step I analyzed whether the overexpression EGFP-Rab26 variants in HeLa have an effect in the autophagosome/lysosome distribution. To validate this hypothesis I used either LC3B or Lysotracker (fluorescent marker for acidic compartments) respectively as a marker for autophagosome and lysosome visualization. The different EGFP-Rab26 constructs were transiently expressed in HeLa and after 24 hours the cells were fixed and immunostained using anti LC3 antibody and subsequently visualized by confocal microscope (Figure 21). EGFP-Rab26WT caused partial clustering of endogenous LC3B. EGFP-Rab26QL appeared to form perinuclear vesicle clusters that included LC3 positive puncta. The dominant negative forms (TN and NI) instead showed small and dispersed puncta that were LC3B free. Further negative controls were performed. Rab26dcc mutant is a variant of a dominant negative form of Rab proteins. This mutant lacks the last four amino acids that contain the two cysteine residues that are essential for the prenylation, a post-translational modification that allows Rabs to be inserted in the membrane (Khosravi-Far *et al.* 1991, Khosravi-Far *et al.* 1992). Without this motif Rab proteins are cytosolic. Indeed EGFP-Rab26dcc was completely diffuse, and did not affect LC3B distribution. The same result was seen in the presence of EGFP only.

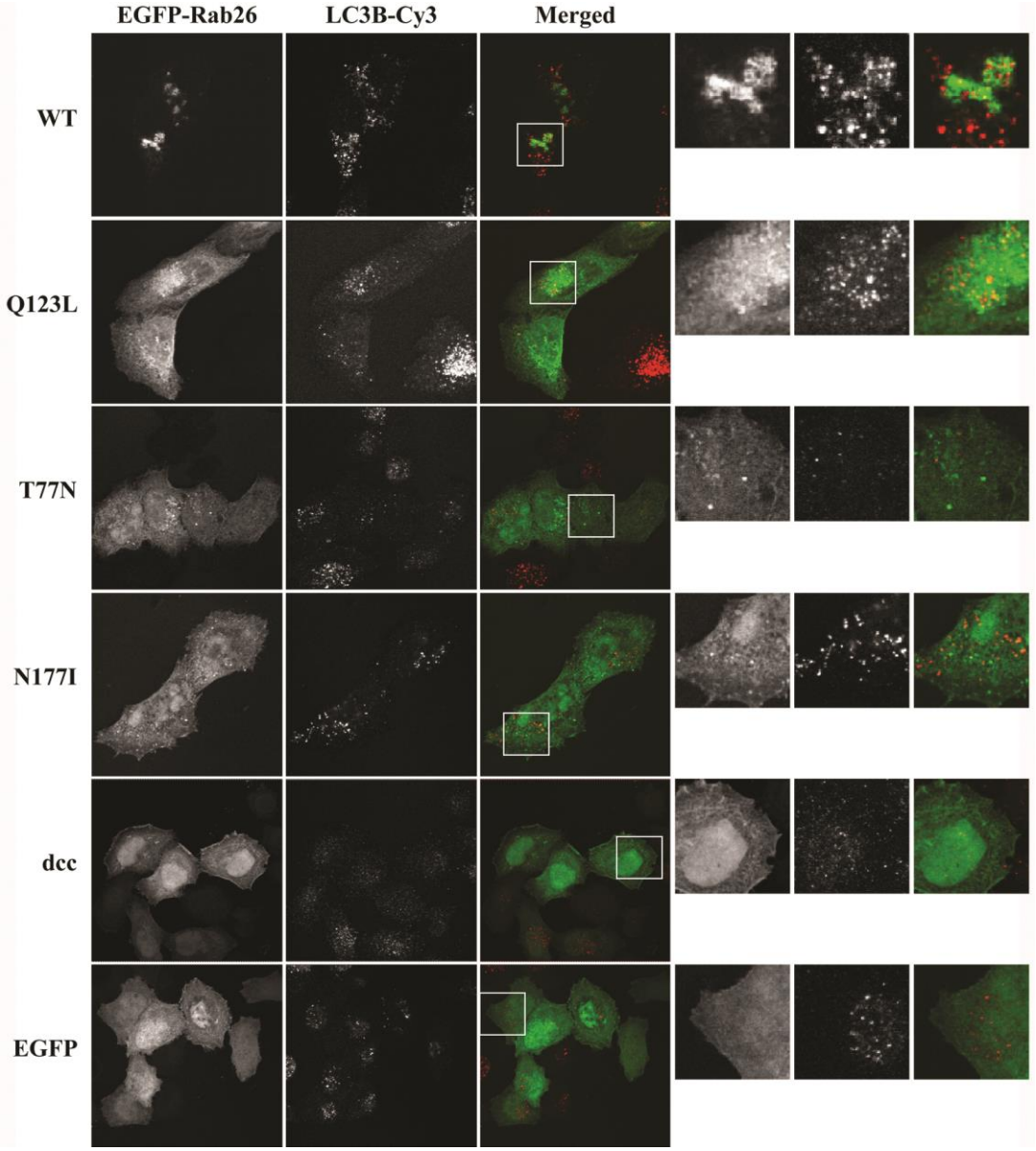

Figure 21 EGFP-Rab26 partially affect autophagosome distribution in HeLa cells

EGFP-Rab26WT and QL, but not TN and NI are partially affecting LC3 distribution. EGFP-Rab26dcc and EGFP itself are negative controls and show diffuse distribution and LC3B puncta appear disperse in the cytoplasm. The white boxes are enlarged as magnified area beside each figure.

Co-staining experiments of EGFP-Rab26 with Lysotracker showed comparable results to the LC3B endogenous stain (Figure 22). After 24 hours of overexpression HeLa cells were incubated for 30 min with Lysotracker (red). Subsequently the samples were fixed and analyzed by confocal microscope the same day to avoid diffusion of the probe. EGFP-Rab26WT and QL were clearly colocalizing with the Lysotracker stain. In the case of EGFP-Rab26TN and NI, the Lysotracker stain was mainly dispersed through the cytosol.

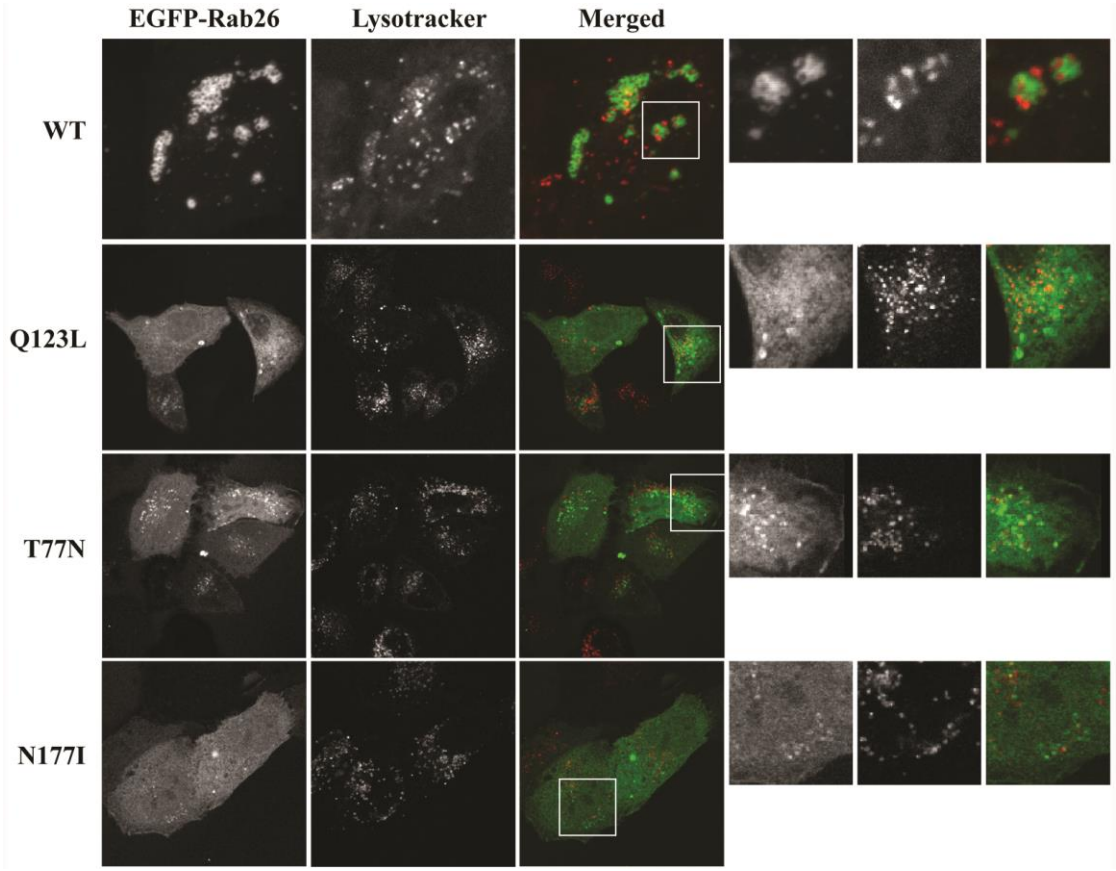

Figure 22 EGFP-Rab26 resides on the acidic compartments

The intracellular distribution of Lysotracker is affected by EGFP-Rab26WT that causes its clustering and moderately by the EGFP-Rab26QL. The presence of the dominant negative forms instead is responsible for more disperse Lysotracker puncta. The region inside the white boxe is represented as a magnified area next to the respective image.

2.4.4 EGFP-Rab26WT induces vesicle aggregate formation in HeLa

As in neurons (Figure 16), the overexpression of the EGFP-Rab26WT in HeLa caused massive vesicle clusters. Cells were transiently transfected with EGFP-Rab26WT for 24 hours and subsequently analyzed by electron microscopy (Figure 23). Compared to the neuronal ultrastructure analysis, in HeLa cells it was possible to read out more informations. We observed the accumulation of huge and massive vesicle aggregates that might be surrounded by membrane structures (indicated by the arrow) or more often without membrane that compartmentalized the vesicle aggregates (arrowhead). We could also observe that vesicle clusters were located inside or in close proximity of degradative compartments that resemble to autolysosomes (arrow and asterisks).

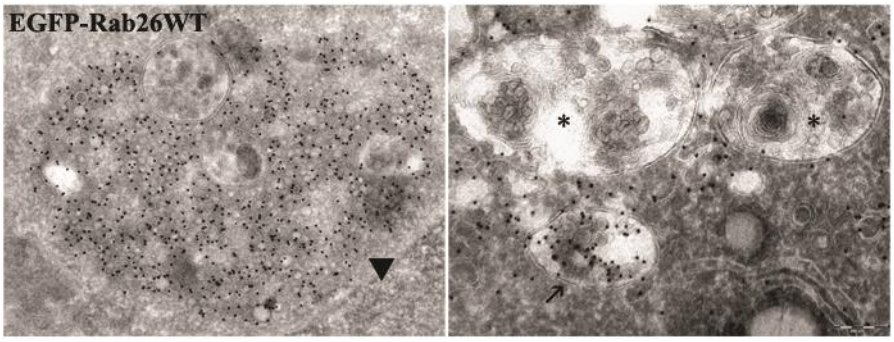

Figure 23 EGFP-Rab26WT provokes vesicle aggregates and autolysosome like-structure cluster.

Overexpression of EGFP-Rab26WT in HeLa causes vesicle clusters that might be surrounded by membrane structures (arrow), or membrane free aggregates (arrowhead). Furthermore EGFP-Rab26 vesicles were in close proximity (asterisk) or inside (arrow) of what resembles autolysosomes. 10 nm gold particles label anti GFP antibody. Scale bar 200 nm. Data analyzed by Dirk Wenzel.

Like in neurons also in the heterologous cell system the expression of Rab26 caused similar effect. In fact investigation of the function of Rab26 in HeLa cells allowed me to better understand and clarify its implication in vesicle clustering and vesicle triggering to the autophagosome/lysosome. But the nature of this vesicles or membranous structures observed in HeLa is mostly unknown. Most importantly HeLa experiments support the hypothesis that Rab26 is sufficient to cause vesicle internalization into a degradative like compartments. The question how this might happen and why particularly in neurons synaptic vesicles are degraded must be better investigated.

2.5 Molecular properties of Rab26

To addressed the hypothesis how Rab26 might cluster vehicles and what is the potential molecular mechanism underling Rab26's physiological activity I employed biochemistry approaches to answer the enigmatic behavior of this small GTPase. In the previous paragraph I showed that Rab26 is associated with a subset of synaptic vesicles. Up to this point there was no evidence showing how this might happen.

2.5.1 Rab26 and Rab27 are resistant to GDI-mediated membrane dissociation

Several studies reported that Rab26 belongs to the secretory Rab subgroup.
It is known that Rab3a cycles between the cytosol pool and the membrane pool while Rab27 appears to be associated with the membrane in a nucleotide independent manner (Pavlos *et al.* 2010). The membrane-cytosol cycle of Rab proteins is regulated by a factor named Rab GDP dissociation inhibitor (RabGDI). This protein extracts the inactive form of Rab, Rab-GDP, from the membrane (for more details see chapter 1.3.1.1). The complex RabGDP·GDI becomes soluble. Therefore the addition of GDP and purified GDI in LP2 or in SV sample allows visualization of any difference in the composition of Rabs in the pellet fraction after the extraction reaction.

I used LP2, the crude synaptic vesicles, as starting material to perform the RabGDI extraction assay (Figure 24) - for the protocol see chapter 4.2.3.5. Despite efficient extraction of the synaptic vesicle marker Rab3a (Lane Rab3, third column), we could see that Rab26 was tightly associated to the membrane in a nucleotide independent manner similarly to the behavior of Rab27 and Rab18 (Pavlos *et al.* 2010) (lane Rab26, column 3). As expected in the absence of RabGDI, and in the presence of PBS (first column), or GDP/GTP$_\gamma$S alone (second and fourth column), no difference in the level of the two Rab proteins could be observed. Synaptophysin was used as a loading control (lane Syph) whereas Rab3 was used as a positive control that showed that in the presence of GDP and GDI Rab3a was remarkably reduced.

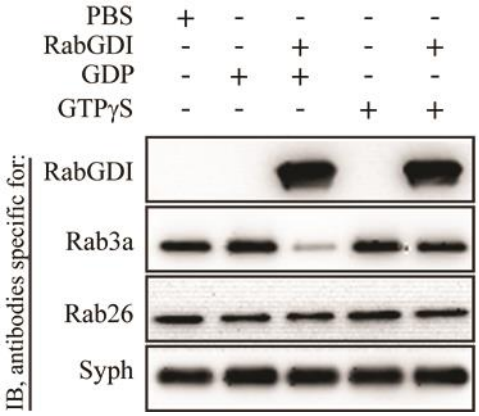

Figure 24 Rab26GDP binds to vesicle membranes

The GDI extraction experiment shows that Rab26 is resistant to extraction in the presence of GDP/ $GTP_{\gamma}S$ and with and without recombinant RabGDI. Rab3a was used as a positive control (column 3, row 2), PBS as a negative control. Synaptophysin (Syph) was the loading control. LP2 was the brain fraction used as a starting material.

2.5.2 Rab26 oligomerization

The observation that Rab26 and Rab27 behave in a similar way on the synaptic vesicle membrane motivated me to check whether Rab26 oligomerizes in a nucleotide dependent manner since it is known that Rab27 forms dimers in a GDP dependent manner (Chavas *et al.* 2007, Pavlos *et al.* 2010). Therefore I tested if Rab26 like Rab27 has the ability to dimerize/oligomerize.

This idea was investigated experimentally by co-immunoprecipitation where EGFP-Rab26WT, EGFP-Rab26QL and EGFP-Rab26TN/NI were cotransfected with Flag-Rab26WT in HEK cells. In Figure 25A the upper blot represents the input fraction in which the coexpression can be observed. The Flag-Rab26WT bands show that equal volume of the samples was added. In the last lane of the input blot I observed only a band for Flag-Rab26WT. It represents the negative control since only Flag-Rab26WT was transfected. Anti GFP antibody was used to perform immunoprecipitation (below panel). The GFP antibody immunoprecipitated EGFP-Rab26WT, QL, TN and NI and in the last lane no bands were observed because there was no EGFP-Rab26 overexpression. Flag-Rab26WT was co-immunoprecipitated with EGFP-Rab26 WT and DN (TN) confirming the hypothesis that Rab26 dimerizes/oligomerizes.
Furthermore oligomerization of both bacteria purified GST-Rab26QL and TN was investigated by native PAGE (Figure 25B). Aggregates were still present after high centrifugation at 20.000 g (see asterisk) but a clear difference between the QL and the TN variant of GST-Rab26 could still be observed. Compared to the QL form that existed preferentially as a monomer (arrowhead) the GST-Rab26TN formed oligomers (see arrows). SDS-PAGE gels showed that in boiled or un-boiled conditions both GST-Rab26QL and TN migrate at the expected molecular weight, 55KD (Figure 25C).

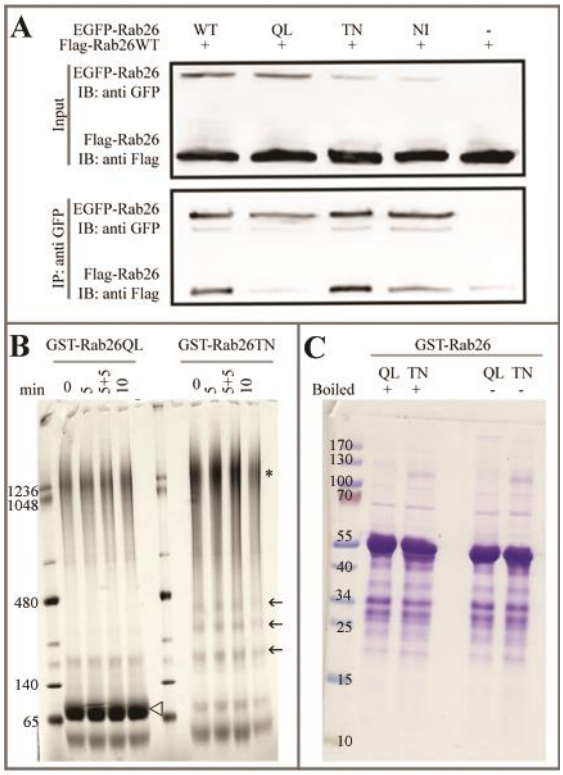

Figure 25 Rab26 self oligomerizes *in vivo* and *in vitro*

(A) Co-immunoprecipitation (CoIP) assay revealed that Rab26 oligomerizes *in vivo*. The upper panel represents the input fraction. The lower panel the IP. Flag-Rab26WT co-immunoprecipitated with the wild-type (WT) and the dominant negative forms (TN and NI) of EGFP-Rab26 but not with the constitutively active form (QL). IB: immunoblot; IP: immunoprecipitation. The assay was performed in HEK 293T cell line. (**B**) The native gel shows that GST-Rab26QL exists prevalently in a monomeric form (arrowhead), whereas the GST-Rab26TN forms multiple bands that correspond to oligomers (arrows). 10 µg per lane were loaded. 0, no centrifugation; 5, 5+5 and 10 are the minutes of centrifugation at 20.000 g to get rid of the possible aggregates indicated with the asterisk (*). (**C**) The SDS-PAGE shows that the GST-Rab26QL and GST-Rab26TN in both condition boiled and not boiled are exist in their monomeric form, at 55 kDa.

2.5.3 Atg16L1 is a novel Rab26 effector protein

The next essential question that required an answer is how Rab26 connects SVs to the autophagy pathway. Is there any regulator or effector protein that acts as a linker between the two pathways? Co-labeling analysis revealed that both endogenous and overexpressed Rab26 co-clusters with Atg16L1 one of the essential members of the pre-autophagosomal machinery. In addition Atg16L1 is reported to be an effector of Rab33 that overlaps partially with Rab26 in HeLa cells (Figure 20C). Therefore I wanted to investigate if Atg16L1 might be also an effector of Rab26. I decided to employ co-immunoprecipitation (Co-IP) and GST-pull down for protein-protein interaction analysis. Co-IP was first performed using HeLa cellular extracts expressing Flag-Rab26WT, QL, and TN. The results are reported in Figure 26A. Excitingly Flag-Rab26QL was capable of immunprecipitating endogenous Atg16L1 in a GTP dependent manner (arrow). More in detail the left blot represents the input fraction and the arrows indicate the relevant Atg16 isoform. The first lane is the negative control that corresponds to the untransfected sample. Lane two to four are respectively WT, QL, and TN of Rab26. Anti-Flag antibody was used to carry out the IP (right panel). The first lane represents the negative control, the second and the third lane show that the Rab26 variants were efficiently and equally extract by anti-Flag antibody. Only in the presence of Flag-Rab26QL the Atg16L1 isoform was co-precipitated (arrow); whereas in the case of the Flag-Rab26WT and TN no signal could be detected.

Subsequently I addressed the question if Atg16L1 is physically interacting with Rab26 *in vitro*. For this purpose GST-pulldown experiments were performed (Figure 26B). Bacteria expressed GST-Rab26QL and TN were immobilized on glutathione beads followed by the addition of a pre-formed complex of His-Atg16L1 N-terminal (NT) and His-Atg5-full length (FL). GST-Rab26QL pulled down His-Atg16L1 and surprisingly His-Atg5 was displaced from the preformed Atg5-Atg16 complex.

These key experiments showed that Atg16L1 interacts preferentially with Rab26 in a GTP dependent manner, and suggest strongly that Atg16L1 might be a novel Rab26 effector protein. These findings contributed to our belief that Rab26 recruits Atg16L1 on synaptic vesicle membranes and targets the vesicles to the autophagy compartment for degradation.

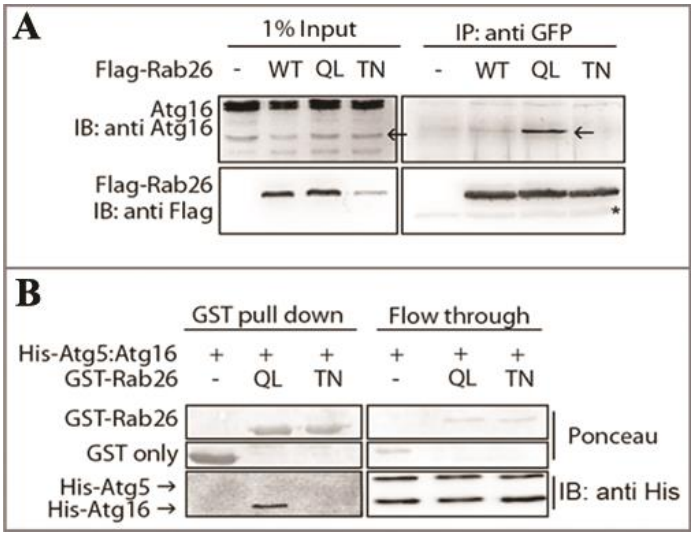

Figure 26 Rab26 interacts directly with Atg16L1

(A) Recombinant Flag-Rab26 co-immunoprecipitates with endogenous Atg16L1 in a GTP dependent manner (arrow). The asterisk indicates the IgG light chain. The heavy chain could not be observed because of the use of a secondary antibody that recognizes only the light chain. For the IP HeLa cell extracts were used. **(B)** Direct interaction of Rab26 with Atg16L1 was confirmed by GST pulldown. The pre-formed complex of Atg5-Atg16L1 is disrupted by the addition of GST-Rab26QL with Atg5 displaced from its binding to Atg16L1.

3 Discussion

3.1 Rab26 targets a subpopulation of SVs.

Rab26 was assigned to be part of the secretory pathway by proteomics (Takamori *et al.* 2006) and phylogenetic (Fukuda 2008) studies. Overexpression of the dominant negative form of Rab26 causes absence of granule formation in the zymogen exocrine cells (Tian *et al.* 2010, Li *et al.* 2012). The first direct evidence about potential physiological implications of Rab26 was published in 2006. The authors showed that Rab26 was associated to mature secretory granules. Furthermore Isoproterenol-induced amylase release was blocked by the introduction of an anti-Rab26 antibody in permeabilized parotid acinar cells. The release response to the stimulation could be rescued with the addition of exogenous GST-Rab26. This assay did not have any effect on the $Ca2^{+}$ dependent stimulation (Nashida *et al.* 2006). They concluded that Rab26 might be involved in $Ca2^{+}$ independent exocytosis.

During my research I confirmed that Rab26 colocalizes with the secretory granule vesicles as overexpression of EGFP-Rab26WT provokes cluster formation of neuropeptides such as NPY and Secretogranin (Figure 12; Figure 13E).

In the very first section of the results I demonstrated that Rab26 is a neuronal and, precisely, a synaptic vesicle protein. Rab26 is recognizing a subset of the SVs. This is supported by the immunoisolation results (Figure 7B Figure 8D). In fact while Synaptophysin was able to pull out all the Rab26 positive particles, Rab26 isolated only a portion of Synaptophysin vesicles. Still a strong signal was detected on the SN. While differences in the efficiency of the antibodies cannot be excluded it seems more likely that the Rab26 vesicle pool is small compared to the Synaptophysin vesicle population. This interpretation is supported by studies which showed that Synaptophysin is one of the most prominent integral component of synaptic vesicles (Jahn *et al.* 1985, Wiedenmann and Franke 1985, Wiedenmann and Huttner 1989), and it is expected to isolate many coupled vesicles in immunoisolation experiments. This assumption was also supported by immunocytochemistry analysis, where Rab26 showed a puncta like pattern which was colocalizing with a subset of Synaptotagmin-1 (Figure 9B).

Different studies suggest that the synapse terminals are composed of different synaptic vesicle populations: from the ready release pool (RRP), to the reserve pool, (RP) and recycling pool (Rizzoli and Betz 2005, Voglmaier and Edwards 2007). It is also believed that these populations, though the ultrastructure analysis was not sufficient to help in distinguishing their morphology, might have different membrane-protein composition. For example VAMP7 (Hua *et al.* 2011), AP3 (Faundez *et al.* 1998, Blumstein *et al.* 2001) and AP1 (Glyvuk *et al.* 2010) appear to be enriched in the resting pool, AP2 in the recycling pool (Di Paolo and De Camilli 2006, Kim and Ryan 2009), VGLUT1 and VGLUT2 in the ready releasable pool (Hua *et al.* 2011).

Furthermore synaptic vesicles are homogenous populations depending on their neurotransmitter contents. The different vesicles that transport different neurotransmitters can be separated from each other. An example is the GABA-synaptic vesicles that can be isolated with high purity from the rest of the other synaptic vesicle populations (Takamori *et al.* 2000).

In the light of my results, it is reasonable to conclude that Rab26 positive compartments are a specific subpopulation of synaptic vesicles.

3.2 Rab26 and Rab27 show common functional features

The neuronal secretory small GTPases are constituted by Rab3s, Rab27 and Rab26 (Fukuda 2008). As discussed in the introduction, Rab27 differs in its membrane cycle from Rab3.

Rab3 appears to shuttle between cytosolic pool and membrane pool in correspondence to the synaptic vesicle exocytosis pathway. During the exocytosis, Rab3 is anchored to the synaptic vesicles assisting their correct tethering, docking and priming toward the presynaptic plasma membrane. After neurotransmitter release, Rab3 is dissociated from the membrane by the action of RabGDI. The Rab3 cycle is essential for the directionality of the synaptic vesicle pathway (Lang and Jahn 2008). Rab27 instead is tightly associated to the synaptic vesicle membrane independent of the synaptic vesicle cycle. In addition the inactive form of Rab27 is found as a dimer (Pavlos *et al.* 2010). The association with the membrane in a nucleotide independent manner and its ability to dimerize resembles Rab26. Co-immunoprecipitation assays in HEK 293T cells (Figure 25) point out that Rab26 might undergo oligomerization by self-association or by mediation of regulator or effector proteins. This capacity is GDP dependent. It is reported that several Rab proteins have the ability to dimerize. For example Rab5 dimerizes (Daitoku *et al.* 2001) though in a GTP bound conformation; Rab11, Rab27 and Rab9 were found to crystalize as a dimer in a GDP-state (Pasqualato *et al*. 2004, Wittmann and Rudolph 2004, Chavas *et al.* 2007).

Like Rab27, Rab26 appears to be bound to the membrane independently of the nucleotide state as suggested by the RabGDI extraction assay. More clearly Rab26 not only binds to the membrane in its active form (GTP bound form) but also in its inactive configuration (GDP- bound state). Several Rab proteins such as Rab27b and Rab18 behave in this way (Pavlos *et al.* 2010). This observation is in apparent contradiction to the partial cytosolic distribution of Rab26TN observed by immunofluorescence. One possible explanation is that the membrane extraction of Rab26 requires additional cytosolic components which are not present in LP2 or Rab26 might shuttle between an active membrane pool and an inactive membrane pool rather than cycle between the membrane and the cytosolic population. The latter mechanism was also speculated for Rab9 and Rab27 (Wittmann and Rudolph 2004, Pavlos *et al.* 2010). Further experiments will be needed to clarify the mechanism of membrane association/dissociation of Rab26.

3.2.1 Rab26 connects SVs with the autophagy pathway

A very recent finding showed for the first time that Rab26 is associated to the lysosomal membrane. Furthermore overexpression of EGFP-Rab26WT causes lysosome clusters and reduction in mitochondria density but not mitochondria functionality (Jin and Mills 2014). This data supports our finding that Rab26 is indeed localizing to a degradative compartment, but it does not specify the mechanism of how Rab26 clusters lysosome and what its physiological role is.

The observation that Rab26 is connected to the SV-autophagy pathway was the most exciting finding of my project. In fact Rab26 colocalizes with several proteins involved in the regulation of the autophagy pathway such as LC3, Atg16L1.

It was very striking to see that the overexpression of Flag-Rab26WT and QL causes autophagosome accumulation along the neurites (Figure 17). Flag-Rab26TN instead does not cluster GFP-LC3B that appears mostly diffuse in the periphery. Moreover most of the expression of Flag-Rab26TN is localized around the soma (probably a "volume" artefact). Also GFP-LC3 seems to be preferentially expressed and punctated at the level of the cell body. This suggests that Rab26 might be important for autophagosome distribution in neurons.

The moderate overlap between Rab33 and Rab26 in HeLa cells, was the key result that allowed me to address the attention of my study to the early stages of autophagosome formation. Atg16L1 was the best candidate for this study, since it was shown that it acts as a Rab33 effector protein (Itoh *et al.* 2008). Combining immunofluorescence and pulldown assays, I identified Atg16L1 as a direct effector protein of Rab26.

Immunofluorescence analysis showed that not only endogenous but also recombinant Rab26 recruits Atg16L1 to the same compartment (Figure 18). Co-IP and GST pull down experiments support this observation. Rab26 interacts directly with the NT-region of Atg16L1 in a GTP dependent manner. The biochemistry studies allowed us to speculate on the dynamic interaction between Rab26, Atg16L1 and Atg5. In fact upon addition of GST-Rab26 on a pre-formed complex between His-Atg16NT and His-Atg5FL, the binary complex is destabilized by Rab26, Atg5 is replaced and a new binary complex (Rab26·Atg16L1) is formed. One possible interpretation for this apparent mutually exclusive interaction is that the interaction between Rab26 and Atg16L1 occurs at an early step before autophagosome formation. This might be possible since it was proposed in yeast that the Atg5·Atg12 complex is first associated to the PAS and that Atg16L1 is

recruited a later stage (Suzuki *et al.* 2007, Suzuki and Ohsumi 2010). Therefore Atg16L1 might be first recruited by Rab26 that transports synaptic vesicles to the new-forming autophagosome, then Atg16L1 interacts with Atg5·Atg12 complex on the isolation membrane.

The mammalian Atg16L1 is one of the essential members of the autophagosome core machinery. It is well investigated both at the functional and structural level. It is composed of three major domains: the N-terminal region or Atg5 binding domain (Fukuda and Itoh 2008; Itoh, Fujita et al. 2008), the coiled coil domains part of which is a Rab33 binding site and a C-terminal WD40 repeats domain with unknown interacting partners (Mizushima *et al.* 2003, Fukuda and Itoh 2008, Itoh *et al.* 2008, Ishibashi *et al.* 2012). In the GST pulldown experiments I could observe an interaction between Rab26QL and the truncated Atg16L1 lacking the WD40 domain. This result suggested that possibly the two Rabs, Rab26 and Rab33B, might compete for the same binding region that corresponds to the coiled-coil motive of Atg16L1 as proposed by Fukuda and Itoh (2008).

Another Atg protein, Atg11, was shown to be a downstream effector of Rab1/Ypt1 in yeast. Interestingly Atg11 interacts with Ypt1 in correspondence of its coiled coil region, similar to Rab26 and Rab33 with Atg16L1. Intriguingly Rab1/Ypt1 is found to be associated with Atg9 positive membranes and together with Atg11 is required for PAS assembly (Lipatova *et al.* 2012). Like Atg11 for Ypt1, Atg16L1 interacts directly with Rab26 and might act as a downstream effector.

Atg16L1 exists in different isoforms. At least three isoforms were identified in mammalian cells (Mizushima *et al.* 2003, Jiang *et al.* 2013). It might be that Rab33a/b and Rab26 each interact with different subsets of the Atg16L1 isoforms that act on different vesicle pools. This scenario is reasonable since Rab26 co-immunoprecipitated a short isoform of Atg16L1, whereas Rab33 interacts with the main isoform (Fukuda and Itoh 2008, Ishibashi *et al.* 2011). In fact the Atg16L1·Rab26 interaction was confirmed with a Co-IP experiment where Flag-Rab26QL but not Flag-Rab26TN precipitated the endogenous Atg16L1 short isoform. Furthermore the partial overlap between Rab26 and Rab33B as well as the colocalization with Rab7 observed in HeLa cells would imply that Rab26 converges with the Rab33B pathway at the very early stages of the autophagosome formation. The Rab33B/Atg16L complex is likely involved in the early tethering/docking of Golgi derived vesicles, whereas the Rab26/Atg16L1 complex in the tethering/docking of synaptic vesicles. The two pathways might converge at some point to a common isolation

membrane containing Atg12·Atg5 complex. Instead Rab26 and Rab7 would only intersect at the stage of fusion of autophagosme with the lysosome.

Rab33A and Atg16L1 are known to regulate the secretion of dense core vesicles in PC12 independently from autophagy (Fukuda et. al 2012). It is likely that Rab26 and Rab33A are regulating different subsets of synaptic vesicles. Nevertheless all these aspects must be further investigated to better clarify the role of Rab26 and Rab33a/b in vesicle targeting and their involvement in the different Atg16L1-dependent vesicle trafficking/degradation processes in neurons.

The fact that Atg16L1 and not LC3 is recruited on EGFP-Rab26WT puncta lead us to speculate how EGFP-Rab26WT, that acts as a functional mutant, causes this vesicle clusters in neurons and in HeLa. First it might be that EGFP-Rab26 actively subtracts synaptic vesicles from their normal pathway to the degradative pathway. The excess recruitment of vesicles stalled the autophagy pathway probably because the degradation machinery cannot keep up with the increased amount of vesicle aggregates. Alternatively EGFP-Rab26 might trap Atg16L1 in a step before its interaction with Atg5-Atg12 that resides on the PAS, preventing therefore LC3 recruitment. Finally it might be that Rab26-Atg16L1 opens a specialized autophagy pathway that is Rab5 independent. This last scenario is not to be excluded since the existence of an Atg5 independent autophagy pathway was reported to exist. Mice atg5 or atg7 knock out are capable to form autophagosome/autolysosome. This work was the first in showing the co-existence of two autophagyc routs: the Atg5/Atg7 dependent pathway and Atg5/Atg7 independent pathway (Nishida *et al.* 2009).

In addition to Atg16 also Rabphilin and RIM might act as Rab26 effector proteins. This hypothesis is based on results reported by Fukuda (2003). In this study it was shown that Rim1 and Rim2 are activated by different Rab proteins and that they are not Rab3 exclusive effectors. Furthermore Fukuda showed that Rab3 interacts with Rim2 and Rabphilin, whereas Rab27 interacts only with Rabphilin. Intriguingly Rab26 was shown to interact with Rim1 only and not with Rim2 and Rabphilin. These are additional proves that Rab26 is diverging functionally from the Rab3 family suggesting that it is regulating a different aspect of synaptic activity. The investigation of a functional interaction between Rab26 and Rim1 in synapses and the implication of this interaction in synaptic vesicle quality control might be a very fascinating project.

3.2.2 Rab26 clusters synaptic vesicles

The oligomerization property of Rab26 might explain the clustering phenotype observed by immunogold electron microscopy both in neurons and in HeLa.

It might be that Rab26WT dimerizes in a “trans” or in a “cis” configuration. More clearly two Rab26 proteins might sit either in different vesicle membrane (“trans dimerization”) or both in the same vesicle (“cis” dimerization) and pull together other vesicles provoking this huge vesicle aggregates with the help of other proteins.

The clustering phenotype is tag independent though the GFP tagged proteins exhibit more dramatic effects. One possible reason is that EGFP weakly dimerizes by its self and therefore possibly enhances the intrinsic ability of Rab26 to cluster vesicles. For this reason EGFP-Rab26WT could act as a functional mutant that might cluster and trap proteins in a particular step slowing down the endocytic pathway and enabling us to understand its role in synaptic vesicle quality control. In fact EGFP-Rab26WT trapped Atg16L1 on the same compartment subtracting it from the recruitment of LC3. The Flag tagged or untagged version of Rab26 is able to recruit LC3 in the same compartments.

It is not the first time that GFP-fused proteins are acting as inhibitors. For example many ESCRT subunits upon fusion with fluorescent proteins are dominant negative and are used to investigate the ESCRT pathway. This functional mutants cause the formation of abnormal endosomal compartments because the ESCRT complexes are trapped (Howard *et al.* 2001, Strack *et al.* 2003, Langelier *et al.* 2006, Tandon *et al.* 2009). EGFP-Rab26 might selectively trap the recycled synaptic vesicles (Figure 15B) at an intermediate stage before fusion with the autolysosome.

3.3 Synaptic vesicle quality control

3.3.1 Rab26-dependent pathway

I showed that Atg16L1 and Rab26 are most likely involved in the membrane trafficking between synaptic vesicles and autophagosomes.

The question that might arise is the following: is Rab26 acting selectively? In other words, which kind of synaptic vesicles are targeted by Rab26?

To address this question I performed a recycling assay as describe in section 2.2.3. This experiment allowed me to visualize how Rab26 targets recycled synaptic vesicles, though it does not exclude that Rab26-induced clusters contain also not recycled vesicles.

On the light of our observation we could conclude that Rab26 might be involved in the regulation of synaptic vesicle turnover. Possibly Rab26 recruits first Atg16L1 on the recycled synaptic vesicles, and then delivers the vesicles and its content to the autophagosome that subsequently fuses with the lysosomes for degradation.

The synaptic vesicle pathway requires a high rate of vesicle and protein turnover. Since the 1950´s several research groups were trying to understand how after neurotransmitter release, the cells were still able to produce new synaptic vesicles capable of release after intensive and extensive depletion of synaptic vesicles at the level of the NMJ of frog and crayfish (Atwood *et al.* 1972, Heuser and Reese 1973).

Ceccarelli *et al.* (1973) showed for the first time that synaptic vesicles are recycled back and reused several times. Although no increase in the number of late endosomes, lysosomes or autophagosomes could be observed under the different conditions the hypothesis was formulated that the newly reformed synaptic vesicles could either be actively re-used as functional synaptic vesicles or re-directed to the late endosome-autolysosome pathway (Holtzman 1971). It is still a very controversial and heavily investigated field. After a certain number of synaptic vesicle cycles, membranes and proteins that are integral components of these vesicles must be re-synthesized *de novo*.

But where are the old synaptic vesicle components going and is there a pathway that controls the quality of synaptic vesicles?

Macroautophagy has already been shown to contribute to regulating postsynaptic receptors. It is still unclear if the presynaptic proteins turnover is regulated by the same pathway. Holtzman (1971) predicted that the turnover of recycled synaptic vesicles might

require lysosomes. David Sulzer´s group demonstrated that presynaptic neurotransmission is modulated by macroautophagy in mice (Hernandez *et al.* 2012). Induction of autophagy by rapamycin causes reduction in presynaptic components. In addition they observed synaptic vesicle like structures inside autophagic vacuoles. This finding led them to hypothesize that the synaptic vesicle membranes are redistributed between endosomes, autophagosomes and lysosomes under normal conditions. They also speculated the existence of an alternative pathway for synaptic vesicle degradation.

This newly discovered role of Rab26 could be seen as an indirect answer to the hypothesis formulated early on by Holtzman and Sulzer.

We offer for the first time a new alternative mode of synaptic vesicle recycling that bypasses the Rab5-dependent pathway and converges with the LE/MVB and autolysosome pathway. A subset of recycled SVs is delivered to the proximal regions of neurons where most of the acidic compartments are localized. Two independent groups suggested that autophagosomes originate distally and through a retrograde transport move towards the cell body. During their travel they undergo fusion with acidic compartments and finally with the lysosomes (Lee, Sato et al. 2011). Maday *et al.* (2012) proposed that the autophagosome can be generated locally along the axons. It is therefore reasonable to think that Rab26 is selectively targeting synaptic vesicles for degradation, contributing to the formation of autophagosomes in the distal and proximal neurite by furnishing membranous structures needed for autophagosome biogenesis. All this data are supporting our theory that Rab26 might be assisting the synaptic vesicle delivery during autophagosome maturation up to the fusion with lysosomes as suggested by the colocalization with LAMP2, the lysosomal receptor protein that modulates selective or Chaperone-mediated autophagy (CMA).

Further investigation in this direction must be performed to better understand the role of Rab26 in regulating the degradation of synaptic vesicle components by the CMA.

4 Materials & Methods

4.1 Materials

4.1.1 Chemicals

All the regular chemicals used during this study were of high purity and only for biochemical analysis. Specific chemicals used for the purpose of this study are listed in the below table (Table 1).

Chemicals	Company
Lysotracker	Invitrogen
DMEM	Lonza
HBSS	Lonza
MITO	Becton Dickinson
Collagen	Becton Dickinson
Neurobasal Medium A (NBA)	Gibco
B-27 Supplement	Gibco
L-glutammine 100X	Lonza
Glutamax –I Supplement	Gibco
Albumin, bovine	Sigma
Penicillin Streptomycin	Roche
FCS	PAA laboratories
Triton-X-100	Sigma-Aldrich
Eupergit C1Z beads	Roehm Pharma
Complete EDTA-free, Protease inhibitor tablet	Roche
IPTG	Formedium
DTT	Formedium
GTPγS	Roche
GDP	Sigma-Aldrich
Eupergit C1Z beads	Roehm Pharma

Table 1 Chemicals

4.1.2 Enzymes

The enzymes used during my studies were purchased from the company listed below (Table 2). They were used according to the manufacturer's protocol.

Enzymes	Company
Restriction Enzyme	NEB
T4 DNA Ligase	NEB
Pfu polymerase	Promega
rApid Alkaline Phosphatase	Roche
Trypsin-EDTA	GIBCO
Papain	Worthington biomedical corporation
Tripsin Inhibitor	Sigma
Thrombin	MP Biomedical
DNaseI	Applichem

Table 2 Enzymes

4.1.3 Kits

Kits used in this study are listed below including the sources from where they were purchased (Table 3). The kits were handled according to the specific instruction given by the company.

Kit	Company
DH5α chemically competent cells	Invitrogen
Gateway pENTR/D-TOPO cloning	Invitrogen
Gateway LR Clonase enzyme mix and reaction buffer	Invitrogen
Lipofectamine ™ 2000	Invitrogen
NucleoSpin ®Plasmid kit	Macherey-Nagel
NucleoSpin® Gel and PCR Clean-up	Macherey-Nagel
NucleoBond® Xtra Midi	Macherey-Nagel
Pierce®BCA Protein assay	Thermo scientific
Western Lightening™ Plus-ECL	Applied Biosystems

Table 3 Kits.

4.1.4 Antibodies

In Table 4 the antibodies used in this study are reported including applications, dilutions and companies.

1° Antibody	Species	Application	Company
Synaptotagmin 41.1	mouse monoclonal	WB (1:1000), ICC (1:400)	Synaptic Systems
Tau	rabbit polyclonal	ICC (1:1000)	Synaptic Systems
Rab26	mouse monoclonal	WB 1:500), ICC (1:100)	Synaptic Systems
Synaptobrevin 69.1	mouse monoclonal	ICC (1:400)	Synaptic Systems
Synaptophysin G96	mouse monoclonal	WB (1:1000), IP,ICC (1:400)	Synaptic Systems
Rab3a	mouse monoclonal	WB (1:100), ICC (1:500)	Synaptic Systems
VAMP4	rabbit polyclonal	ICC (1:500)	Synaptic Systems
Syntaxin6	rabbit polyclonal	ICC (1:500)	Synaptic Systems
Vti1b	rabbit polyclonal	ICC (1:500)	Synaptic Systems
GFP	rabbit polyclonal	WB (1:10.000), IP	Synaptic Systems
Flag	mouse monoclonal	WB (1:20000), ICC (1:1000), IP	Sigma-Aldrich
RFP	rabbit polyclonal	WB (1:1000)	Abcam
LC3B	rabbit polyclonal	WB (1:2000), ICC (1:500-1000)	Novus Biological
EEA1	mouse monoclonal	WB (1.2000), ICC (1:400)	BD Transduction Laboratories™
GM130	mouse monoclonal	ICC (1:200)	BD Transduction Laboratories™
Mitofilin	mouse monoclonal	WB (1:1000), ICC (1:200)	Abcam
Atg16L1	rabbit polyclonal	WB (1:500)	Medical and biological laboratories
Atg16L1	rabbit polyclonal	ICC (1:200-400)	Cosmo Bio *Co.*
LAMP2	mouse monoclonal	ICC (1:200)	Developmental Studies Hybridoma Bank
2° Antibody	**Species**	**Application**	**Company**
mouse IgG (Alexa fluor 488)	goat polyclonal,	WB (1:400), ICC (1:400)	Jackson ImmunoResearch
mouse IgG (Cy2 or Cy3 labeled)	goat polyclonal	WB (1:400), ICC (1:400)	Jackson ImmunoResearch
rabbit IgG (Cy2 or Cy3 labeled)	goat polyclonal	WB (1:400), ICC (1:400)	Jackson ImmunoResearch
mouse IgG (HRP labeled)	goat polyclonal	WB (1:400), ICC (1:400)	BioRad
rabbit IgG (HRP labeled)	goat polyclonal	WB (1:400), ICC (1:400)	BioRad

Table 4 Antibodies

4.1.5 Buffers and Media

The common buffers used during this study are listed in Table 5: Phosphate Buffered Saline (PBS); Tris-Buffered Saline and Tween 20 (TBST); paraformaldehyd(PFA) used for immunocytochemistry (ICC); lysis buffer used to lyse cells; The running buffer was used for Laemmli SDS-PAGE for protein separation. The transfer buffer was used to transfer proteins from the SDS-PAGE gel to the nitrocellulose or PVDF membrane for WB. The blocking buffers were employed respectively to block the membrane prior to WB using dry milk as a blocking reagent or the cells during the ICC procedure using normal goat serum (NGS) as a blocking reagent.

Buffer recipes								
Buffers (1X)	**PBS**	**TBST**	**Running**	**Transfer**	**Blocking (WB)**	**Lysis**	**PFA**	**Blocking (ICC)**
Composition	2.7 mM KCl 1.5 mM KH2PO4 137 mM NaCl 8 mM Na2HPO4 pH 7,4- to filter	150 mM Tris-HCl 1.5 M NaCl 0.5 % Tween 20	25mM Tris-HCl 192 mM Glycine 0.1 % SDS	200 mM Glycin 25 mM Tris 0,04% SDS 20% EtOH	5% dry milk 1XTBST	50 mM HEPES 150 mM NaCl 1mM MgCl2 1% Tx-100 Protease inhibitors pH 7,4- to filter	4% PFA 1XPBS pH 7,4- to filter	10% NGS 1XPBS 0.2% Tx-100 pH 7,4- to filter

Table 5 Buffers and media recipes

4.1.5.1 Antibiotics

Ampicillin and kanamycin were the two antibiotics used in this study for DNA amplification and protein expression in bacteria strains. The following antibiotics were prepared using deionized water. Ampicillin 100 µg/ml (w/v) and Kanamycin 30 µg/ml (w/v).

4.1.5.2 Neuronal culture media

The neuronal culture media is based on the NBA solution that contains: 500 ml Neurobasal A, 50 ml B-27-supplement, 5 ml Glutamax I-stock, 100 U/ml Penicillin/streptomycin.

4.1.5.3 HeLa and HEK 293T feeding media

The feeding media (D10) for HeLa and HEK cells is prepared as follow: DMEM, 10 % FCS, 4 mM glutamine, 100 U/ml penicillin and Streptomycin

4.1.5.4 Bacteria media

E.coli strains were grown in a Luria Bertani (LB) medium containing 10 g tryptone, 5 g yeast extract and 10 g NaCl per 1iter (l).

4.1.6 Mammalian cell lines and bacteria strains

During this study different cell lines were used in different experiments.
The neuronal cultures, from rat brain, and the HeLa ss6 cell lines were used for overexpression studies and immunocytochemistry (ICC) analysis. HeLa and Human Embryonic Kidney 293T (HEK293T) cells were both used for transient transfection and for biochemistry studies. For molecular cloning and for protein expression respectively *E.coli* DH5α and *E.coli* BL21 (DE3) strains were used.

4.1.7 DNA constructs

In Table 6 all the DNA constructs used in this study are listed

Vector	Gene	Mutations site	Tag	Resistance	Source
pEGFP	Rab26	WT; Q123L; T77N; N177I	EGFP	Kan^R	N. Pavlos
pEGFP	Rab26	dcc	EGFP	Kan^R	B. Binotti
mGFP	Rab26	WT	GFP	Kan^R	J. Chua
pCMV-Tag2a	Rab26	WT; Q123L; T77N	Flag	Kan^R	B. Binotti
pcDNA 3.1(+)	Rab26	WT; Q123L; T77N	-	Kan^R	B. Binotti
pGEX-KG	Rab26	WT; Q123L; T77N; N177I	GST	Amp^R	N. Pavlos
pEGFP	Rab7	WT	EGFP	Kan^R	N. Pavlos
pEGFP	Rab33	WT	EGFP	Kan^R	N. Pavlos
GFP	LC3B	WT	GFP	Kan^R	Z. Elazar
mRFP	LC3A	WT	RFP	Kan^R	B. Binotti
mRFP	Rab5	WT; Q79L	RFP	Kan^R	S. Kioke

Table 6 DNAs and Vectors

4.1.8 Primers

Primers used for cloning Rab26 and LC3 in the different vectors are listed below in Table 7

Sequences: 5´-3´	Name	Restriction site	Vectors
CGCGGATCCCATGTCCAGGAA	Rab26_forward	BamHI	pCMV-Tag2a
CCGCTCGAGTCATCAAGGGCG	Rab26_reverse	XhoI	pCMV-Tag2a
CGCGGATCCCACCATGGACGT CGCCTTCAAGGTCATGC	Rab26_forward	BamHI	pcDNA3.1(+)
CCGCTCGAGTCATCAAGGGCG GCAGCAGGA	Rab26_reverse	XhoI	pcDNA3.1(+)
GAGAAGATCTATGTCCAGGAAG AAGACCCCCA	Rab26dcc_forward	BaglII	pEGFP-C1
CGCGGATCCTCAGGAGGCCCC	Rab26dcc_reverse	BamHI	pEGFP-C1
CCGCTCGAGCTATGCCCTCCGA CCGGCCTTTC	LC3A_forward	XhoI	pmRFP-C1
CGCGGATCCTCAGAAGCCGAAG GTTTCTTGGGAG	LC3A_reverce	BamHI	pmRFP-C1

Table 7 Oligonucleotides

4.2 Methods

4.2.1 Molecular biology methods

4.2.1.1 Molecular cloning

Standard cloning procedures were used to generate the different Rab26 constructs that include not only the WT but also the constitutively active (CA)/GTP locked form and the dominant negative (DN)/GDP locked form. Rab proteins share the same and well characterized organization of the small GTPase domain. The point mutations to get either the CA, or the DN forms are well defined (Li and Stahl 1993). The single point mutations for Rab26 were identified by alignment with the closest relative mRab37 which shares 74% sequence identity with Rab26 and for which the mutation sites were already characterized (Masuda *et al.* 2000). The sequences alignment between *Mus musculus* Rab37 (gi|112293035|) and *Homo sapiens* Rab26 (gi|46361978|) was performed using T-coffee algorithm. Rab26 CA could be generated by replacing the Glutamine residue Q123 with a Lysine (L) and the DNs by substituting Threonine T77 with Asparagine (N) or substituting Asparagine 177 (N177) with Isoleucine (I) (Figure 27, green boxes). The different Rab26 constructs were obtained using a standard PCR protocol. Specific primers for the specific vectors are listed in Table 7.

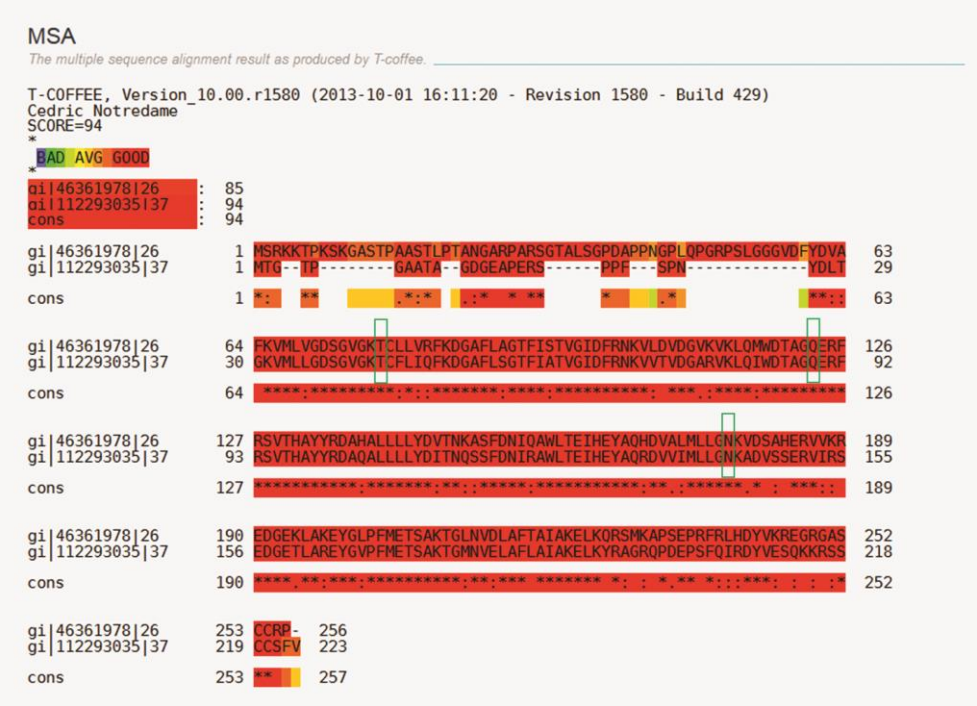

Figure 27 Rab26 and Rab37 sequence alignment

Human Rab26 and mouse Rab37 are close relatives. They share 74% of sequence identity (Masuda *et al.* 2000). Rab37Q89L corresponds to Rab26Q123L; whereas Rab37T43N corresponds to Rab26T77N. The two position are highlighted with green rectangles. The third green rectangle is the Asparagine residue that once substituted with the Isoleucine (I) gives the nucleotide-free state of the Rab protein. T-coffee is the algorithm used for the sequence alignment.

4.2.1.2 Cloning procedure

To clone genes into specific vectors the desired cDNA was amplified using a standard PCR protocol. The PCR products were obtained using the DNA polymerase *Pfu* (Promega) following the protocol in Table 8.

Master Mix (PCR buffer reaction)	**100 µl reaction**	**PCR cycles**	
Buffer (10X)	10	(1) Initial denaturation	98 °C, 1 min
water	77	(2) Denaturation	98 °C, 30 sec
dNTPs (10 mM)	4	(3) Annealing	65°C, 30 sec
Template (5 nM)	4	(4) Elongation	72°C, 2 min/1kb
Primer_forward (15 µM)	2	n° of cycles	Step 2 to 4 performed 30X
Primer_reverse (15 µM)	2	(5) Final extension	72°C, 5 min
Pfu	1	pause	4°C

Table 8 PCR cycles**.**

The PCR products (or inserts) obtained were monitored by agarose gel electrophoresis and purified by gel extraction using a commercial kit (4.1.3). The DNA was loaded on 1% agarose gel using 100 mM Tris-boric acid EDTA-free buffer. Subsequently the purified PCR products were digested for 3 hours at 37°C with the specific restriction enzymes (NEB) and subjected to a second purification step using a PCR clean up kit (4.1.3). At the same time the vectors were digested with the same restriction enzymes and gel purified. Insert and vector were then ligated using the same amount of mole ratio, or with excess of insert. The ligation was performed in 10 µl of reaction using T4-DNA ligase (NEB) according to the manufacturer's protocol. 3 to 4 µl of the reaction were then used for heat shock transformation.

4.2.1.3 Bacteria transformation

Chemically competent *E.coli* DH5α (Invitrogen) were transformed using a heat shock transformation protocol that consists in incubating 50 µl of the competent cells with either normal plasmid or with the ligation reaction in a 2 ml Eppendorf tube. The DNA/cells mixture was then incubated for 30 min on ice. Afterwards the sample was heat shocked for 50 sec at 42°C, let recover on ice for 2 min and for 45-60 min at 37°C in presence of 500-1000 µl of SOC medium under constant agitation. Finally the cells were shortly centrifuge at 13.000 rpm for 1 min, the supernatant was discarded and a fresh LB medium (around 150 µl) was used to re-suspend the pellet. The cells were plated on agar plate with the desired antibiotic for colony selection. The positive colonies were isolated to check for the presence of the insert.

4.2.1.4 Plasmid purification

A single positive colony was grown overnight (ON) in a 13 ml round bottom tube (SARSTED) with 6 ml LB-medium in presence of antibiotic. Then the culture was centrifuged for 10 min at 4.000 rpm using a micro centrifuge (Eppendorf centrifuge 5702R). The medium was discarded and the plasmids were extracted from the cell pellet using a plasmid extraction kit (NucleoSpin ®Plasmid kit). The DNA concentration was measured using a NanoDrop machine (NanoDrop® ND 1000 PEQLAB, Thermo Scientific). 200 ng of the purified plasmid was then subjected to digestion and the fragments were analyzed by

agarose gel. 1 µg of the positive plasmid were then sent for DNA sequencing (eurofins genomics mwg/operon)

4.2.1.5 Protein expression and purification

Human Rab26 was cloned in a pGEX-KG vector using the EcoRI and BamHI cleavage sites. The plasmid was then transformed in BL21 (D3). 200 ml pre-culture were grown at 37°C ON. 10 ml of ON culture were inoculated in 1l fresh LB medium supplemented with 100 µg/ml Ampicillin for 2.5 hours up to an OD of 0.6-0.8. Subsequently before IPTG induction, the cultures were let grow for 1 hour at 16°C. The expression was achieved by addition of 1 mM IPTG ON at 16°C. The cells were harvested by centrifugation at 4000 rpm for 10 min using a Bachman centrifuge. 1l pellet was re-suspended in 25 mL protein buffer (PB) (50 mM HEPES pH 7.4, 500 mM NaCl, 5 mM DTT, 5 mM $MgCl_2$, complete protease inhibitor, 100 µM GTPγS/GDP) and supplemented with a few crystals of DNase. The samples were left for 10-15 min at 4°C and subsequently sonicated 4 times for 30 sec each, with 1 min interval on ice to cool down, using a Branson Sonifier 450. The lysate was then cleared at 13.000 rpm using SLA 1500 rotor for 40 min at 4°C. The supernatant was collected and filtered using a 0, 45 µm Whatman filter. The sample was afterwards loaded onto a GST-column (GST Trap4B GE Healthcare) and eluted using 30 mM glutathione in PB. The eluted fractions were collected and dialyzed using PB to remove glutathione, three times for 3 hours each. The purified proteins were then used for GST pull down assay (4.2.3.7) or frozen in liquid nitrogen and kept at -80°C

4.2.2 Cell biology methods

4.2.2.1 Mammalian cell cultures

4.2.2.1.1 Cell lines and primary neuronal cultures

HeLa ss6 and HEK 293T were cultured using D10 medium containing DMEM, 10% fetal calf serum (FCS), 4 mM glutamine and 100 units/ml penicillin/streptomycin. They were maintained in a 10-cm petri dishes for 2-3 days at 37°C and 90% humidity in 5% CO_2. When they reached the confluence of 80%-90% they were passaged and diluted (usually 1:10). The splitting procedure was as follows: first the cells were washed once with a pre-warmed (37°C) 1X PBS, and then they were incubated with 1 ml of Trypsin EDTA for 4 min in at 37°C or 1 min at RT for HEK cells. Subsequently the trypsin activity was inhibited by the addition of fresh medium (around 10 ml). The cells were then collected in a 15 ml Falcon tube and centrifuged at 1000 g for 2 min at room temperature (RT). The supernatant was discarded and the cell pellet was re-suspended in 10 ml fresh D10 medium. 1 ml of the suspension was then added on the 10-cm petri dish containing 9 ml D10 medium. The cells were then re-incubated until the next passage. All the steps were carried out in a sterile condition under a lamina-hood

Primary hippocampal neurons were used to prepare high dense cultures. The hippocampal regions were first isolated from the brain of a new born rat (day of in vitro development 0, DIV 0). 75 000 cells were seeded in a 12 well plate and maintained till DIV 20 in a medium containing NBA solution (4.1.5.2). The cells were grown and developed at 37°C and 95% humidity in 5% CO_2. The cultures were kindly prepared by Sigrid Schmidt.

4.2.2.2 Transient transfection

Mammalian cell lines were transiently transfected using Lipofectamin™ 2000 (Invitrogen) following manufacturer's instructions. Briefly cells were seeded a day before in 12 well plates until the confluence was about 70%-80%. 3 µl/well of Lipofectamine was diluted in 100 µl of DMEM without supplement for 5 min. Subsequently 1 µg of DNA diluted in 100 µl of DMEM was combined with the diluted Lipofectamine. The transfection mix was then incubated at RT for 20 min and after addition to the cells, incubated at 37°C for 4 hours. Finally the medium was replaced with fresh D10 medium. The plate was then incubated for 24-48 hours at 37°C. Subsequently the transiently expressing cells were either fixed and subjected to ICC for microscope analysis or lysed for biochemistry studies.

The transfection protocol was optimized for neuronal culture. Neurons were transfected at DIV 7-9. First the cells were moved into a new 12-well plate with 800 µl freshly prepared NBA medium. The old medium was put back in the incubator. 160 µl of transfection mix containing 1 µg of DNA and 2 µl Lipofectamine were added on top of each well. The neurons were then incubated for 4 hours. Subsequently the cells were washed once with pre-warmed fresh NBA medium and then they were placed back into the initial growing medium for another 24-48 hours. In the experiments performed in Figure 12 and Figure 13 neurons were transiently transfected for 48 hours using a calcium phosphate transfection method (for protocol see Pavlos *et al.* (2010)).

4.2.2.3 Transferrin assay

For the transferrin uptake, Alexa Fluor 488-conjugated transferrin was diluted 1:100 in pre-warmed (37°C) OptiMEM medium and added on the neuronal or HeLa cultures for 5 min or 30 min (to label recycled and early endosomes). After incubation the cells were washed 3 times in PBS and fixed with 4 % PFA for direct microscopy analysis.

4.2.2.4 Lysosome stain

LysoTracker® Red (Invitrogen) is a florescent-labeled dye that is canonically used to visualize acidic compartments such as lysosomes in live cells. Cultured neurons and HeLa cells were labeled with Lysotracker following the manufacturer's instructions.

4.2.2.5 In vivo recycling assay

For the *in vivo* recycling assay neurons were incubated for 24 hours with anti Synaptotagimin-Oyster-550 labeled antibody (Synaptic Systems) that recognizes the luminal domain of Synaptotagmin. The incubation was performed during all the time of transient expression of EGFP-Rab26 constructs. Subsequently the cells were washed twice with PBS then they were directly fixed and analyzed under the microscope.

4.2.2.6 Immunofluorescence stain

Transiently transfected cells or neurons from DIV-12 to DIV-16 were washed once with PBS to remove the serum. Then the cells were fixed using 4% PFA for 15 min at RT. The fixative was removed and the cells were washed 3 times 5 min each with PBS. Afterward the cells were blocked with 10% NGS and 0, 2% Triton-X-100 in PBS for 1 hour. The coverslips were inverted on top of a drop of 45-50 µl of primary antibody diluted in blocking buffer. The incubation was performed in a dark and humidified chamber for 1 to 2 hours at RT or ON at 4°C. Subsequently the coverslips were placed back in their 12-well plates and washed 3 times for 5 min each with PBS and incubated again following the same procedure with the secondary antibody for 1 hour at RT. Finally the cells were washed as previously described and mounted on a microscope slides using a mounting media (Fuoro-Gel, Electron Microscopy Sciences, or VECTASHIELD HardSet Mounting Medium with DAPI, Vector Laboratory). The mounting media was let dry ON at 4°C.

4.2.2.7 Image acquisition and processing

For the image acquisition of immunostained samples AOBS SP2 (Leica), or LSM 780 (ZEISS) confocal microscopes were used. The images shown in Figure 20 were acquired using an epifluorescence microscope (Axioverter 200M, ZEISS). ImageJ or LAS AF Lite software from Leica were used for colocalization studies (linescans).

4.2.2.8 Electron microscopy

For immunoelectron microscopy, ultrathin cryosections were prepared as described previously in (Tokuyasu 1973, Tokuyasu 1980, Zink *et al.* 2009). The images were processed by Dirk Wenzel (Facility for transmission electron microscopy, MPI for Biophysical Chemistry, Göttingen). For the ultrastucural analysis of immunoisolated synaptic vesicles the same procedure described in Takamori *et al.* (2000) was applied. Image acquisition and data processing was performed by Dietmar Riedel (Facility for transmission electron microscopy, MPI for Biophysical Chemistry, Göttingen).

4.2.3 Biochemistry methods

4.2.3.1 SDS polyacrylamide gels (SDS-PAGE) and Western Blotting (WB)

To separate proteins and cell protein extracts a denaturing polyacrylamide gel was applied (Laemmli 1970). The Laemmli method is based on a discontinuous PAGE system composed of a collecting or stacking gel (4% bis-acrylamide, 0.1% SDS, 1 M Tris pH 6,8) and of a separating gel (10% bis-acrylamide, 0.1% SDS, 10% glycerol, 1 M Tris pH 8.45). The polymerization reaction was catalyzed by the addition of ammoniumpersulfate (APS) and TEMED. 2X loading dye (120 mM Tris pH 8,8, 20% (v/v) glycerol, 4% (w/v) SDS, 0,02% (w/v) bromophenol blue, 5% (v/v) β-Mercaptoethanol) was added in the samples which then were boiled for 5 min at 95°C prior loading them on the gel. The gel was run using SDS-PAGE running buffer (25mM Tris-HCl, 192 mM Glycine, 0.1 % SDS). The gel was stopped and subjected to visualization either by coomassie blue stain, or by WB.

For Western blotting detection, proteins separated by SDS-PAGE were transferred onto a nitrocellulose membrane (Potran 0, 2 µm nitrocellulose transfer membrane PerkinElmer) or polyvinylidenfluorid (PVDF) (0, 45µm Millipore) membrane. Transfer was performed using transfer buffer (200 mM Glycin 25 mM Tris 0,04% SDS 20% EtOH) either in a semidry system (Semi dry blotter PEGASUS) applying 50 mA current per gel for 1 hour at RT, or in wet system (BioRad) using 70V for 1 hour at 4°C.
After checking the transfer by Ponceau S stain, the membrane was first washed once with TBST buffer and incubated for at least 1 hour at RT with blocking solution containing 5% of nonfat milk powder in TBST. Subsequently a primary antibody diluted in the blocking buffer was applied and the membrane was incubated ON at 4° on an agitating platform. Afterwards the membrane was washed 3 times for 10 min each prior to incubation for 1 hour at RT with an HRP-conjugated secondary antibody. Finally the membrane was washed again 3 times for 10 min and incubated for 1 min with the Western Lightening™ *Plus*-ECL reagent that allowed the detection of the protein bands using a chemiluminescence detection apparatus (FUJIFILM LAS-1000).

4.2.3.2 Native gel

To observe the behavior of proteins in their native condition, a blue native protein gel (Invitrogen) was used according to the manufacturer's instructions.

4.2.3.3 Differential centrifugation

Transiently transfected HeLa cells (two 15-cm petri dishes) were first washed with pre-warmed PBS and then detached from the plates using Trypsin EDTA for 4 min at 37°C. The Trypsin activity was inactivated by the addition of pre-warmed growing media (D10). The cell were collected in a Falcon tube and centrifuged once at 1000 g for 3 min. The medium was removed, the cell pellet was washed once with ice-cold PBS, centrifuged again as before, and the supernatant (SN) was discarded. Subsequently the pellet was washed once with ice-cold homogenization buffer (250 mM sucrose and 3 mM imidazole at pH 7, 4), and centrifuged as before. Twice the volume of the pellet of homogenization buffer supplemented

with complete EDTA-free protease inhibitors was used to re-suspend the cells. The cells were then applied through a pre-equilibrated and pre-cooled ball homogenizer with a 1 ml syringe at least 10 times to break the plasma membranes. The homogenized cells were then transferred to a 1.5 ml test tube and subjected to 2000 g centrifugation for 15 min. The nuclear pellet (P1) was kept. The post nuclear supernatant (PNS) was centrifuged at 32.000 g using a Beckmann centrifuge in a TLS 55 rotor for 15 min. In this way a pellet (P2) and a soluble fraction (S2) were generated. Finally the S2 was centrifuged at 100.000 g for 30 min allowing the separation of a pellet (P3) and the supernatant (S3) fraction. Each step was carried out at 4°C. The protein concentration of all the fractions was measured using BCA protein assay Kit (ThermoFischer) following the manufacturer's instructions. 10 µg of each fraction were loaded on a SDS-PAGE and the protein profile was analyzed by WB (see section 4.2.3.1).

4.2.3.4 Brain subcellular fractionation

The isolation and characterization of highly purified rat SVs is based on the protocol described in Huttner *et al.* (1983) and Takamori *et al.* (2006). Briefly rat brain homogenate was centrifuged to get the synaptosome pellet (P2´) and the cytosol (S3) fraction. Subsequently the synaptosomes were lysed by osmotic shock and then subjected to two low speed centrifugation steps to obtain a crude synaptic vesicle pellet (LP2) and the cytosol SN (LS2) fractions. High pure synaptic vesicles were obtained by purifying LP2 first by sucrose density gradient centrifugation and then by size exclusion chromatography.

4.2.3.5 RabGDI extraction assay

The RabGDI assay was performed as described in Pavlos *et al.* (2010). The crude synaptic vesicles (LP2) were used as a starting material. 50 µg of LP2 were pre-incubated with 500 µM GDP or 500 µM GTPγS for 15 min at 37°C in 200 µl of extraction buffer (EB) containing 50 mM HEPES-KOH pH 7, 4; 100 mM KCl; 5 mM $MgCl_{2;}$ 10 mM EDTA; protease inhibitors. Then in each sample both PBS (control) or 5 µM HIS-GDI were added and the samples were re-incubated for additional 45 min at 37 °C. The samples were then kept on ice and subsequently centrifuged for 20 min at 200.000 g (95.000 rpm) at 4 °C using S100 AT3

rotor. The supernatants were collected for further analysis and the pellet was re-suspended in 50 µl 2X LDS, boiled at 95°C for 5 min and analyzed by WB.

4.2.3.6 Antibody coupling and Immunoisolation

For the immunoisolation of a subpopulation of synaptic vesicles from the rat brain LP2 fraction, the monoclonal Rab26 antibody (clone 163E12, Synaptic Systems) and the monoclonal Synaptophysin antibody (clone 7.2, Synaptic Systems) were coupled to immunobeads (Eupergit C1Z methacrylate microbeads; Röhm Pharmaceuticals) as previously described (Burger *et al.* 1989, Takamori *et al.* 2000, Boyken *et al.* 2013).

Precisely 1,5 mg/ml of affinity purified Rab26 antibody was loaded into dialysis cassettes (10.000 MW, cut off Thermo Scientific) and dialyzed for 3 days in 500 ml of 150 mM NaCl (three changes per day). After dialysis the antibody solution was centrifuged at 10.000 g for 15 min, the supernatant (SN) was collected and the concentration was measured and kept for coupling. Meanwhile the beads were weight. 25 mg of beads were used for 1 mg/ml of antibody. Beads were washed twice with water followed each time by vigorous vortexing and 2 minute sonication to break down the clumped beads in isolated particles. They were then spinned down at 4500 rpm for 6 min. After removing the SN from the second wash, the pellet was incubated with the antibody after vigorous vortexing and incubated for 8 hours on a rotating wheel at 21°C. Then the beads were centrifuged for 6 min at 4500 rpm and the supernatant was saved to measure the coupling efficiency by determining the antibody concentration from the SN. Usually the coupling efficiency was around 35%- 40%. 1 M glycin was then added to the bead pellet and incubated ON under constant rotation at 21°C to quench unspecific binding sites. Afterwards the beads were pelleted at 4500 rpm for 6 min and the supernatant was discarded. Finally the beads were washed three times alternating two different buffers containing 0,1 M Na-Acetate, 0, 5 M NaCl pH 4,5 and 0,1 M Tris, 0, 5 M NaCl pH 8,0. After washing once with PBS, the beads were stored in 4 volumes of PBS. The coupled beads were then used for immunoisolation.

For the immunoisolation of vesicles from LP2 a protocol previously describe in (Boyken *et al.* (2013)) was used. Briefly 10 µl of immunobeads were incubated with 400 µg of LP2 re-suspended in the immunoisolation buffer (IB) that contains 1X PBS, 3 mg/ml BSA, 2,25 mM HEPES pH 7,4, protease inhibitor cocktail (Roche) in a final volume of 500 µl in the presence or in the absence of 1% Tx-100 and incubated ON at 4°C under constant rotation. Then the

samples were centrifuged at 2000 rpm at 4°C for 2 min and the SN was collected for further analysis. The beads were subjected to 3 washes with PBS. Each wash was performed for 5 min at 4°C on a rotating wheel followed by 2 min of centrifugation at 2000 rpm. After the third wash, the beads were centrifuged at 6000 g for 1 min to completely remove the SN. At this point the pellet was either send for electron microscopy (EM) analysis or the protein composition was characterized by WB or mass spectrometry (MS).

4.2.3.7 Immunoprecipitation and GST-pull down

Transiently transfected cells were washed once with ice-cold PBS and then lysed using lysis buffer (50 mM HEPES, 150 mM NaCl, 5mM $MgCl_2$, 1% Tx-100 and protease inhibitor) for 30 min. The lysate was then pre-cleared by centrifugation at 10.000 g for 10 min. 30 µl of the SN were collected for the input, and the rest was incubated with the antibody (anti mouse Flag or anti rabbit GFP antibody) for 2 hours on a rotating wheel. Meanwhile the IgG Sepharose beads (GE Healthcare*)* were first washed once with water and then equilibrated with lysis buffer until use. Subsequently the samples were incubated with 30 µl of pre-equilibrated slurry beads for 1 hour under constant rotation. After incubation the samples were centrifuged at 3000 g for 1 min. The SN was collected and the beads were washed 3 times for 1 min at 3000 g with lysis buffer. After the third wash, the beads were centrifuged for 1 min at 12.000 g to completely remove the buffer. The samples were kept at 4°C or on ice during all the steps. Finally the beads were eluted with 25-30 µl of 2X loading dye (LDS), and together with the input were boiled at 95°C for 5 min. 15 µl of the IP samples and 5 µl of the input were loaded on the SDS-PAGE and subsequently transferred onto nitrocellulose or PVDF membrane. The membrane was then probed with the primary antibody against the protein of interest. WB was performed as describe in section 4.2.3.1.

For GST pulldown assay 10 µg of purified GST-Rab26 variants were incubated with Sepharose Glutathione beads (Glutathione Sepharouse^{TM} Fast Flow GE Healthcare) for 1 hour under constant rotation in presence of protein buffer (50 mM HEPE pH 7.4, 200 mM NaCl, 5 mM DTT, 5 mM $MgCl_2$, 10 µM GTPγS/GDP, 1% NP40). Subseq uently a pre-formed complex His-Atg16L1^{NT}/His-Atg5^{FL} was added to the beads and incubated for an additional 2 hours under the same conditions. The samples were then washed 3 times with the protein buffer. Each wash was followed by a centrifugation step for 2 min at 3000 g. Each step was

accomplished on ice or at 4°C. 2X LDS was used to elute the proteins from the beads and 15 µl of each sample were subjected to SDS-PAGE and then analyzed by western blot.

5 References

Aakalu, G., W. B. Smith, N. Nguyen, *et al.* (2001). "Dynamic Visualization of Local Protein Synthesis in Hippocampal Neurons." Neuron **30**(2): 489-502.

Albert, S. and D. Gallwitz (1999). "Two new members of a family of Ypt/Rab GTPase activating proteins. Promiscuity of substrate recognition." J Biol Chem **274**(47): 33186-33189.

Albert, S., E. Will and D. Gallwitz (1999). "Identification of the catalytic domains and their functionally critical arginine residues of two yeast GTPase-activating proteins specific for Ypt/Rab transport GTPases." EMBO J **18**(19): 5216-5225.

Aravamudan, B., T. Fergestad, W. S. Davis, *et al.* (1999). "Drosophila UNC-13 is essential for synaptic transmission." Nat Neurosci **2**(11): 965-971.

Atwood, H. L., F. Lang and W. A. Morin (1972). "Synaptic vesicles: selective depletion in crayfish excitatory and inhibitory axons." Science **176**(4041): 1353-1355.

Augustin, I., C. Rosenmund, T. C. Sudhof, *et al.* (1999). "Munc13-1 is essential for fusion competence of glutamatergic synaptic vesicles." Nature **400**(6743): 457-461.

Balaji, J. and T. A. Ryan (2007). "Single-vesicle imaging reveals that synaptic vesicle exocytosis and endocytosis are coupled by a single stochastic mode." Proc Natl Acad Sci U S A **104**(51): 20576-20581.

Barr, F. and D. G. Lambright (2010). "Rab GEFs and GAPs." Curr Opin Cell Biol **22**(4): 461-470.

Becherer, U. and J. Rettig (2006). "Vesicle pools, docking, priming, and release." Cell Tissue Res **326**(2): 393-407.

Bedford, F. K., J. T. Kittler, E. Muller, *et al.* (2001). "GABA(A) receptor cell surface number and subunit stability are regulated by the ubiquitin-like protein Plic-1." Nat Neurosci **4**(9): 908-916.

Berg, T. O., M. Fengsrud, P. E. Stromhaug, *et al.* (1998). "Isolation and characterization of rat liver amphisomes. Evidence for fusion of autophagosomes with both early and late endosomes." J Biol Chem **273**(34): 21883-21892.

Betz, A., P. Thakur, H. J. Junge, *et al.* (2001). "Functional interaction of the active zone proteins Munc13-1 and RIM1 in synaptic vesicle priming." Neuron **30**(1): 183-196.

Blondeau, F., B. Ritter, P. D. Allaire, *et al.* (2004). "Tandem MS analysis of brain clathrin-coated vesicles reveals their critical involvement in synaptic vesicle recycling." Proc Natl Acad Sci U S A **101**(11): 3833-3838.

Blumcke, S., H. R. Niedorf, J. Rode, *et al.* (1968). "[Degeneration of peripheral aminergic nerves]." Verh Dtsch Ges Pathol **52**: 228-233.

Blumer, J., J. Rey, L. Dehmelt, *et al.* (2013). "RabGEFs are a major determinant for specific Rab membrane targeting." J Cell Biol **200**(3): 287-300.

Blumstein, J., V. Faundez, F. Nakatsu, *et al.* (2001). "The neuronal form of adaptor protein-3 is required for synaptic vesicle formation from endosomes." J Neurosci **21**(20): 8034-8042.

Boyken, J., M. Grønborg, D. Riedel, *et al.* (2013). "Molecular Profiling of Synaptic Vesicle Docking Sites Reveals Novel Proteins but Few Differences between Glutamatergic and GABAergic Synapses." Neuron **78**(2): 285-297.

Brighouse, A., J. B. Dacks and M. C. Field (2010). "Rab protein evolution and the history of the eukaryotic endomembrane system." Cellular and Molecular Life Sciences **67**(20): 3449-3465.

Brose, N., C. Rosenmund and J. Rettig (2000). "Regulation of transmitter release by Unc-13 and its homologues." Curr Opin Neurobiol **10**(3): 303-311.

Burger, P. M., E. Mehl, P. L. Cameron, *et al.* (1989). "Synaptic vesicles immunoisolated from rat cerebral cortex contain high levels of glutamate." Neuron **3**(6): 715-720.

Busse, R. A., A. Scacioc, J. M. Hernandez, *et al.* (2013). "Qualitative and quantitative characterization of protein-phosphoinositide interactions with liposome-based methods." Autophagy **9**(5): 770-777.

Campbell, D. S. and C. E. Holt (2001). "Chemotropic responses of retinal growth cones mediated by rapid local protein synthesis and degradation." Neuron **32**(6): 1013-1026.

Ceccarelli, B., W. P. Hurlbut and A. Mauro (1973). "Turnover of transmitter and synaptic vesicles at the frog neuromuscular junction." J Cell Biol **57**(2): 499-524.

Chang-Ileto, B., S. G. Frere, R. B. Chan, *et al.* (2011). "Synaptojanin 1-mediated PI(4,5)P2 hydrolysis is modulated by membrane curvature and facilitates membrane fission." Dev Cell **20**(2): 206-218.

Chapman, E. R., S. An, J. M. Edwardson, *et al.* (1996). "A novel function for the second C2 domain of synaptotagmin. Ca2+-triggered dimerization." J Biol Chem **271**(10): 5844-5849.

Chapman, E. R., P. I. Hanson, S. An, *et al.* (1995). "Ca2+ regulates the interaction between synaptotagmin and syntaxin 1." J Biol Chem **270**(40): 23667-23671.

Chavas, L. M., S. Torii, H. Kamikubo, *et al.* (2007). "Structure of the small GTPase Rab27b shows an unexpected swapped dimer." Acta Crystallogr D Biol Crystallogr **63**(Pt 7): 769-779.

Cherfils, J. and M. Zeghouf (2013). "Regulation of small GTPases by GEFs, GAPs, and GDIs." Physiol Rev **93**(1): 269-309.

Chiang, H. L. and J. F. Dice (1988). "Peptide sequences that target proteins for enhanced degradation during serum withdrawal." J Biol Chem **263**(14): 6797-6805.

Chua, C. E., B. Q. Gan and B. L. Tang (2011). "Involvement of members of the Rab family and related small GTPases in autophagosome formation and maturation." Cell Mol Life Sci **68**(20): 3349-3358.

Chua, J. J., S. Kindler, J. Boyken, *et al.* (2010). "The architecture of an excitatory synapse." J Cell Sci **123**(Pt 6): 819-823.

Clayton, E. L. and M. A. Cousin (2008). "Differential labelling of bulk endocytosis in nerve terminals by FM dyes." Neurochemistry International **53**(3–4): 51-55.

Colicelli, J. (2004). "Human RAS superfamily proteins and related GTPases." Sci STKE **2004**(250): RE13.

Cuervo, A. M. and J. F. Dice (2000). "Regulation of lamp2a levels in the lysosomal membrane." Traffic **1**(7): 570-583.

Cuervo, A. M., L. Stefanis, R. Fredenburg, *et al.* (2004). "Impaired degradation of mutant alpha-synuclein by chaperone-mediated autophagy." Science **305**(5688): 1292-1295.

d'Azzo, A., A. Bongiovanni and T. Nastasi (2005). "E3 ubiquitin ligases as regulators of membrane protein trafficking and degradation." Traffic **6**(6): 429-441.

Dahm, R., M. Zeitelhofer, B. Götze, *et al.* (2008). Visualizing mRNA Localization and Local Protein Translation in Neurons. Methods in Cell Biology. F. S. Kevin, Academic Press. **Volume 85:** 293-327.

Dai, H., N. Shen, D. Arac, *et al.* (2007). "A quaternary SNARE-synaptotagmin-Ca2+-phospholipid complex in neurotransmitter release." J Mol Biol **367**(3): 848-863.

Daitoku, H., J. Isida, K. Fujiwara, *et al.* (2001). "Dimerization of small GTPase Rab5." Int J Mol Med **8**(4): 397-404.

Delprato, A., E. Merithew and D. G. Lambright (2004). "Structure, exchange determinants, and family-wide rab specificity of the tandem helical bundle and Vps9 domains of Rabex-5." Cell **118**(5): 607-617.

Di Paolo, G. and P. De Camilli (2006). "Phosphoinositides in cell regulation and membrane dynamics." Nature **443**(7112): 651-657.

DiAntonio, A., A. P. Haghighi, S. L. Portman, *et al.* (2001). "Ubiquitination-dependent mechanisms regulate synaptic growth and function." Nature **412**(6845): 449-452.

Dice, J. F. (2007). "Chaperone-mediated autophagy." Autophagy **3**(4): 295-299.

Dice, J. F. and H. L. Chiang (1989). "Peptide signals for protein degradation within lysosomes." Biochem Soc Symp **55**: 45-55.

Du, L. L., R. N. Collins and P. J. Novick (1998). "Identification of a Sec4p GTPase-activating protein (GAP) as a novel member of a Rab GAP family." J Biol Chem **273**(6): 3253-3256.

Dunn, W. A., Jr. (1994). "Autophagy and related mechanisms of lysosome-mediated protein degradation." Trends Cell Biol **4**(4): 139-143.

Fader, C. M. and M. I. Colombo (2009). "Autophagy and multivesicular bodies: two closely related partners." Cell Death Differ **16**(1): 70-78.

Fader, C. M., D. Sanchez, M. Furlan, *et al.* (2008). "Induction of autophagy promotes fusion of multivesicular bodies with autophagic vacuoles in k562 cells." Traffic **9**(2): 230-250.

Fader, C. M., D. G. Sanchez, M. B. Mestre, *et al.* (2009). "TI-VAMP/VAMP7 and VAMP3/cellubrevin: two v-SNARE proteins involved in specific steps of the autophagy/multivesicular body pathways." Biochim Biophys Acta **1793**(12): 1901-1916.

Fasshauer, D., W. K. Eliason, A. T. Brunger, *et al.* (1998). "Identification of a minimal core of the synaptic SNARE complex sufficient for reversible assembly and disassembly." Biochemistry **37**(29): 10354-10362.

Faundez, V., J. T. Horng and R. B. Kelly (1998). "A function for the AP3 coat complex in synaptic vesicle formation from endosomes." Cell **93**(3): 423-432.

Ferguson, M. L., K. Prasad, H. Boukari, *et al.* (2008). "Clathrin Triskelia Show Evidence of Molecular Flexibility." Biophysical Journal **95**(4): 1945-1955.

Ferguson, S. M., G. Brasnjo, M. Hayashi, *et al.* (2007). "A selective activity-dependent requirement for dynamin 1 in synaptic vesicle endocytosis." Science **316**(5824): 570-574.

Fesce, R., F. Grohovaz, F. Valtorta, *et al.* (1994). "Neurotransmitter release: fusion or 'kiss-and-run'?" Trends in Cell Biology **4**(1): 1-4.

Finley, D. (2009). "Recognition and processing of ubiquitin-protein conjugates by the proteasome." Annu Rev Biochem **78**: 477-513.

Finn, P. F. and J. F. Dice (2005). "Ketone bodies stimulate chaperone-mediated autophagy." J Biol Chem **280**(27): 25864-25870.

Fuchs, E., A. K. Haas, R. A. Spooner, *et al.* (2007). "Specific Rab GTPase-activating proteins define the Shiga toxin and epidermal growth factor uptake pathways." J Cell Biol **177**(6): 1133-1143.

Fukuda, M. (2003). "Distinct Rab binding specificity of Rim1, Rim2, rabphilin, and Noc2. Identification of a critical determinant of Rab3A/Rab27A recognition by Rim2." J Biol Chem **278**(17): 15373-15380.

Fukuda, M. (2008). "Regulation of secretory vesicle traffic by Rab small GTPases." Cell Mol Life Sci **65**(18): 2801-2813.

Fukuda, M. and T. Itoh (2008). "Direct link between Atg protein and small GTPase Rab: Atg16L functions as a potential Rab33 effector in mammals." Autophagy **4**(6): 824-826.

Gallwitz, D., C. Donath and C. Sander (1983). "A yeast gene encoding a protein homologous to the human c-has/bas proto-oncogene product." Nature **306**(5944): 704-707.

Garrett, M. D., J. E. Zahner, C. M. Cheney, *et al.* (1994). "GDI1 encodes a GDP dissociation inhibitor that plays an essential role in the yeast secretory pathway." EMBO J **13**(7): 1718-1728.

Geppert, M., Y. Goda, R. E. Hammer, *et al.* (1994). "Synaptotagmin I: a major Ca2+ sensor for transmitter release at a central synapse." Cell **79**(4): 717-727.

Gerondopoulos, A., L. Langemeyer, J. R. Liang, *et al.* (2012). "BLOC-3 mutated in Hermansky-Pudlak syndrome is a Rab32/38 guanine nucleotide exchange factor." Curr Biol **22**(22): 2135-2139.

Glyvuk, N., Y. Tsytsyura, C. Geumann, *et al.* (2010). "AP-1/sigma1B-adaptin mediates endosomal synaptic vesicle recycling, learning and memory." EMBO J **29**(8): 1318-1330.

Goody, R. S., A. Rak and K. Alexandrov (2005). "The structural and mechanistic basis for recycling of Rab proteins between membrane compartments." Cell Mol Life Sci **62**(15): 1657-1670.

Granseth, B., B. Odermatt, S. J. Royle, *et al.* (2006). "Clathrin-mediated endocytosis is the dominant mechanism of vesicle retrieval at hippocampal synapses." Neuron **51**(6): 773-786.

Grosshans, B. L., D. Ortiz and P. Novick (2006). "Rabs and their effectors: Achieving specificity in membrane traffic." Proceedings of the National Academy of Sciences **103**(32): 11821-11827.

Gutierrez, M. G., D. B. Munafo, W. Beron, *et al.* (2004). "Rab7 is required for the normal progression of the autophagic pathway in mammalian cells." J Cell Sci **117**(Pt 13): 2687-2697.

Haas, A. K., E. Fuchs, R. Kopajtich, *et al.* (2005). "A GTPase-activating protein controls Rab5 function in endocytic trafficking." Nat Cell Biol **7**(9): 887-893.

Haas, A. K., S. Yoshimura, D. J. Stephens, *et al.* (2007). "Analysis of GTPase-activating proteins: Rab1 and Rab43 are key Rabs required to maintain a functional Golgi complex in human cells." J Cell Sci **120**(Pt 17): 2997-3010.

Haberman, A., W. R. Williamson, D. Epstein, *et al.* (2012). "The synaptic vesicle SNARE neuronal Synaptobrevin promotes endolysosomal degradation and prevents neurodegeneration." J Cell Biol **196**(2): 261-276.

Haglund, K., P. P. Di Fiore and I. Dikic (2003). "Distinct monoubiquitin signals in receptor endocytosis." Trends Biochem Sci **28**(11): 598-603.

Hamasaki, M., N. Furuta, A. Matsuda, *et al.* (2013). "Autophagosomes form at ER-mitochondria contact sites." Nature **495**(7441): 389-393.

Hammarlund, M., M. T. Palfreyman, S. Watanabe, *et al.* (2007). "Open syntaxin docks synaptic vesicles." PLoS Biol **5**(8): e198.

Hegde, A. N., A. L. Goldberg and J. H. Schwartz (1993). "Regulatory subunits of cAMP-dependent protein kinases are degraded after conjugation to ubiquitin: a molecular mechanism underlying long-term synaptic plasticity." Proc Natl Acad Sci U S A **90**(16): 7436-7440.

Hegde, A. N., K. Inokuchi, W. Pei, *et al.* (1997). "Ubiquitin C-terminal hydrolase is an immediate-early gene essential for long-term facilitation in Aplysia." Cell **89**(1): 115-126.

Hemelaar, J., V. S. Lelyveld, B. M. Kessler, *et al.* (2003). "A single protease, Apg4B, is specific for the autophagy-related ubiquitin-like proteins GATE-16, MAP1-LC3, GABARAP, and Apg8L." J Biol Chem **278**(51): 51841-51850.

Hernandez, D. T., C. A.Setlik, W.Cebrian, C.Mosharov, E. V.Tang, G., H. C. K. Cheng, N.Yarygina, O. and R. E. G. Burke, M.Sulzer, D. (2012). "Regulation of presynaptic neurotransmission by macroautophagy." Neuron **74**(2): 277-284.

Hershko, A. and A. Ciechanover (1998). "The ubiquitin system." Annu Rev Biochem **67**: 425-479.

Heuser, J. E. and T. S. Reese (1973). "Evidence for recycling of synaptic vesicle membrane during transmitter release at the frog neuromuscular junction." J Cell Biol **57**(2): 315-344.

Hinshaw, J. E. and S. L. Schmid (1995). "Dynamin self-assembles into rings suggesting a mechanism for coated vesicle budding." Nature **374**(6518): 190-192.

Holt, Christine E. and Erin M. Schuman (2013). "The Central Dogma Decentralized: New Perspectives on RNA Function and Local Translation in Neurons." Neuron **80**(3): 648-657.

Holtzman, E., A. B. Novikoff and H. Villaverde (1967). "Lysosomes and GERL in normal and chromatolytic neurons of the rat ganglion nodosum." J Cell Biol **33**(2): 419-435.

Holtzman, E. F., A. R. ; Kashner, L. A. (1971). "Stimulation-dependent alterations in peroxidase uptake at lobster neuromuscular junctions." Science **173**(3998): 733-736.

Howard, T. L., D. R. Stauffer, C. R. Degnin, *et al.* (2001). "CHMP1 functions as a member of a newly defined family of vesicle trafficking proteins." J Cell Sci **114**(Pt 13): 2395-2404.

Hua, Z., S. Leal-Ortiz, S. M. Foss, *et al.* (2011). "v-SNARE composition distinguishes synaptic vesicle pools." Neuron **71**(3): 474-487.

Hutagalung, A. H. and P. J. Novick (2011). "Role of Rab GTPases in membrane traffic and cell physiology." Physiol Rev **91**(1): 119-149.

Huttner, W. B., W. Schiebler, P. Greengard, *et al.* (1983). "Synapsin I (protein I), a nerve terminal-specific phosphoprotein. III. Its association with synaptic vesicles studied in a highly purified synaptic vesicle preparation." J Cell Biol **96**(5): 1374-1388.

Hyttinen, J. M. T., M. Niittykoski, A. Salminen, *et al.* (2013). "Maturation of autophagosomes and endosomes: A key role for Rab7." Biochimica et Biophysica Acta (BBA) - Molecular Cell Research **1833**(3): 503-510.

Ignatev, A., S. Kravchenko, A. Rak, *et al.* (2008). "A structural model of the GDP dissociation inhibitor rab membrane extraction mechanism." J Biol Chem **283**(26): 18377-18384.

Ishibashi, K., N. Fujita, E. Kanno, *et al.* (2011). "Atg16L2, a novel isoform of mammalian Atg16L that is not essential for canonical autophagy despite forming an Atg12-5-16L2 complex." Autophagy **7**(12): 1500-1513.

Ishibashi, K., T. Uemura, S. Waguri, *et al.* (2012). "Atg16L1, an essential factor for canonical autophagy, participates in hormone secretion from PC12 cells independently of autophagic activity." Mol Biol Cell **23**(16): 3193-3202.

Itakura, E., C. Kishi-Itakura and N. Mizushima (2012). "The hairpin-type tail-anchored SNARE syntaxin 17 targets to autophagosomes for fusion with endosomes/lysosomes." Cell **151**(6): 1256-1269.

Itoh, M. F. a. T. (2008). "Direct link between Atg protein and small GTPase Rab Atg16L functions as a potential Rab33 effector in mammals." Autophagy **4**(6): 824-826.

Itoh, T., N. Fujita, E. Kanno, *et al.* (2008). "Golgi-resident small GTPase Rab33B interacts with Atg16L and modulates autophagosome formation." Mol Biol Cell **19**(7): 2916-2925.

Iwasaki, K., J. Staunton, O. Saifee, *et al.* (1997). "aex-3 encodes a novel regulator of presynaptic activity in C. elegans." Neuron **18**(4): 613-622.

Jager, S., C. Bucci, I. Tanida, *et al.* (2004). "Role for Rab7 in maturation of late autophagic vacuoles." J Cell Sci **117**(Pt 20): 4837-4848.

Jahn, R. and D. Fasshauer (2012). "Molecular machines governing exocytosis of synaptic vesicles." Nature **490**(7419): 201-207.

Jahn, R. and D. Fasshauer (2012). "Molecular machines governing exocytosis of synaptic vesicles." Nature **490**(7419): 201-207.

Jahn, R. and R. H. Scheller (2006). "SNAREs [mdash] engines for membrane fusion." Nat Rev Mol Cell Biol **7**(9): 631-643.

Jahn, R., W. Schiebler, C. Ouimet, *et al.* (1985). "A 38,000-dalton membrane protein (p38) present in synaptic vesicles." Proc Natl Acad Sci U S A **82**(12): 4137-4141.

Jahn, R. and T. C. Sudhof (1994). "Synaptic vesicles and exocytosis." Annu Rev Neurosci **17**: 219-246.

Jiang, T., B. Qin, J. He, *et al.* (2013). "Three isoforms of the Atg16L1 protein contribute different autophagic properties." Mol Cell Biochem.

Jin, R. U. and J. C. Mills (2014). "RAB26 coordinates lysosome traffic and mitochondrial localization." J Cell Sci.

Jockusch, W. J., G. J. Praefcke, H. T. McMahon, *et al.* (2005). "Clathrin-dependent and clathrin-independent retrieval of synaptic vesicles in retinal bipolar cells." Neuron **46**(6): 869-878.

Kabeya, Y., N. N. Noda, Y. Fujioka, *et al.* (2009). "Characterization of the Atg17–Atg29–Atg31 complex specifically required for starvation-induced autophagy in Saccharomyces cerevisiae." Biochem Biophys Res Commun **389**(4): 612-615.

Kaeser, P. S. and T. C. Sudhof (2005). "RIM function in short- and long-term synaptic plasticity." Biochem Soc Trans **33**(Pt 6): 1345-1349.

Katzmann, D. J., G. Odorizzi and S. D. Emr (2002). "Receptor downregulation and multivesicular-body sorting." Nat Rev Mol Cell Biol **3**(12): 893-905.

Khosravi-Far, R., G. J. Clark, K. Abe, *et al.* (1992). "Ras (CXXX) and Rab (CC/CXC) prenylation signal sequences are unique and functionally distinct." J Biol Chem **267**(34): 24363-24368.

Khosravi-Far, R., R. J. Lutz, A. D. Cox, *et al.* (1991). "Isoprenoid modification of rab proteins terminating in CC or CXC motifs." Proc Natl Acad Sci U S A **88**(14): 6264-6268.

Kiffin, R., C. Christian, E. Knecht, *et al.* (2004). "Activation of chaperone-mediated autophagy during oxidative stress." Mol Biol Cell **15**(11): 4829-4840.

Kim, S. H. and T. A. Ryan (2009). "Synaptic vesicle recycling at CNS snapses without AP-2." J Neurosci **29**(12): 3865-3874.

Klionsky, D. J., H. Abeliovich, P. Agostinis, *et al.* (2008). "Guidelines for the use and interpretation of assays for monitoring autophagy in higher eukaryotes." Autophagy **4**(2): 151-175.

Komander, D. and M. Rape (2012). "The ubiquitin code." Annu Rev Biochem **81**: 203-229.

Koushika, S. P., J. E. Richmond, G. Hadwiger, *et al.* (2001). "A post-docking role for active zone protein Rim." Nat Neurosci **4**(10): 997-1005.

Krick, R., R. A. Busse, A. Scacioc, *et al.* (2012). "Structural and functional characterization of the two phosphoinositide binding sites of PROPPINs, a beta-propeller protein family." Proc Natl Acad Sci U S A **109**(30): E2042-2049.

Laemmli, U. K. (1970). "Cleavage of structural proteins during the assembly of the head of bacteriophage T4." Nature **227**(5259): 680-685.

Lamb, C. A., T. Yoshimori and S. A. Tooze (2013). "The autophagosome: origins unknown, biogenesis complex." Nat Rev Mol Cell Biol **14**(12): 759-774.

Lampert, P. W. and S. S. Schochet, Jr. (1968). "Demyelination and remyelination in lead neuropathy. Electron microscopic studies." J Neuropathol Exp Neurol **27**(4): 527-545.

Lang, T. and R. Jahn (2008). "Core proteins of the secretory machinery." Handb Exp Pharmacol(184): 107-127.

Langelier, C., U. K. von Schwedler, R. D. Fisher, *et al.* (2006). "Human ESCRT-II complex and its role in human immunodeficiency virus type 1 release." J Virol **80**(19): 9465-9480.

Lee, S. H., J. H. Choi, N. Lee, *et al.* (2008). "Synaptic protein degradation underlies destabilization of retrieved fear memory." Science **319**(5867): 1253-1256.

Lee, S. H., A. Simonetta and M. Sheng (2004). "Subunit rules governing the sorting of internalized AMPA receptors in hippocampal neurons." Neuron **43**(2): 221-236.

Li, C., Y. Fan, T. H. Lan, *et al.* (2012). "Rab26 modulates the cell surface transport of alpha2-adrenergic receptors from the Golgi." J Biol Chem **287**(51): 42784-42794.

Li, G. and P. D. Stahl (1993). "Structure-function relationship of the small GTPase rab5." J Biol Chem **268**(32): 24475-24480.

Li, W. W., J. Li and J. K. Bao (2012). "Microautophagy: lesser-known self-eating." Cell Mol Life Sci **69**(7): 1125-1136.

Lipatova, Z., N. Belogortseva, X. Q. Zhang, *et al.* (2012). "Regulation of selective autophagy onset by a Ypt/Rab GTPase module." Proc Natl Acad Sci U S A **109**(18): 6981-6986.

Lonart, G. and T. C. Sudhof (2000). "Assembly of SNARE core complexes prior to neurotransmitter release sets the readily releasable pool of synaptic vesicles." J Biol Chem **275**(36): 27703-27707.

Lynch-Day, M. A. and D. J. Klionsky (2010). "The Cvt pathway as a model for selective autophagy." FEBS Lett **584**(7): 1359-1366.

Maday, S., K. E. Wallace and E. L. Holzbaur (2012). "Autophagosomes initiate distally and mature during transport toward the cell soma in primary neurons." J Cell Biol **196**(4): 407-417.

Mahoney, T. R., Q. Liu, T. Itoh, *et al.* (2006). "Regulation of synaptic transmission by RAB-3 and RAB-27 in Caenorhabditis elegans." Mol Biol Cell **17**(6): 2617-2625.

Maiuri, M. C., E. Zalckvar, A. Kimchi, *et al.* (2007). "Self-eating and self-killing: crosstalk between autophagy and apoptosis." Nat Rev Mol Cell Biol **8**(9): 741-752.

Mari, M., J. Griffith, E. Rieter, *et al.* (2010). "An Atg9-containing compartment that functions in the early steps of autophagosome biogenesis." J Cell Biol **190**(6): 1005-1022.

Mari, M. and F. Reggiori (2010). "Atg9 reservoirs, a new organelle of the yeast endomembrane system?" Autophagy **6**(8): 1221-1223.

Martin, K. C. (2010). "Anchoring Local Translation in Neurons." Cell **141**(4): 566-568.

Masuda, E. S., Y. Luo, C. Young, *et al.* (2000). "Rab37 is a novel mast cell specific GTPase localized to secretory granules." FEBS Lett **470**(1): 61-64.

Mayle, K. M., A. M. Le and D. T. Kamei (2012). "The intracellular trafficking pathway of transferrin." Biochimica et Biophysica Acta (BBA) - General Subjects **1820**(3): 264-281.

McMahon, H. T. and E. Boucrot (2011). "Molecular mechanism and physiological functions of clathrin-mediated endocytosis." Nat Rev Mol Cell Biol **12**(8): 517-533.

Miller, T. M. and J. E. Heuser (1984). "Endocytosis of synaptic vesicle membrane at the frog neuromuscular junction." J Cell Biol **98**(2): 685-698.

Mizushima, N. (2011). "Autophagy in protein and organelle turnover." Cold Spring Harb Symp Quant Biol **76**: 397-402.

Mizushima, N., A. Kuma, Y. Kobayashi, *et al.* (2003). "Mouse Apg16L, a novel WD-repeat protein, targets to the autophagic isolation membrane with the Apg12-Apg5 conjugate." J Cell Sci **116**(Pt 9): 1679-1688.

Mizushima, N., H. Sugita, T. Yoshimori, *et al.* (1998). "A new protein conjugation system in human. The counterpart of the yeast Apg12p conjugation system essential for autophagy." J Biol Chem **273**(51): 33889-33892.

Mizushima, N., T. Yoshimori and Y. Ohsumi (2011). "The role of Atg proteins in autophagosome formation." Annu Rev Cell Dev Biol **27**: 107-132.

Muralidhar, M. G. and J. B. Thomas (1993). "The Drosophila bendless gene encodes a neural protein related to ubiquitin-conjugating enzymes." Neuron **11**(2): 253-266.

Murphey, R. K., S. J. Froggett, P. Caruccio, *et al.* (2003). "Targeted expression of shibire ts and semaphorin 1a reveals critical periods for synapse formation in the giant fiber of Drosophila." Development **130**(16): 3671-3682.

Nakatogawa, H., K. Suzuki, Y. Kamada, *et al.* (2009). "Dynamics and diversity in autophagy mechanisms: lessons from yeast." Nat Rev Mol Cell Biol **10**(7): 458-467.

Nashida, T., A. Imai and H. Shimomura (2006). "Relation of Rab26 to the amylase release from rat parotid acinar cells." Arch Oral Biol **51**(2): 89-95.

Ng, E. L. and B. L. Tang (2008). "Rab GTPases and their roles in brain neurons and glia." Brain Res Rev **58**(1): 236-246.

Nishida, Y., S. Arakawa, K. Fujitani, *et al.* (2009). "Discovery of Atg5/Atg7-independent alternative macroautophagy." Nature **461**(7264): 654-658.

Noda, T., J. Kim, W. P. Huang, *et al.* (2000). "Apg9p/Cvt7p is an integral membrane protein required for transport vesicle formation in the Cvt and autophagy pathways." J Cell Biol **148**(3): 465-480.

Nonet, M. L., J. E. Staunton, M. P. Kilgard, *et al.* (1997). "Caenorhabditis elegans rab-3 mutant synapses exhibit impaired function and are partially depleted of vesicles." J Neurosci **17**(21): 8061-8073.

Novick, P., C. Field and R. Schekman (1980). "Identification of 23 complementation groups required for post-translational events in the yeast secretory pathway." Cell **21**(1): 205-215.

Novick, P. and R. Schekman (1979). "Secretion and cell-surface growth are blocked in a temperature-sensitive mutant of Saccharomyces cerevisiae." Proc Natl Acad Sci U S A **76**(4): 1858-1862.

Orsi, A., H. E. J. Polson and S. A. Tooze (2010). "Membrane trafficking events that partake in autophagy." Curr Opin Cell Biol **22**(2): 150-156.

Ostrowski, M., N. B. Carmo, S. Krumeich, *et al.* (2010). "Rab27a and Rab27b control different steps of the exosome secretion pathway." Nat Cell Biol **12**(1): 19-30; sup pp 11-13.

Pan, X., S. Eathiraj, M. Munson, *et al.* (2006). "TBC-domain GAPs for Rab GTPases accelerate GTP hydrolysis by a dual-finger mechanism." Nature **442**(7100): 303-306.

Pankiv, S., E. A. Alemu, A. Brech, *et al.* (2010). "FYCO1 is a Rab7 effector that binds to LC3 and PI3P to mediate microtubule plus end-directed vesicle transport." J Cell Biol **188**(2): 253-269.

Pasqualato, S., F. Senic-Matuglia, L. Renault, *et al.* (2004). "The structural GDP/GTP cycle of Rab11 reveals a novel interface involved in the dynamics of recycling endosomes." J Biol Chem **279**(12): 11480-11488.

Patrick, G. N., B. Bingol, H. A. Weld, *et al.* (2003). "Ubiquitin-mediated proteasome activity is required for agonist-induced endocytosis of GluRs." Curr Biol **13**(23): 2073-2081.

Pavlos, N. J., M. Gronborg, D. Riedel, *et al.* (2010). "Quantitative analysis of synaptic vesicle Rabs uncovers distinct yet overlapping roles for Rab3a and Rab27b in Ca2+-triggered exocytosis." J Neurosci **30**(40): 13441-13453.

Pavlos, N. J., J. Xu, D. Riedel, *et al.* (2005). "Rab3D regulates a novel vesicular trafficking pathway that is required for osteoclastic bone resorption." Mol Cell Biol **25**(12): 5253-5269.

Pearse, B. M. (1976). "Clathrin: a unique protein associated with intracellular transfer of membrane by coated vesicles." Proc Natl Acad Sci U S A **73**(4): 1255-1259.

Pfeffer, S. and D. Aivazian (2004). "Targeting Rab GTPases to distinct membrane compartments." Nat Rev Mol Cell Biol **5**(11): 886-896.

Pfeffer, S. R. (2005). "Structural clues to Rab GTPase functional diversity." J Biol Chem **280**(16): 15485-15488.

Raiborg, C. and H. Stenmark (2009). "The ESCRT machinery in endosomal sorting of ubiquitylated membrane proteins." Nature **458**(7237): 445-452.

Renna, M., C. Schaffner, A. R. Winslow, *et al.* (2011). "Autophagic substrate clearance requires activity of the syntaxin-5 SNARE complex." J Cell Sci **124**(Pt 3): 469-482.

Richmond, J. E., W. S. Davis and E. M. Jorgensen (1999). "UNC-13 is required for synaptic vesicle fusion in C. elegans." Nat Neurosci **2**(11): 959-964.

Rizzoli, S. O. and W. J. Betz (2005). "Synaptic vesicle pools." Nat Rev Neurosci **6**(1): 57-69.

Rizzoli, S. O. and R. Jahn (2007). "Kiss-and-run, collapse and 'readily retrievable' vesicles." Traffic **8**(9): 1137-1144.

Roberts, R. L., M. A. Barbieri, K. M. Pryse, *et al.* (1999). "Endosome fusion in living cells overexpressing GFP-rab5." J Cell Sci **112 (Pt 21)**: 3667-3675.

Roux, A., K. Uyhazi, A. Frost, *et al.* (2006). "GTP-dependent twisting of dynamin implicates constriction and tension in membrane fission." Nature **441**(7092): 528-531.

Roxrud, I., C. Raiborg, N. M. Pedersen, *et al.* (2008). "An endosomally localized isoform of Eps15 interacts with Hrs to mediate degradation of epidermal growth factor receptor." J Cell Biol **180**(6): 1205-1218.

Rubinsztein, D. C., A. M. Cuervo, B. Ravikumar, *et al.* (2009). "In search of an "autophagomometer"." Autophagy **5**(5): 585-589.

Salminen, A. and P. J. Novick (1987). "A ras-like protein is required for a post-Golgi event in yeast secretion." Cell **49**(4): 527-538.

Sanford, J. C., J. Yu, J. Y. Pan, *et al.* (1995). "GDP dissociation inhibitor serves as a cytosolic acceptor for newly synthesized and prenylated Rab5." J Biol Chem **270**(45): 26904-26909.

Sasaki, T., A. Kikuchi, S. Araki, *et al.* (1990). "Purification and characterization from bovine brain cytosol of a protein that inhibits the dissociation of GDP from and the subsequent binding of GTP to smg p25A, a ras p21-like GTP-binding protein." J Biol Chem **265**(4): 2333-2337.

Schlote, W. (1966). "[The structure of stratified bodies in the axoplasm of dissected fibers of the optic nerve situated distally from the lesion]." J Ultrastruct Res **16**(5): 548-568.

Schluter, O. M., F. Schmitz, R. Jahn, *et al.* (2004). "A complete genetic analysis of neuronal Rab3 function." J Neurosci **24**(29): 6629-6637.

Schluter, O. M., E. Schnell, M. Verhage, *et al.* (1999). "Rabphilin knock-out mice reveal that rabphilin is not required for rab3 function in regulating neurotransmitter release." J Neurosci **19**(14): 5834-5846.

Schmitt, H. D., M. Puzicha and D. Gallwitz (1988). "Study of a temperature-sensitive mutant of the ras-related YPT1 gene product in yeast suggests a role in the regulation of intracellular calcium." Cell **53**(4): 635-647.

Schmitt, H. D., P. Wagner, E. Pfaff, *et al.* (1986). "The ras-related YPT1 gene product in yeast: a GTP-binding protein that might be involved in microtubule organization." Cell **47**(3): 401-412.

Schwamborn, J. C., M. Müller, A. H. Becker, *et al.* (2007). "Ubiquitination of the GTPase Rap1B by the ubiquitin ligase Smurf2 is required for the establishment of neuronal polarity." EMBO J **26**(5): 1410-1422.

Seki, N., T. Yoshikawa, A. Hattori, *et al.* (2000). "cDNA cloning of a human RAB26-related gene encoding a Ras-like GTP-binding protein on chromosome 16p13.3 region." J Hum Genet **45**(5): 309-314.

Shehata, M., H. Matsumura, R. Okubo-Suzuki, *et al.* (2012). "Neuronal Stimulation Induces Autophagy in Hippocampal Neurons That Is Involved in AMPA Receptor Degradation after Chemical Long-Term Depression." Journal of Neuroscience **32**(30): 10413-10422.

Sivars, U., D. Aivazian and S. R. Pfeffer (2003). "Yip3 catalyses the dissociation of endosomal Rab-GDI complexes." Nature **425**(6960): 856-859.

Slepnev, V. I. and P. De Camilli (2000). "Accessory factors in clathrin-dependent synaptic vesicle endocytosis." Nat Rev Neurosci **1**(3): 161-172.

Sonnichsen, B., S. De Renzis, E. Nielsen, *et al.* (2000). "Distinct membrane domains on endosomes in the recycling pathway visualized by multicolor imaging of Rab4, Rab5, and Rab11." J Cell Biol **149**(4): 901-914.

Sorensen, J. B., K. Wiederhold, E. M. Muller, *et al.* (2006). "Sequential N- to C-terminal SNARE complex assembly drives priming and fusion of secretory vesicles." EMBO J **25**(5): 955-966.

Speese, S. D., N. Trotta, C. K. Rodesch, *et al.* (2003). "The ubiquitin proteasome system acutely regulates presynaptic protein turnover and synaptic efficacy." Curr Biol **13**(11): 899-910.

Stanley, R. E., M. J. Ragusa and J. H. Hurley (2013). "The beginning of the end: how scaffolds nucleate autophagosome biogenesis." Trends Cell Biol.

Stenmark, H. (2009). "Rab GTPases as coordinators of vesicle traffic." Nat Rev Mol Cell Biol **10**(8): 513-525.

Stenmark, H. and V. M. Olkkonen (2001). "The Rab GTPase family." Genome Biol **2**(5): REVIEWS3007.

Stenmark, H., R. G. Parton, O. Steele-Mortimer, *et al.* (1994). "Inhibition of rab5 GTPase activity stimulates membrane fusion in endocytosis." EMBO J **13**(6): 1287-1296.

Steward, O. and W. B. Levy (1982). "Preferential localization of polyribosomes under the base of dendritic spines in granule cells of the dentate gyrus." J Neurosci **2**(3): 284-291.

Strack, B., A. Calistri, S. Craig, *et al.* (2003). "AIP1/ALIX is a binding partner for HIV-1 p6 and EIAV p9 functioning in virus budding." Cell **114**(6): 689-699.

Strom, M., P. Vollmer, T. J. Tan, *et al.* (1993). "A yeast GTPase-activating protein that interacts specifically with a member of the Ypt/Rab family." Nature **361**(6414): 736-739.

Südhof, T. (2008). Neurotransmitter Release. Pharmacology of Neurotransmitter Release. T. Südhof and K. Starke, Springer Berlin Heidelberg. **184:** 1-21.

Sudhof, T. C. (2004). "The synaptic vesicle cycle." Annu Rev Neurosci **27**: 509-547.

Südhof, Thomas C. (2012). "The Presynaptic Active Zone." Neuron **75**(1): 11-25.

Südhof, Thomas C. (2013). "Neurotransmitter Release: The Last Millisecond in the Life of a Synaptic Vesicle." Neuron **80**(3): 675-690.

Suzuki, K., Y. Kubota, T. Sekito, *et al.* (2007). "Hierarchy of Atg proteins in pre-autophagosomal structure organization." Genes to Cells **12**(2): 209-218.

Suzuki, K. and Y. Ohsumi (2010). "Current knowledge of the pre-autophagosomal structure (PAS)." FEBS Lett **584**(7): 1280-1286.

Takamori, S., M. Holt, K. Stenius, *et al.* (2006). "Molecular anatomy of a trafficking organelle." Cell **127**(4): 831-846.

Takamori, S., D. Riedel and R. Jahn (2000). "Immunoisolation of GABA-specific synaptic vesicles defines a functionally distinct subset of synaptic vesicles." J Neurosci **20**(13): 4904-4911.

Takats, S., P. Nagy, A. Varga, *et al.* (2013). "Autophagosomal Syntaxin17-dependent lysosomal degradation maintains neuronal function in Drosophila." J Cell Biol **201**(4): 531-539.

Tandon, R., D. P. AuCoin and E. S. Mocarski (2009). "Human cytomegalovirus exploits ESCRT machinery in the process of virion maturation." J Virol **83**(20): 10797-10807.

Tanida, I., N. Minematsu-Ikeguchi, T. Ueno, *et al.* (2005). "Lysosomal turnover, but not a cellular level, of endogenous LC3 is a marker for autophagy." Autophagy **1**(2): 84-91.

Tanida, I., Y. Sou, N. Minematsu-Ikeguchi, *et al.* (2006). "Atg8L/APg8L is the fourth mammalian modifier of mammalian Atg8 conjugation mediated by human Atg4B, Atg7 and Atg3." Febs Journal **273**(11): 2553-2562.

Tanida, I., Y. S. Sou, J. Ezaki, *et al.* (2004). "HsAtg4B/HsApg4B/autophagin-1 cleaves the carboxyl termini of three human Atg8 homologues and delipidates microtubule-associated protein light chain 3- and GABAA receptor-associated protein-phospholipid conjugates." J Biol Chem **279**(35): 36268-36276.

Tanida, I., E. Tanida-Miyake, M. Komatsu, *et al.* (2002). "Human Apg3p/Aut1p homologue is an authentic E2 enzyme for multiple substrates, GATE-16, GABARAP, and

MAP-LC3, and facilitates the conjugation of hApg12p to hApg5p." J Biol Chem **277**(16): 13739-13744.

Thomas, J. B. and R. J. Wyman (1984). "Mutations altering synaptic connectivity between identified neurons in Drosophila." Journal of Neuroscience **4**(2): 530-538.

Thrower, J. S., L. Hoffman, M. Rechsteiner, *et al.* (2000). "Recognition of the polyubiquitin proteolytic signal." EMBO J **19**(1): 94-102.

Thumm, M., R. A. Busse, A. Scacioc, *et al.* (2013). "It takes two to tango: PROPPINs use two phosphoinositide-binding sites." Autophagy **9**(1): 106-107.

Tian, X., R. U. Jin, A. J. Bredemeyer, *et al.* (2010). "RAB26 and RAB3D are direct transcriptional targets of MIST1 that regulate exocrine granule maturation." Mol Cell Biol **30**(5): 1269-1284.

Tokuyasu, K. T. (1973). "A technique for ultracryotomy of cell suspensions and tissues." J Cell Biol **57**(2): 551-565.

Tokuyasu, K. T. (1980). "Immunochemistry on ultrathin frozen sections." Histochem J **12**(4): 381-403.

Tsukita, S. and H. Ishikawa (1980). "The movement of membranous organelles in axons. Electron microscopic identification of anterogradely and retrogradely transported organelles." J Cell Biol **84**(3): 513-530.

Tucker, K. A., F. Reggiori, W. A. Dunn, Jr., *et al.* (2003). "Atg23 is essential for the cytoplasm to vacuole targeting pathway and efficient autophagy but not pexophagy." J Biol Chem **278**(48): 48445-48452.

van den Bogaart, G., K. Meyenberg, U. Diederichsen, *et al.* (2012). "Phosphatidylinositol 4,5-bisphosphate increases Ca2+ affinity of synaptotagmin-1 by 40-fold." J Biol Chem **287**(20): 16447-16453.

Verhage, M. and J. B. Sorensen (2008). "Vesicle docking in regulated exocytosis." Traffic **9**(9): 1414-1424.

Voges, D., P. Zwickl and W. Baumeister (1999). "The 26S proteasome: a molecular machine designed for controlled proteolysis." Annu Rev Biochem **68**: 1015-1068.

Voglmaier, S. M. and R. H. Edwards (2007). "Do different endocytic pathways make different synaptic vesicles?" Curr Opin Neurobiol **17**(3): 374-380.

Wagner, A. C., M. Z. Strowski, B. Goke, *et al.* (1995). "Molecular cloning of a new member of the Rab protein family, Rab 26, from rat pancreas." Biochem Biophys Res Commun **207**(3): 950-956.

Watanabe, S., Q. Liu, M. W. Davis, *et al.* (2013). "Ultrafast endocytosis at Caenorhabditis elegans neuromuscular junctions." Elife **2**: e00723.

Waters, M. G. and S. R. Pfeffer (1999). "Membrane tethering in intracellular transport." Curr Opin Cell Biol **11**(4): 453-459.

Webber, J. L. and S. A. Tooze (2010). "New insights into the function of Atg9." FEBS Lett **584**(7): 1319-1326.

Wennerberg, K., K. L. Rossman and C. J. Der (2005). "The Ras superfamily at a glance." J Cell Sci **118**(Pt 5): 843-846.

Wettstein, R. and J. R. Sotelo (1963). "Electron microscope study on the regenerative process of peripheral nerves of mice." Z Zellforsch Mikrosk Anat **59**: 708-730.

Wiedenmann, B. and W. W. Franke (1985). "Identification and localization of synaptophysin, an integral membrane glycoprotein of Mr 38,000 characteristic of presynaptic vesicles." Cell **41**(3): 1017-1028.

Wiedenmann, B. and W. B. Huttner (1989). "Synaptophysin and chromogranins/secretogranins--widespread constituents of distinct types of neuroendocrine vesicles and new tools in tumor diagnosis." Virchows Arch B Cell Pathol Incl Mol Pathol **58**(2): 95-121.

Willeumier, K., S. M. Pulst and F. E. Schweizer (2006). "Proteasome inhibition triggers activity-dependent increase in the size of the recycling vesicle pool in cultured hippocampal neurons." J Neurosci **26**(44): 11333-11341.

Wittmann, J. G. and M. G. Rudolph (2004). "Crystal structure of Rab9 complexed to GDP reveals a dimer with an active conformation of switch II." FEBS Lett **568**(1-3): 23-29.

Wu, Y. W., L. K. Oesterlin, K. T. Tan, *et al.* (2010). "Membrane targeting mechanism of Rab GTPases elucidated by semisynthetic protein probes." Nat Chem Biol **6**(7): 534-540.

Xie, Z. and D. J. Klionsky (2007). "Autophagosome formation: core machinery and adaptations." Nat Cell Biol **9**(10): 1102-1109.

Xu-Friedman, M. A., K. M. Harris and W. G. Regehr (2001). "Three-dimensional comparison of ultrastructural characteristics at depressing and facilitating synapses onto cerebellar Purkinje cells." J Neurosci **21**(17): 6666-6672.

Yao, I., H. Takagi, H. Ageta, *et al.* (2007). "SCRAPPER-dependent ubiquitination of active zone protein RIM1 regulates synaptic vesicle release." Cell **130**(5): 943-957.

Yen, W. L., J. E. Legakis, U. Nair, *et al.* (2007). "Atg27 is required for autophagy-dependent cycling of Atg9." Mol Biol Cell **18**(2): 581-593.

Yi, J. J. and M. D. Ehlers (2007). "Emerging roles for ubiquitin and protein degradation in neuronal function." Pharmacological Reviews **59**(1): 14-39.

Yoshimura, S., A. Gerondopoulos, A. Linford, *et al.* (2010). "Family-wide characterization of the DENN domain Rab GDP-GTP exchange factors." J Cell Biol **191**(2): 367-381.

Zhang, J. Z., B. A. Davletov, T. C. Südhof, *et al.* (1994). "Synaptotagmin I is a high affinity receptor for clathrin AP-2: Implications for membrane recycling." Cell **78**(5): 751-760.

Zink, S., D. Wenzel, C. A. Wurm, *et al.* (2009). "A link between ER tethering and COP-I vesicle uncoating." Dev Cell **17**(3): 403-416.

6 Appendix

6.1 Abbreviations

α	alpha
γ	gamma
µ	micro
Atg	autophagy related gene
ATP	Adenosine triphosphate
AZ	Active Zone
c	control
C. elegans	*Caenorhabditis elegans*
CA	Costitutively Active
Ca^{2+}	calcium ion
CAZ	Cytomatrix of active zone
CCV	clathrin coated vesicles
cDNA	complementary DANN
CMA	chaperone-mediated autophagy
CME	Clathrin-mediated endocytosis
CNS	central nervous system
CT	C-terminal
DIV	Day of *in vitro* development
DN	Dominant negative
DTT	Dithiothreitol
e. coli	*Escherichia coli*
ECL	Enhanced chemiluminescence
EDTA	Ethylenediaminetetraacetic acid
EEA1	Early endosome antige 1
EGFP	Enahanced Green fluorescent protein
ESCRT	Endosomal sorting complex for transport
et al.	et alii
FL	Full lenght
g	Gram/centrifugal force
GAP	GTPase-activating proteins
GDF	GDI-displacement factor
GDI	GDP dissociator inhibitor
GDP	Guanosine diphosphate
GEF	Guanin exchange factor
GFP	Green Fluorescent Protein
GGTase	Geranylgeranyltransferase
GTP	Guanosine triphosphate--S
HEPES	*N*-(*2*-Hydroxyethyl)piperazine-N-3-propanesulfonic acid
His	Histidine

IgG	Immunglobuline G
II	Immunoisolation
ILV	intraluminal vesicles
IP	Immunoprecipitation
KO	Knock out
l	liter
LAMP2A	Lysosomal associated membrane *protein*-2
LB- Medium	Luria-Bertani- Medium
LE	late endosomes
m	mitochondria
mA	milli Ampere
mGFP	monomeric Green fluorescent protein
min	minute
mM	milli Molar
MVB	Multivesicular body
MVE	Multivesicle endosome
NGS	Normal goat serum
NMJ	Neuro Muscular Junction
NT	N-terminal
PAGE	Polyacrylamide gel electrophoresis
PAS	Pre-autophagosomal structure
PBS	Phosphate-Buffered Saline
PE	Phosphatidylethanolamine
pH	preponderance of hydrogen ions
PIP2	Phosphatidylinositol-4,5-bisphosphate
PM	Plasma membrane
PNS	Post nuclear supernatant
REP	Rab escort proteins
rpm	revolutions per minute
RRP	Ready releasable pool
RT	Room temperature
SDS	Sodium dodecyl sulfate
sec	second
sec	secretory mutant
SN	Supernatant
SNARE	soluble N-ethylmalemide–sensitive factor attachment *protein* receptor
SOC medium	Super Optimal broth with Catabolite repression
SV	Synaptic sesicle
TB	Tris-boric acid
TBST	Tris-Buffered Saline and Tween 20
TEMED	*N*,*N*,*N´*, *N*′-Tetramethylethylenediamine
Tris	tris-(hydroxymethyl)-aminomethane
ts	temperature senitive
UPS	Ubiquitin proteasome system

V	Volt
v/v	volume per volume
VPS9	Vacuolar sorting protein 9
WB	Wetern blotting
w/v	weight per volume
X	Time

6.2 Acknowledgments

My first acknowledgement goes to Professor Reinhard Jahn not only because he allowed me to be part of his group, but in particularly for his way to think science, for his passion for research, for his immense knowledge and his always renewed excitement for my project. I thank him for his constant support and enthusiasm that were a great driving force to proceed with this fascinating project. I am honored to be his student.

Special thanks go to Dr. John Chua for his supervision and constant supports, for his patients in keeping always open his door, for the friendly discussions we had during this four years.

I do not forget Dr. Nathan Pavlos who left me the project at the right time and right moment. Thank you for your availability and contributions in trying to understand Rab26 function from the other side of the world.

I would like to direct my acknowledgements to Dr. Dietmar Riedel and Dr. Dirk Wenzel for the electron microscopy images; to professor Henning Urlaub and Monika Raabe for the mass spectrometry analysis; to Dr. Gerd Vorbrüggen and to Dr. Janina Boiken for the helpful collaborations. Special thanks also to Dr. Karin Kühnel for the Atg16 and Atg5 purified proteins; to Dr. Seiichi Koike for RFP-Rab5 constructs and for the nice discussions, Zohreh Farsi and Momchil Ninov for the brain fractions.

My gratitude goes to Sigrid Schmidt and to Brigitte Barg-Kues for the help during my last period of my PhD. I also thank Dr. Dieter Schmitt and Dr. Gottfried Mieskes who were heart and soul of this laboratory. Without them nothing would work. I really appreciated your kindness and time.

To the entire Neurobiology department for the wonderful and friendly environment.

Particular thanks go to Momchil, Hale, Angel, Dominika and Partho for their friendship. Thank you guys for listening and sharing concerns and the good time we had together. Thank you to Neva, Kemal and little Alya with whom I shared unforgettable times during this four years.

Last but not least I want to thank my family for being always close during all my walk of life, side by side with countless love. For supporting and encouraging me any time I was in front of an important decision. My thanks will never be enough for what you have done and you are still doing.